

Ultraviolet Absorption Cross Sections and Reaction Kinetics and Mechanisms for Peroxy Radicals in the Gas Phase

T. J. WALLINGTON*

Research Staff, SRL-E3083, Ford Motor Company, P.O. Box 2053, Dearborn, Michigan 48121-2053

P. DAGAUT

Laboratoire de Combustion et Systèmes Réactifs, Centre National de la Recherche Scientifique, 1C, Avenue de la Recherche Scientifique, 45071 Orleans Cedex 2, France

M. J. KURYLO

The Chemical Kinetics and Thermodynamics Division, National Institute of Standards and Technology, Gaithersburg, Maryland 20899

Received August 26, 1991 (Revised Manuscript Received March 19, 1992)

Contents

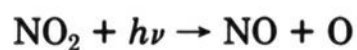
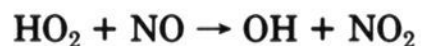
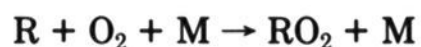
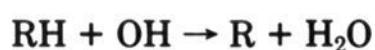
I. Introduction	668	B. HO ₂ + CH ₃ O ₂	692
II. Ultraviolet Absorption Spectra	669	C. HO ₂ + CD ₃ O ₂	694
A. HO ₂	669	D. HO ₂ + C ₂ H ₅ O ₂	694
B. CH ₃ O ₂	672	E. HO ₂ + HOCH ₂ O ₂	694
C. C ₂ H ₅ O ₂	673	F. HO ₂ + HOCH ₂ CH ₂ O ₂	695
D. <i>n</i> -C ₃ H ₇ O ₂	673	G. HO ₂ + CH ₃ C(O)O ₂	695
E. <i>i</i> -C ₃ H ₇ O ₂	674	V. Kinetics and Mechanisms of RO ₂ + NO Reactions	696
F. <i>t</i> -C ₄ H ₉ O ₂	674	A. HO ₂ + NO	696
G. (CH ₃) ₃ CCH ₂ O ₂	675	B. CH ₃ O ₂ + NO	697
H. CH ₂ ClO ₂	675	C. C ₂ H ₅ O ₂ + NO	697
I. CH ₂ FO ₂	675	D. (CH ₃) ₂ CHO ₂ + NO	697
J. HOCH ₂ O ₂	675	E. (CH ₃) ₃ CO ₂ + NO	699
K. CH ₂ ClCH ₂ O ₂	676	F. CH ₃ C(O)O ₂ + NO	699
L. HOCH ₂ CH ₂ O ₂	676	G. CFCl ₂ O ₂ + NO	700
M. CH ₃ C(O)O ₂	676	H. CF ₂ ClO ₂ + NO	700
N. CH ₃ OCH ₂ O ₂	677	I. CF ₃ O ₂ + NO	700
O. CH ₃ COCH ₂ O ₂	677	J. CCl ₃ O ₂ + NO	700
P. CF ₃ CCl ₂ O ₂ , CF ₃ CFHO ₂ , CFCl ₂ CH ₂ O ₂ , and CF ₂ ClCH ₂ O ₂	677	VI. Kinetics and Mechanisms of RO ₂ + NO ₂ Reactions	700
III. Kinetics and Mechanisms of Peroxy Radical Self-Reactions and Cross Reactions	679	A. HO ₂ + NO ₂	700
A. CH ₃ O ₂ + CH ₃ O ₂	679	B. CH ₃ O ₂ + NO ₂	700
B. C ₂ H ₅ O ₂ + C ₂ H ₅ O ₂	685	C. C ₂ H ₅ O ₂ + NO ₂	701
C. <i>n</i> -C ₃ H ₇ O ₂ + <i>n</i> -C ₃ H ₇ O ₂	686	D. (CH ₃) ₂ CHO ₂ + NO ₂	701
D. <i>i</i> -C ₃ H ₇ O ₂ + <i>i</i> -C ₃ H ₇ O ₂	686	E. CF ₂ ClO ₂ + NO ₂	701
E. <i>t</i> -C ₄ H ₉ O ₂ + <i>t</i> -C ₄ H ₉ O ₂	687	F. CFCl ₂ O ₂ + NO ₂	702
F. neo-C ₅ H ₁₂ O ₂ + neo-C ₅ H ₁₂ O ₂	688	G. CH ₃ C(O)O ₂ + NO ₂	702
G. CH ₂ ClO ₂ + CH ₂ ClO ₂	688	H. CCl ₃ O ₂ + NO ₂	703
H. CH ₂ FO ₂ + CH ₂ FO ₂	689	I. CF ₃ O ₂ + NO ₂	703
I. HOCH ₂ O ₂ + HOCH ₂ O ₂	689	VII. Discussion	703
J. CH ₂ ClCH ₂ O ₂ + CH ₂ ClCH ₂ O ₂	689	A. Absorption Spectra	703
K. HOCH ₂ CH ₂ O ₂ + HOCH ₂ CH ₂ O ₂	690	B. Kinetics and Mechanisms of Self-Reactions	705
L. CH ₃ C(O)O ₂ + CH ₃ C(O)O ₂	690	C. Kinetics and Mechanisms of RO ₂ + HO ₂ Reactions	707
M. CH ₃ OCH ₂ O ₂ + CH ₃ OCH ₂ O ₂	690	D. Kinetics and Mechanisms of RO ₂ + NO _x Reactions	707
N. CH ₃ COCH ₂ O ₂ + CH ₃ COCH ₂ O ₂	691	VIII. Conclusions	708
O. CH ₃ C(O)O ₂ + CH ₃ O ₂	691	IX. Acknowledgment	709
P. (CH ₃) ₃ CO ₂ + CH ₃ O ₂	691	X. References	709
IV. Kinetics and Mechanisms of RO ₂ + HO ₂ Reactions	691		
A. HO ₂ + HO ₂	691		



Timothy Wallington was born in England in 1958. He received his B.A. in Natural Sciences from Oxford University in 1981 and a Ph.D. in physical chemistry under the supervision of Richard Wayne in 1983. In 1984 he moved to the Statewide Air Pollution Research Center in Riverside, CA to take up a postdoctoral fellowship with James N. Pitts, Jr. and Roger Atkinson. At Riverside he studied mechanisms of urban smog formation. In 1986 he moved to the National Bureau of Standards (now the National Institute of Standards and Technology) in Gaithersburg, MD to take up a postdoctoral fellowship with Michael J. Kurylo. At NBS he studied the kinetics of OH reactions with organics and the atmospheric chemistry of alkyl peroxy radicals with Philippe Dagaut. In 1987 he moved to the Scientific Research Laboratory of Ford Motor Company in Dearborn, MI. He is currently a Senior Research Scientist working to establish the effect of vehicle and manufacturing emissions on the environment.

I. Introduction

Alkyl peroxy radicals, RO_2 , play important roles as reaction intermediates in the atmospheric oxidation and low-temperature combustion of every hydrocarbon.¹⁻³ In such degradation processes, alkyl radicals (formed via H-atom abstraction by OH or NO_3 radicals or Cl or O atoms) are rapidly converted into peroxy radicals by combination with molecular oxygen. Following such formation, under tropospheric conditions these alkyl peroxy radicals react with NO, NO_2 , HO_2 , themselves, or other alkyl peroxy radicals. For example, RO_2 radicals are responsible for the formation of ozone in urban areas by the following series of reactions:



Thus, a complete mechanistic understanding of hydrocarbon degradation and its role in atmospheric chemistry requires detailed information on a multitude of RO_2 reactions. In addition, studies of RO_2 self-re-



Philippe Dagaut was born in France in 1960. He worked for a Ph.D. degree in the CRCCHT, CNRS at Orléans (France) in the field of Combustion Chemistry under the supervision of Michel Cathonnet. He received his Ph.D. in Physical Chemistry from the University of Paris (VI) in 1986. After a postdoctoral fellowship with Michael J. Kurylo at NIST (USA), where he studied the kinetics of OH reactions with organics and the spectroscopy and kinetics of peroxy radicals reactions, in collaboration with Timothy J. Wallington, he moved back in 1988 to the Laboratoire de Combustion et Systèmes Réactifs (Formerly CRCCHT), CNRS at Orléans. He is currently studying the kinetics and mechanisms of the gas-phase oxidation of hydrocarbons. He is developing comprehensive chemical kinetic reaction mechanisms for the oxidation of hydrocarbons.

Michael Kurylo was born in Wallingford, CT, in 1945. He received his B.S. in Chemistry from Boston College in 1966 and a Ph.D. in Physical Chemistry from the Catholic University of America under the supervision of Richard B. Timmons in 1969. He was awarded a National Research Council Postdoctoral Associateship in 1969 and worked with Walter Braun at the National Bureau of Standards (now the National Institute of Standards and Technology, NIST) on the study of gas-phase atom and free-radical kinetics. He has continued his research at the NIST laboratories in Gaithersburg, MD, in the areas of gas-phase photochemistry and kinetics with an emphasis on atmospheric and combustion processes. In 1983, he was awarded the U.S. Department of Commerce Bronze Medal for significant contribution to the study of the kinetics of chemical reactions. More recently (in October, 1991) he was awarded the U.S. Department of Commerce Silver Medal for leadership in providing a scientific basis for understanding the effects of man-made chemicals on the Earth's atmosphere.

activity have played a central role in the development and testing of combination rate theory. Recognition of the central role of gas-phase peroxy radical reactivity from both a practical and theoretical standpoint has fostered considerable research over the last decade. This, in turn, has made possible a timely review and evaluation of our present state of understanding of gas-phase RO_2 chemistry.

In this article we review the available spectroscopic, kinetic, and mechanistic data concerning alkyl peroxy radicals in the gas phase. Our purpose is to provide an up to date, comprehensive source of such data for inclusion into chemical models of atmospheric and combustion processes. Where possible, recommended values are given and discrepancies and uncertainties in

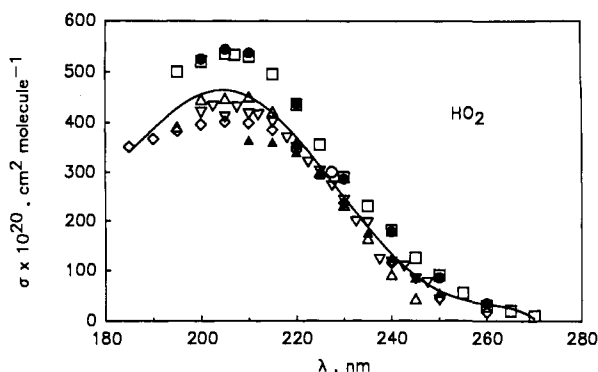


Figure 1. Absorption cross section data for HO₂ at 298 K from McAdam et al.⁸ (filled circles), Moortgat et al.¹⁰ (open squares), Paukert and Johnston⁴ (filled and open inverse triangles), Cox and Burrows⁵ (open triangles), Hohanadel et al.⁶ (1980) (open diamonds), Sander et al.⁷ (open circle), Kurylo et al.⁹ (filled triangles), recommended spectrum (full line).

the data are highlighted. This review is broken down into four sections dealing with (i) ultraviolet absorption cross sections of RO₂ radicals, (ii) branching ratios and kinetics of self-reactions and cross reactions, (iii) the kinetics of peroxy radical reactions with HO₂ radicals, and (iv) the kinetics of the reaction of peroxy radicals with NO_x. We have restricted ourselves to articles published before June 1991.

Where multiple studies exist, we have based our recommendations on an average of those studies appearing to be most reliable. Where only a single investigation has been reported the results of that study are recommended providing that there is a consistency with analogous systems.

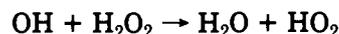
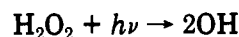
II. Ultraviolet Absorption Spectra

The most convenient and hence widely used method for monitoring peroxy radicals is via their strong absorption in the ultraviolet over the range 200–300 nm. Since these absorptions are an important facet of studies of peroxy radical reaction kinetics, we shall first review the available literature data on the UV absorption cross sections. In all cases no evidence for fine structure has been discerned with the spectral resolutions employed (typically 1–3 nm). Direct comparison of the reported absorption cross sections is then possible. Table I lists the literature data for peroxy radical absorption cross sections (base *e*) in units of cm² molecule⁻¹.

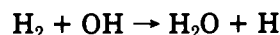
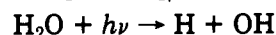
A. HO₂

UV absorption cross sections at room temperature have been reported by Paukert and Johnston,⁴ Hohanadel et al.,^{6,44} Cox and Burrows,⁵ Sander et al.,⁷ McAdam et al.,⁸ Kurylo et al.,⁹ and Moortgat et al.¹⁰ The measurement techniques fall into two groups, either molecular modulation spectroscopy (Paukert and Johnston,⁴ and Cox and Burrows⁵) or flash photolysis/absorption spectroscopy (Hohanadel et al.,^{6,44} Sander et al.,⁷ McAdam et al.,⁸ Kurylo et al.,⁹ and Moortgat et al.¹⁰). HO₂ radicals have been generated using a variety of chemical systems. Paukert and

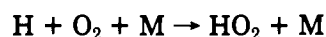
Johnston⁴ used photolysis of hydrogen peroxide in helium at 253.7 nm



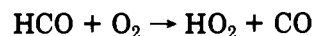
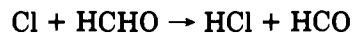
and photolysis of H₂O in H₂/O₂ mixtures



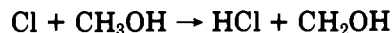
In their latest study, Hohanadel et al.⁶ produced HO₂ radicals by photolysis of CO/H₂O/O₂ mixtures and by photolysis of He/H₂O/O₂ mixtures. Cox and Burrows⁵ generated HO₂ by photolysis of chlorine in the presence of excess H₂ and O₂



or in the presence of formaldehyde and O₂



Sander et al.⁷ used the photolysis ($\lambda > 300$ nm) of Cl₂/H₂/O₂ and Cl₂/CH₃OH/O₂ mixtures to produce HO₂



The methanol system was also used by McAdam et al.,⁸ Kurylo et al.,⁹ and Moortgat et al.¹⁰ Replacing methanol by CH₃OD or CD₃OD and H₂ by D₂, Sander et al.⁷ also determined $\sigma(\text{DO}_2) = (2.5 \pm 0.33) \times 10^{-18}$ cm² molecule⁻¹ at 227.5 nm.

As seen from Figure 1, there are significant discrepancies in the values of $\sigma(\text{HO}_2)$. In this evaluation we have normalized the first spectrum obtained by Hohanadel et al.⁴⁴ to the value of $\sigma(\text{HO}_2) = 4.05 \times 10^{-18}$ cm² molecule⁻¹ at 220 nm obtained in subsequent work by these authors.⁶ Below 220 nm the remaining set of data falls into two groups: one with high σ values (McAdam et al.⁸ and Moortgat et al.¹⁰) and one with low σ values (Paukert and Johnston,⁴ Cox and Burrows,⁵ Hohanadel et al.,⁶ Sander et al.,⁷ and Kurylo et al.⁹). Above 220 nm, good agreement between all these data is found. No definitive explanation of the short wavelength differences can be offered at the present time. Thus our recommended cross sections come from a fit (fifth-order regression) to the composite data set. This fit is represented by the solid line in Figure 1, with a maximum of absorption of 4.65×10^{-18} cm² molecule⁻¹ at 205 nm.

No pressure dependence has been observed for σ (HO₂) over the range 120–760 Torr. However, a small temperature dependence has been reported by Kijewski and Troe⁴⁵ and Lightfoot et al.⁴⁶ that can be represented by

$$(\sigma_T/\sigma_{300\text{K}})_{210\text{nm}} = 1.0 - 2.16 \times \exp(-1801/T)$$

over the temperature range 300–1100 K.

TABLE I. Measured Absorption Cross Sections for Peroxy Radicals

HO ₂								
wavelength (nm)	σ (10 ⁻²⁰ cm ² molecule ⁻¹)							
	ref 4 ^a	ref 5	ref 6	ref 7	ref 8	ref 9	ref 10	recommendation
185			351					344
190			367					387
195	391		383				500	430
200	445	419	396		525		520	458
202.5		431						
205	447	410	401		544		535	465
207							533	
207.5		428						
210	450	417	399		537	365	530	454
212		415						
215	421	399	385			360	495	422
218		368						
220	358	345	345		437	340	435	373
222.5		320						
225	299	302				295	355	316
227.5		272		300		265		
230	231	242	236		286	235	290	245
232.5		198						
235	163	196				175	230	192
237.5		122						
240	91	116	115		177	125	180	135
242.5		108						
245	43	83				85	125	92
247.5		76						
250		41	45		85	55	90	60
255							55	46
260			18		35		30	36
265							20	25
270							10	7

CH ₃ O ₂																
wavelength (nm)	σ (10 ⁻²⁰ cm ² molecule ⁻¹)															
	refs 11 and 12	ref 16	ref 13	refs 17 and 18	ref 14	ref 19	ref 15	ref 8	ref 9	ref 20	ref 10	ref 21	ref 21	ref 22	ref 28	recommendation
195											145					
200											165					165
205										165						190
210									231	235	237	250	153		213	212
215					363				318	280		320	215		273	268
220					382				378	315	370	390	278	260	325	327
225					485				415	340		440	325		384	386
230					485				492	365	492	470	381	374	423	430
235		332			573					380		480	393		447	443
240	550		313 ^c		592				486	380	497	480	403	380	452	389
245					573					360		460	384		443	426
250		291 ^b		390	493	245			441	330	425	440	365	348	414	392
255					439		370 ^d		412	295		410	320		377	362
260					378				368	255	353	360	284	279	334	318
265			202		332				312	215		310	245		285	279
270					306				260	175	238	255	200		236	238
275					218							220	149		190	161
280					145					100		175	120	108	147	145
285													81		110	104
290								40					47		78	66
295															54	42
300																8

C ₂ H ₅ O ₂							
wavelength (nm)	σ (10 ⁻²⁰ cm ² molecule ⁻¹)						
	ref 23	ref 26	ref 24	ref 27	ref 25	ref 28	recommendation
215						250	230
220	215				281	290	282
225	295				363	330	330
230	347		539		431	380	376
235	389				474 ^e	405	408
240	367	619	519		459	415	415
245	332				418	410	406
250	316				401	390	379
255	285				368	360	338
260	248				320	320	296
265	202				263	270	245
270	167				219	205	192

TABLE I (Continued)

C ₂ H ₅ O ₂								
wavelength (nm)	σ (10 ⁻²⁰ cm ² molecule ⁻¹)							recommendation
	ref 23	ref 26	ref 24	ref 27	ref 25	ref 28		
275	129							149
280	104						130	112
285								85
290							60	60
295								45
300							25	25

n-C ₃ H ₇ O ₂ and i-C ₃ H ₇ O ₂								
wavelength (nm)	σ (10 ⁻²⁰ cm ² molecule ⁻¹)		wavelength (nm)	σ (10 ⁻²⁰ cm ² molecule ⁻¹)		wavelength (nm)	σ (10 ⁻²⁰ cm ² molecule ⁻¹)	
	n-C ₃ H ₇ O ₂ , ref 29	i-C ₃ H ₇ O ₂ , ref 29		n-C ₃ H ₇ O ₂ , ref 29	i-C ₃ H ₇ O ₂ , ref 29		n-C ₃ H ₇ O ₂ , ref 29	i-C ₃ H ₇ O ₂ , ref 29
215	205	-	240	423	487	265	272	295
220	249	264	245	408	469	270	223	231
225	321	405	250	382	441	275	166	156
230	385	474	255	352	400	280	138	123
235	478	492	260	315	354			

t-C ₄ H ₉ O ₂											
wavelength (nm)	σ (10 ⁻²⁰ cm ² molecule ⁻¹)					wavelength (nm)	σ (10 ⁻²⁰ cm ² molecule ⁻¹)				
	ref 30	refs 32 and 33	ref 31	ref 34	recommen- dation		ref 30	refs 32 and 33	ref 31	ref 34	recommen- dation
210				145 (160) ^f	136	260	309		318 (350)	298	
215					210	265	-			245	
220		317		264 (290)	285	270	189		200 (220)	193	
225		386			361	275	-			150	
230		430		373 (410)	412	280	103		127 (140)	106	
235		470			440	285					
240	220	458	400	427 (470)	446	290					
245		458			430	295					
250		403		382 (420)	398	300					
255		-			350						

(CH ₃) ₃ CH ₂ O ₂								
wavelength (nm)	σ (10 ⁻²⁰ cm ² molecule ⁻¹)			wavelength (nm)	σ (10 ⁻²⁰ cm ² molecule ⁻¹)			recommendation
	ref 34	ref 35	recommendation		ref 34	ref 35	recommendation	
210	191 (210) ^f	225	210	260	509 (560)	450	450	
215		265	265	265		415	415	
220	327 (360)	320	320	270	373 (410)	350	350	
225		385	385	275		285	285	
230	482 (530)	455	455	280	236 (260)	220	220	
235		505	505	285		170	170	
240	564 (620)	525	530	290	154 (170)	120	120	
245		540	555	295		75	75	
250	546 (600)	520	525	300		25	25	
255		500	500					

CH ₃ COCH ₂ O ₂							
wavelength (nm)	σ (10 ⁻²⁰ cm ² molecule ⁻¹), ref 36	wavelength (nm)	σ (10 ⁻²⁰ cm ² molecule ⁻¹), ref 36	wavelength (nm)	σ (10 ⁻²⁰ cm ² molecule ⁻¹), ref 36		
225	433	260	186	330		130	
227.5	402	270	137	340		98	
230	345	280	148	350		66	
235	311	290	141	360		44	
240	276	300	150	370		27	
245	254	310	148	380		9	
250	214	320	141				

CH ₂ ClO ₂ , CH ₂ FO ₂ , and HOCH ₂ O ₂						
wavelength (nm)	σ (10 ⁻²⁰ cm ² molecule ⁻¹)					
	CH ₂ ClO ₂ , ref 37	CH ₂ FO ₂ , ref 37	HOCH ₂ O ₂			recommendation
			ref 38	ref 39		
200			273 (295) ^g			273
210	245	340	315 (340)			305
215	285	400	-	310		325
220	305	460	334 (360)	350		342
225	345	475	-	375		355
230	370	460	352 (380)	370		365
235	375	415	-			365

TABLE I (Continued)

CH ₂ ClO ₂ , CH ₂ FO ₂ , and HOCH ₂ O ₂					
wavelength (nm)	σ (10 ⁻²⁰ cm ² molecule ⁻¹)				
	CH ₂ ClO ₂ , ref 37	CH ₂ FO ₂ , ref 37	ref 38	HOCH ₂ O ₂ ref 39	recommendation
240	370	370	334 (360)	360	355
245	340	320	—	355	335
250	314	265	278 (300)	300	305
255	275	210	—	275	265
260	240	155	213 (230)	230	216
265	200	125	—	165	165
270	160	85	120 (130)	125	123
275	120	70	—	90	90
280	90	50	—	65	65
285	—	—	—	—	—
290	30	30	—	—	—
CH ₂ ClCH ₂ O ₂ , HOCH ₂ CH ₂ O ₂ , CH ₃ (O)O ₂ , and CH ₃ OCH ₂ O ₂					
wavelength (nm)	σ (10 ⁻²⁰ cm ² molecule ⁻¹)				
	CH ₂ ClCH ₂ O ₂ , ref 40	HOCH ₂ CH ₂ O ₂ , ref 41	CH ₃ COO ₂ , ref 10	CH ₃ OCH ₂ O ₂ , ref 42	
195	—	—	428 (500) ^h	—	
200	—	—	702 (820)	—	
205	—	79	797 (930)	—	
207	—	—	814 (950)	—	
210	215	112	771 (900)	340	
215	—	147	612 (715)	360	
220	270	179	488 (570)	395	
225	—	210	355 (415)	400	
230	355	235	291 (340)	400	
235	390	255	300 (350)	390	
240	400	264	313 (365)	365	
245	390	259	317 (370)	335	
250	365	245	287 (335)	295	
255	325	—	253 (295)	260	
260	280	198	214 (250)	220	
265	220	—	184 (215)	175	
270	180	122	146 (170)	140	
275	—	—	120 (140)	—	
280	110	58	94 (110)	80	
285	85	—	—	—	
290	45	21	—	35	
CF ₃ CCl ₂ O ₂ , CF ₃ CFHO ₂ , CFCl ₂ CH ₂ O ₂ , and CFCICH ₂ O ₂					
wavelength (nm)	σ (10 ⁻²⁰ cm ² molecule ⁻¹)				
	CF ₃ CCl ₂ O ₂ , ref 43	CF ₃ CFHO ₂ , ref 43	CFCl ₂ CH ₂ O ₂ , ref 43	CF ₂ CICH ₂ O ₂ , ref 43	
200	—	306	—	—	
210	—	386	—	196	
220	216	335	355	286	
230	223	282	387	333	
240	206	205	375	342	
250	181	121	322	288	
260	160	55	221	187	
270	116	26	156	115	
280	63	—	79	48	
290	29	—	—	—	

^a Average values. ^b At 248.2 nm. ^c At 239 nm. ^d At 254 nm. ^e At 236 nm. ^f Values in parentheses were measured relative to $\sigma(\text{CH}_3\text{O}_2)$ values reported by Moortgat et al.;¹⁰ these values have been rescaled using our recommended values for $\sigma(\text{CH}_3\text{O}_2)$. ^g Values in parentheses are based upon $\sigma(\text{HO}_2)$ 210 nm = 4.9×10^{-18} , results have been rescaled to our recommended value for $\sigma(\text{HO}_2)$. ^h Values in parentheses are relative to $\sigma(\text{HO}_2)$ 210 nm = 5.3×10^{-18} , results have been rescaled to our recommended value for $\sigma(\text{HO}_2)$.

B. CH₃O₂

UV absorption cross sections of CH₃O₂ radicals have been reported by Parkes et al.,^{11,12} Hochenadel et al.,¹⁶ Kan et al.,¹³ Cox and Tyndall,^{17,18} Adachi et al.,¹⁴ Sander and Watson,¹⁹ Pilling and Smith,¹⁵ McAdam et al.,⁸ Kurylo et al.,⁹ Jenkin et al.,²⁰ Wallington et al.,²⁸ Moortgat et al.,¹⁰ Dagaut and Kurylo,²¹ and Simon et al.²² and are listed in Table I. In addition, Jenkin and Cox⁴¹ have reported a relative spectrum of CH₃O₂. As

in the case of HO₂, the experimental techniques used fall into two groups, either molecular modulation spectroscopy (Parkes et al.^{11,12} Cox and Tyndall,^{17,18} Simon et al.,²² and Jenkin and Cox⁴¹ or flash/laser photolysis coupled with absorption spectroscopy (Hochenadel et al.,¹⁶ Kan et al.,¹³ Adachi et al.,¹⁴ Sander and Watson,¹⁹ Pilling and Smith,¹⁵ McAdam et al.,⁸ Kurylo et al.,⁹ Moortgat et al.,¹⁰ Wallington et al.,²⁸ and Dagaut and Kurylo²¹). In all cases methyl radicals are generated in the presence of an excess of molecular oxygen

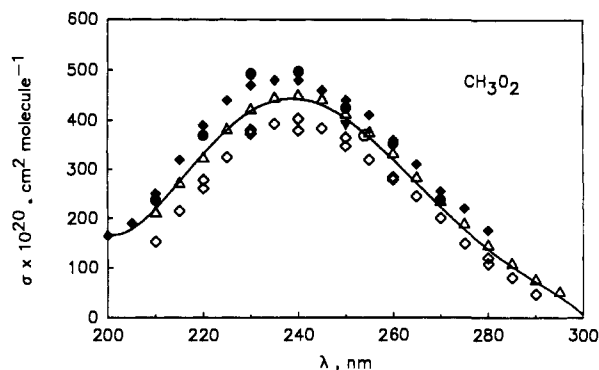
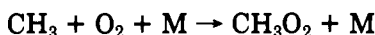
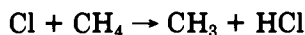
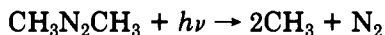


Figure 2. Absorption cross section data for CH_3O_2 reported by Cox and Tyndall¹⁷ (filled inverse triangle), Pilling and Smith¹⁵ (open circle), Jenkin et al.²⁰ (filled circles), Moortgat et al.¹⁰ (filled diamonds), Simon et al.²² (open triangles), and Dagaut and Kurylo²¹ (open diamonds). The solid line is our recommended spectrum.

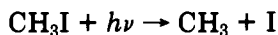
to yield CH_3O_2 radicals



The reaction of methyl radicals with O_2 is pressure dependent with a pseudo-second-order rate constant varying between 0.3 and $1.0 \times 10^{-12} \text{ cm}^3 \text{ molecule}^{-1} \text{ s}^{-1}$ over the pressure range 100–700 Torr of air.⁴⁷ In all the studies listed in Table I the molecular oxygen concentration was sufficient to assure rapid conversion of CH_3 to CH_3O_2 . With the exception of the most recent study by Jenkin and Cox⁴¹ the chemical system used to prepare CH_3 radicals in these studies was the photolysis of either azomethane or Cl_2/CH_4 mixtures.



Jenkin and Cox⁴¹ used the photolysis of CH_3I as a source of CH_3 radicals.



As seen from Table I, the data from most of the earlier studies yield significantly higher^{11,12,14} or lower^{13,16,19} cross sections than do the more recent investigations, although there is good agreement on the shape of the spectrum from all studies. Our recommended spectrum is derived from a fifth-order regression fit to the results from Pilling and Smith,¹⁵ Cox and Tyndall,^{17,18} Jenkin et al.,²⁰ Moortgat et al.,¹⁰ Dagaut and Kurylo,²¹ and Simon et al.²² These data and our recommendation are shown in Figure 2.

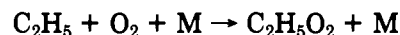
The values reported by McAdam et al.,⁸ Kurylo et al.,⁹ and Wallington et al.²⁸ were excluded from this analysis. The value reported by McAdam et al.⁹ was modified as a result of subsequent checks by these authors and is superseded by the data reported by Moortgat et al.¹⁰ The Kurylo et al.⁹ data are superseded by the work of Dagaut and Kurylo²¹ which the authors believe to be subject to less systematic error. Finally, the data reported by Wallington et al.²⁸ was essentially a repeat of the experiments of Kurylo et al.⁹ with the exception that values of $\sigma(\text{CH}_3\text{O}_2)$ were measured relative to $\sigma(\text{C}_2\text{H}_5\text{O}_2)$ and hence have an additional uncertainty associated with them.

There have been several studies of the effect of temperature and pressure on $\sigma(\text{CH}_3\text{O}_2)$. No variation of $\sigma(\text{CH}_3\text{O}_2)$ has been reported over the temperature range 240–600 K,^{19,48} although above 600 K a slight broadening of the spectrum has been observed.⁴⁹ No variation in $\sigma(\text{CH}_3\text{O}_2)$ with pressure has been reported over the range 120–760 Torr.⁴⁸

C. $\text{C}_2\text{H}_5\text{O}_2$

UV absorption cross sections have been reported by Adachi et al.,²³ Anastasi et al.,^{26,25} Munk et al.,²⁴ Cattell et al.,²⁷ and Wallington et al.²⁸ As in the case of investigations of the spectrum of methyl peroxy radicals, studies to measure the UV spectrum of ethyl peroxy radicals have employed chemical systems that generate the corresponding alkyl radical in the presence of an excess of molecular oxygen. Sources of ethyl radicals which have been used are photolysis of azoethane (Adachi et al.,²³ Anastasi et al.,^{25,26} and Cattell et al.²⁷), reaction of H atoms with ethene (Munk et al.²⁴), and photolysis of $\text{Cl}_2/\text{C}_2\text{H}_6$ mixtures (Wallington et al.²⁸).

In the presence of excess molecular oxygen, ethyl radicals are rapidly converted to ethyl peroxy radicals



This reaction is pressure dependent with a pseudo-second-order rate constant varying between 4.6 and $4.8 \times 10^{-12} \text{ cm}^3 \text{ molecule}^{-1} \text{ s}^{-1}$ over the pressure range 100–700 Torr of air.⁴⁷ Plumb and Ryan⁵⁰ have suggested that there is a pressure-independent channel of the reaction of ethyl radicals with O_2 which leads to the formation of ethene and HO_2 , and that at atmospheric pressure this channel accounts for $\approx 5\%$ of the loss of C_2H_5 . However, recent experimental and theoretical work^{51–54} have shown that, at room temperature and pressures > 50 Torr of nitrogen, the ethene yield from the reaction of ethyl radicals with O_2 is $< 1\%$. All studies of the spectra of $\text{C}_2\text{H}_5\text{O}_2$ given in Table I were obtained at total pressures > 50 Torr and thus are not subject to complications arising from the formation of ethene and HO_2 .

Three different experimental techniques have been used to measure $\sigma(\text{C}_2\text{H}_5\text{O}_2)$. These are molecular modulation spectroscopy (Anastasi et al.,^{25,26} and Cattell et al.,²⁷), flash photolysis (Adachi et al.²³ and Wallington et al.²⁸), and pulse radiolysis (Munk et al.²⁴). As seen from Table I, with the exception of the first determination of Anastasi et al.²⁶ and that of Munk et al.²⁴ (in which unusually high values of σ were obtained) all the studies are in agreement within the combined experimental errors. Thus we chose to fit a fifth-order regression to all the data, with the exception of those from refs 24 and 26, to derive our recommended spectrum. Recommended values of $\sigma(\text{C}_2\text{H}_5\text{O}_2)$ are given in Table I and are plotted as a solid line in Figure 3 along with those data used in its calculation.

D. $n\text{-C}_3\text{H}_7\text{O}_2$

The n -propyl peroxy radical UV absorption spectrum has been investigated by Adachi and Basco²⁹ using the flash photolysis technique. The absorption cross sections estimated from the spectrum published by these authors are listed in Table I and plotted in Figure 4.

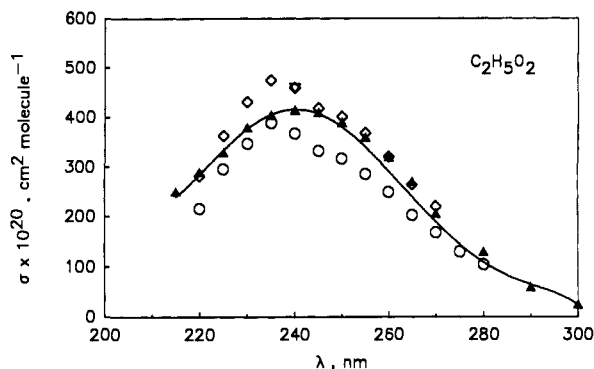


Figure 3. Absorption cross section data for $C_2H_5O_2$ reported by Adachi et al.²³ (open circles), Cattell et al.²⁷ (open diamonds), Anastasi et al.²⁵ (open inverse triangle), and Wallington et al.²⁸ (filled triangles). The solid line is our recommended spectrum.

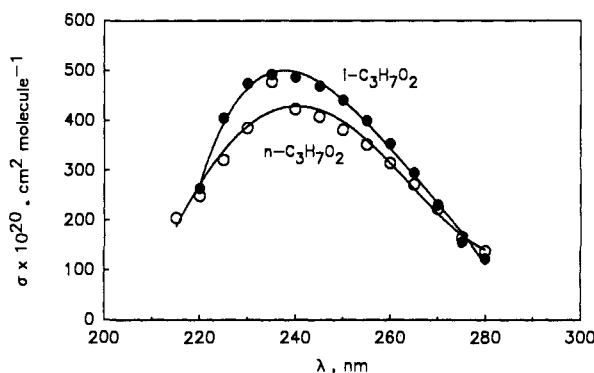
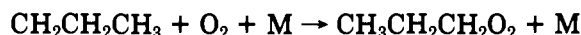
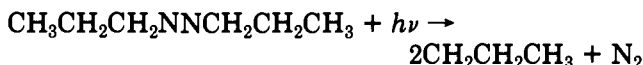


Figure 4. Absorption spectra for *n*-propyl and isopropyl peroxy reported by Adachi and Basco.²⁹

Propyl peroxy radicals were generated by photolysis of 1,1'-azo-*n*-propane in the presence of excess molecular oxygen:



The absolute calibration of the spectrum was obtained by measurements of the N_2 photolytic yield in the absence of molecular oxygen. As seen from Figure 4 the 235-nm absorption cross section is approximately 10% larger than expected on the basis of an extrapolation of the cross-section data at higher and lower wavelengths. This difference is within the experimental uncertainties. As the only published data available, we recommend the spectrum of Adachi and Basco.²⁹

E. *i*- $C_3H_7O_2$

The isopropyl peroxy radical UV absorption spectrum has been investigated by Kirsch et al.⁵⁵ using the molecular modulation spectroscopy technique and by Adachi and Basco²⁹ using flash photolysis. Good agreement was found for the shape of the UV spectrum determined in these studies. However, actual UV absorption cross sections were only reported by Adachi and Basco.²⁹ In both studies, isopropyl peroxy radicals were generated by photolysis of 2,2'-azoisopropane in presence of excess molecular oxygen:

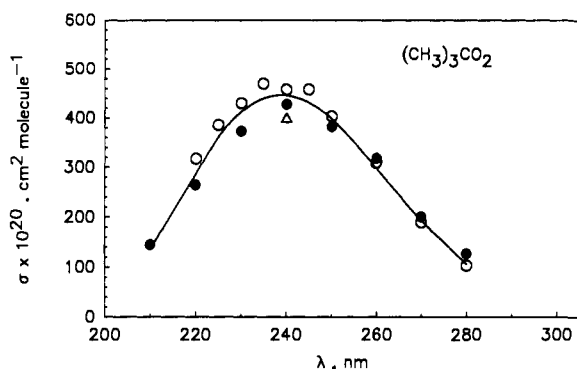
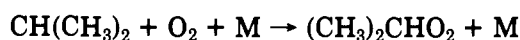
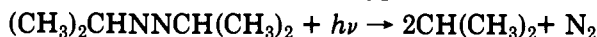
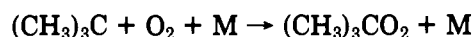
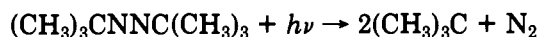


Figure 5. Absorption cross section data for $(CH_3)_3CO_2$ reported by Anastasi et al.^{32,33} (open circles), Kirsch and Parkes³¹ (triangle), and Lightfoot et al.³⁴ (filled circles). The solid line is a fifth-order fit to our recommended spectrum.

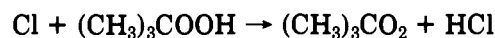
Figure 4 shows the UV absorption spectrum measured by Adachi and Basco using the same calibration procedure as for the *n*-propyl peroxy radical discussed above. As can be seen, the isopropyl peroxy radical has a slightly stronger absorption (by ~10–20%) in the wavelength range 225–260 nm than the *n*-propyl peroxy radical. Although it should be noted that within the combined experimental errors this difference is probably not significant. As the only published data available, we recommend the spectrum of Adachi and Basco.²⁹

F. *t*- $C_4H_9O_2$

The *tert*-butyl peroxy radical UV absorption spectrum has been investigated by Parkes³⁰ and Kirsch and Parkes³¹ using molecular modulation spectroscopy and by Anastasi et al.^{32,33} and Lightfoot et al.³⁴ using flash photolysis. Parkes,³⁰ Kirsch and Parkes,³¹ and Anastasi et al.^{32,33} generated peroxy radicals by photolysis of azo-*tert*-butane in the presence of excess molecular oxygen:



Lightfoot et al.³⁴ used photolysis of Cl_2 in the presence of *t*- C_4H_9OOH :



Lightfoot et al.³⁴ calibrated their *tert*-butyl peroxy spectra against that of methyl peroxy at 230–250 nm.⁵⁶ The values listed in Table I, and plotted in Figure 5, have been recalculated using the present recommendations for $\sigma(CH_3O_2)$ at 230–250 nm. Anastasi et al.^{32,33} did not report absolute cross-section values but did compare their spectrum with that of CH_3O_2 measured in the same study. At 225 nm the observed absorption for both peroxy radicals was equal: we have, therefore, used our recommended value of $\sigma(CH_3O_2) = 3.86 \times 10^{-18} \text{ cm}^2 \text{ molecule}^{-1}$ to place the *tert*-butyl peroxy radical spectrum of Anastasi et al.^{32,33} on an absolute scale.

Parkes³⁰ reported a determination of $\sigma(t-C_4H_9O_2)$ at 240 nm only. Kirsch and Parkes³¹ later reported a cross-section value twice as large at this wavelength. As seen from Figure 5 there is good agreement in the reported spectra of Kirsch and Parkes,³¹ Anastasi et al.,^{32,33} and Lightfoot et al.³⁴ Our recommendation for

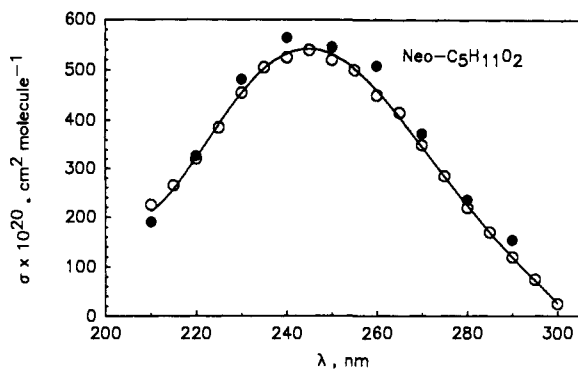
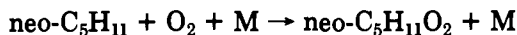


Figure 6. Absorption cross section data for $(\text{CH}_3)_3\text{CCH}_2\text{O}_2$ reported by Dagaut and Kurylo³⁵ (open symbols) and Lightfoot et al.³⁴ (filled symbols). The solid line is a fifth-order fit to both data sets and is our recommended spectrum.

the absorption spectrum of *tert*-butyl peroxy radicals is obtained from a fifth-order regression analysis to these data sets and is shown in Figure 5.

G. $(\text{CH}_3)_3\text{CCH}_2\text{O}_2$

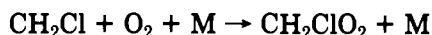
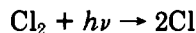
The absorption spectrum of neopentyl peroxy radicals has been measured by Dagaut and Kurylo³⁵ and Lightfoot et al.³⁴ using flash photolysis. In both studies the peroxy radicals were produced by photolysis of neo- $\text{C}_5\text{H}_{12}/\text{Cl}_2/\text{O}_2$ mixtures. In the presence of excess molecular oxygen, neopentyl radicals were rapidly converted to neopentyl peroxy radicals:



Dagaut and Kurylo³⁵ calibrated their absorption spectrum using chlorine actinometry. Lightfoot et al.³⁴ measured their neopentyl peroxy spectrum relative to that of CH_3O_2 . The values listed in Table I and plotted in Figure 6 have been recalculated using the present recommendations for $\sigma(\text{CH}_3\text{O}_2)$ at each wavelength. As seen from Figure 6, after the normalization procedure, there is good agreement between the two studies. Our recommended spectrum is a fifth-order regression fit to the results from both studies and is listed in Table I and plotted in Figure 6.

H. CH_2ClO_2

UV absorption cross sections of chloromethyl peroxy radicals have been measured by Dagaut et al.³⁷ using the flash photolysis/absorption spectroscopy technique. The peroxy radicals were generated by photolysis of $\text{Cl}_2/\text{CH}_3\text{Cl}/\text{O}_2/\text{N}_2$ mixtures with oxygen in excess:



An absolute value of the cross section of CH_2ClO_2 at 250 nm was obtained using chlorine actinometry by comparing the initial increase in absorption at 250 nm upon flashing $\text{Cl}_2/\text{CH}_3\text{Cl}/\text{O}_2/\text{N}_2$ mixtures with the loss of molecular chlorine per flash (determined by the decrease in absorption at 330 nm upon flashing $\text{Cl}_2/\text{O}_2/\text{N}_2$ mixtures). The absolute value for $\sigma(\text{CH}_2\text{ClO}_2)$ at 250 nm thus determined was used to scale the initial absorptions between 210 and 290 nm and hence derive the absorption spectrum. The spectrum is broad and featureless (see Figure 7) with an absorption maximum at

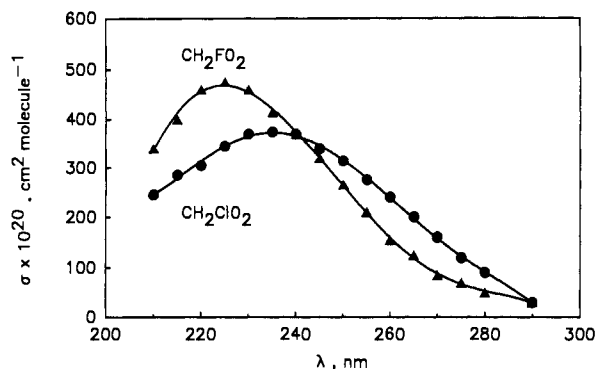
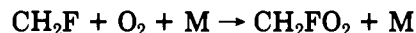


Figure 7. Absorption spectra for CH_2FO_2 and CH_2ClO_2 reported by Dagaut et al.³⁷

~ 235 nm and thus is similar to that measured for CH_3O_2 . This similarity indicates that there is little or no interaction between the Cl atom and the chromophore group in CH_2ClO_2 . We recommend the spectrum of CH_2ClO_2 reported by Dagaut et al.³⁷

I. CH_2FO_2

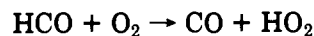
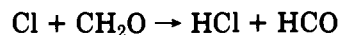
UV absorption cross sections of fluoromethyl peroxy radicals have been reported by Dagaut et al.³⁷ using the flash photolysis/absorption spectroscopy technique. The peroxy radicals were generated by photolysis of $\text{Cl}_2/\text{CH}_3\text{F}/\text{O}_2/\text{N}_2$ mixtures with oxygen in excess:



An absolute value of the cross section of CH_2FO_2 at 240 nm was obtained by chlorine actinometry using a procedure similar to that used for CH_2ClO_2 . The absolute value for $\sigma(\text{CH}_2\text{FO}_2)$ at 240 nm was then used to scale the initial absorptions between 210 and 290 nm to derive the absorption spectrum. The spectrum is broad and featureless with an absorption maximum at ~ 225 nm. As can be seen from Figure 7 the cross-section values differ significantly from those determined for $\sigma(\text{CH}_2\text{ClO}_2)$ and $\sigma(\text{CH}_3\text{O}_2)$: the absorption maximum for CH_2FO_2 is shifted by ~ 10 – 15 nm to shorter wavelength and the peak cross section is increased by 10–25%. This behavior indicates a significant interaction between the F atom and the chromophore group in CH_2FO_2 . We recommend the spectrum of CH_2FO_2 reported by Dagaut et al.³⁷

J. HOCH_2O_2

The UV absorption spectrum of hydroxymethyl peroxy radicals has been measured by Veyret et al.³⁸ using the flash photolysis/absorption spectroscopy technique and by Burrows et al.³⁹ using molecular modulation spectroscopy. The spectrum is broad and featureless with an absorption maximum at ~ 230 nm. In both studies hydroxymethyl peroxy radicals were produced by flash photolysis of chlorine in presence of oxygen and formaldehyde:



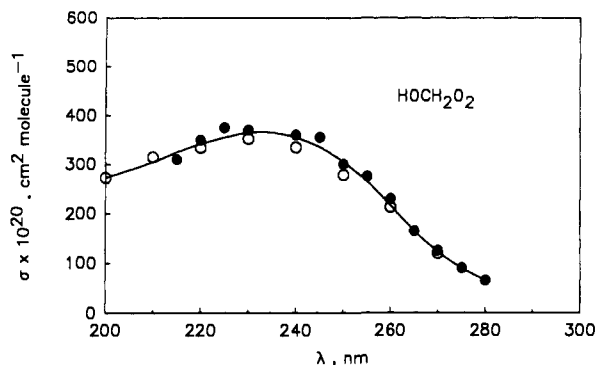


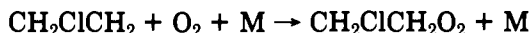
Figure 8. Absorption cross section data for HOCH_2O_2 reported by Veyret et al.³⁸ (open symbols) and Burrows et al.³⁹ (filled symbols). The solid line represents our recommended spectrum.

As seen from Figure 8, the measured cross sections reported by Veyret et al.³⁸ and Burrows et al.³⁹ are in excellent agreement. Our recommended spectrum is a fifth-order regression fit to the data from both studies and is listed in Table I and plotted in Figure 8. As for chloromethyl peroxy, the spectrum of hydroxymethyl peroxy differs only slightly from that of methyl peroxy. The slightly greater cross section at shorter wavelengths suggests that there is only a small interaction between the HO group and the chromophore in HOCH_2O_2 .

It should be noted that Veyret et al.³⁸ determined the hydroxymethyl peroxy radical UV spectrum relative to a $\sigma(\text{HO}_2)$ value at 210 nm of $4.9 \times 10^{-18} \text{ cm}^2 \text{ molecule}^{-1}$. The values tabulated for these authors in Table I and plotted in Figure 8 were rescaled using the value of $\sigma(\text{HO}_2)$ at 210 nm = $4.54 \times 10^{-18} \text{ cm}^2 \text{ molecule}^{-1}$ recommended here.

K. $\text{CH}_2\text{ClCH}_2\text{O}_2$

UV absorption cross sections of 2-chloroethyl peroxy radicals have been determined by Dagaut et al.⁴⁰ using the flash photolysis/absorption spectroscopy technique. The peroxy radicals were generated by photolysis of $\text{Cl}_2/\text{C}_2\text{H}_4/\text{O}_2/\text{N}_2$ mixtures with oxygen in excess:



This preparation isolates the formation of the 2-chloro isomer. The absolute values of the cross sections between 210 and 290 nm were obtained from chlorine actinometry absolute calibration at 250 nm. As seen from Figure 9, the spectrum is broad and featureless with a maximum of absorption at ~ 240 nm and with cross-sections values that are indistinguishable from those determined for the ethyl peroxy radical. Similar observations on the negligible effect of a single chlorine substitution were made for CH_2ClO_2 .³⁷ We recommend the spectrum of $\text{CH}_2\text{ClCH}_2\text{O}_2$ reported by Dagaut et al.⁴⁰

L. $\text{HOCH}_2\text{CH}_2\text{O}_2$

The UV absorption spectrum of $\text{HOCH}_2\text{CH}_2\text{O}_2$ radicals has been measured by Jenkin and Cox⁴¹ using the molecular modulation technique. The $\text{HOCH}_2\text{CH}_2\text{O}_2$

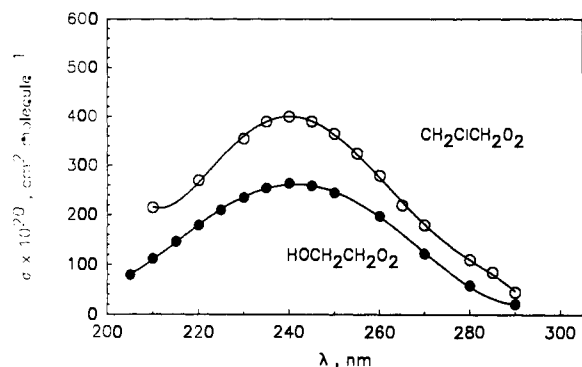


Figure 9. Absorption cross section data for $\text{CH}_2\text{ClCH}_2\text{O}_2$ and $\text{HOCH}_2\text{CH}_2\text{O}_2$ reported by Dagaut et al.⁴⁰ (open circles) and Jenkin and Cox⁴¹ (filled circles), respectively. Solid lines are fourth-order fits to these data sets.

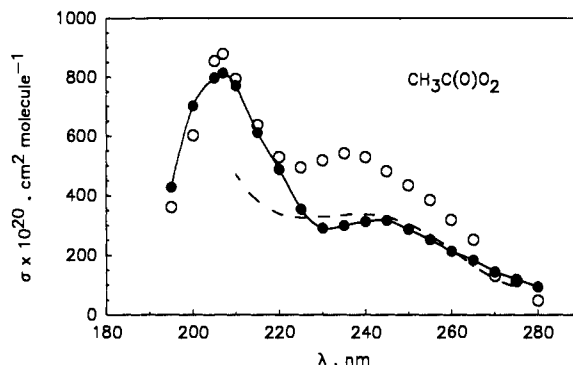
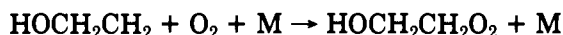
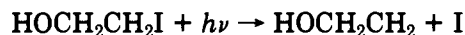


Figure 10. Absorption cross section data for acetyl peroxy radical reported by Moortgat et al.¹⁰ (filled circles and full line; cubic spline), Basco and Parmer⁵⁸ (open circles), and Addison et al.⁵⁷ (dotted line).

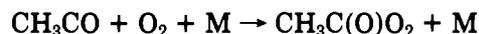
radicals were produced by the 254-nm photolysis of $\text{HOCH}_2\text{CH}_2\text{I}$:



The radical flux in these experiments was obtained by observing the first-order decay of the ethyl hydroxy iodide. This decay rate and the observed modulated absorption were then used to calculate the absolute absorption cross sections which are listed in Table I. The shape of the $\text{HOCH}_2\text{CH}_2\text{O}_2$ spectrum is identical to that for ethyl peroxy and 2-chloroethyl peroxy with the cross sections reduced by $\sim 35\%$ (see Figure 9).

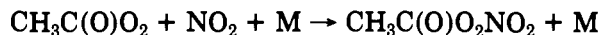
M. $\text{CH}_3\text{C}(\text{O})\text{O}_2$

UV absorption cross sections of acetyl peroxy radicals have been published by Addison et al.,⁵⁷ Basco and Parmer,⁵⁸ and Moortgat et al.¹⁰ Figure 10 shows the spectra obtained by these authors. The last two groups used the flash photolysis of $\text{Cl}_2/\text{excess O}_2/\text{CH}_3\text{CHO}$ mixtures to produce the acetyl peroxy radicals and measured the spectrum by absorption spectroscopy:



Addison et al.⁵⁷ used the molecular modulation spectroscopy technique and generated acetyl peroxy radical

through the same scheme as above but in presence of NO_2 . Acetyl peroxy radicals react rapidly with NO_2 to give peroxy acetyl nitrate (PAN):



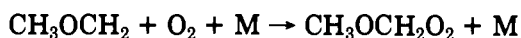
Addison et al. were able to determine $\sigma(\text{CH}_3\text{C}(\text{O})\text{O}_2)$ by subtracting the contribution due to PAN from the observed modulated absorption over the range 210–280 nm.

There is an inconsistency in the manuscript of Basco and Parmer⁵⁸ with regard to the position of the absorption maximum; in the text the maximum is repeatedly given as 207 nm but in Figure 6 of ref 58 the maximum is drawn at 211 nm. In this review we assume that the error lies in the labeling of the x axis in Figure 6 of the manuscript of Basco and Parmer and that the absorption maximum did indeed occur at 207 nm.

As can be seen from Figure 10 there are significant discrepancies between the reported spectra. Possible causes of these differences have been outlined by Moortgat et al.¹⁰ For example, the spectrum of Addison et al.⁵⁷ was calibrated at 210 nm where absorption by PAN is considerable. Correction for such absorption could have introduced significant errors into the measurements, particularly at the shorter wavelengths. The absorption spectrum reported by Basco and Parmer is similar in shape to that measured by Moortgat et al. However, the absorption at 240 nm is significantly greater. The reason for this discrepancy has not been delineated. Clearly, further work is needed to better define and quantify this spectrum. We recommend the spectrum obtained by Moortgat et al., noting that there is good agreement between the data of Addison et al. and Moortgat et al. at wavelengths greater than 230 nm. It should be noted that Moortgat et al.¹⁰ calculated their absorption cross sections relative to a $\sigma(\text{HO}_2)$ at 210 nm of $5.3 \times 10^{-18} \text{ cm}^2 \text{ molecule}^{-1}$. The values listed in Table I and plotted in Figure 10 have been recalculated using the value of $\sigma(\text{HO}_2)$ at 210 nm of $4.54 \times 10^{-18} \text{ cm}^2 \text{ molecule}^{-1}$ recommended here.

N. $\text{CH}_3\text{OCH}_2\text{O}_2$

UV absorption cross sections of methoxymethyl peroxy radicals have been reported by Dagaut et al.⁴² using the flash photolysis/absorption spectroscopy technique. The peroxy radicals were generated by photolysis of $\text{Cl}_2/\text{CH}_3\text{OCH}_3/\text{O}_2/\text{N}_2$ mixtures with oxygen in excess:



The absolute values of the cross sections between 210 and 290 nm were obtained from a chlorine actinometry absolute calibration at 240 nm. The spectrum (see Figure 11) is broad and featureless with a maximum at ~ 220 nm. As observed in the case of F substitution on CH_3O_2 , the CH_3O group shifts the absorption maximum to shorter wavelength. As the only published data available it is the basis of our recommendation.

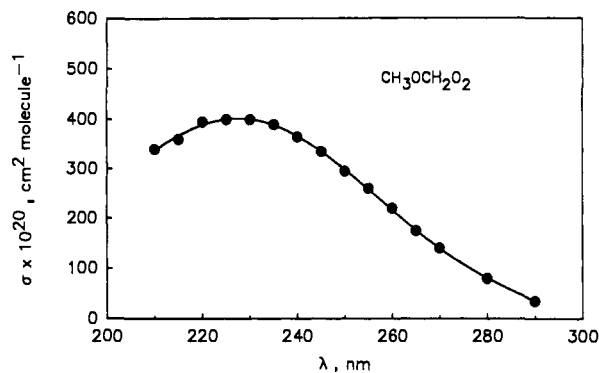


Figure 11. Absorption cross section data for $\text{CH}_3\text{OCH}_2\text{O}_2$ reported by Dagaut et al.⁴² The solid line is a fifth-order fit.

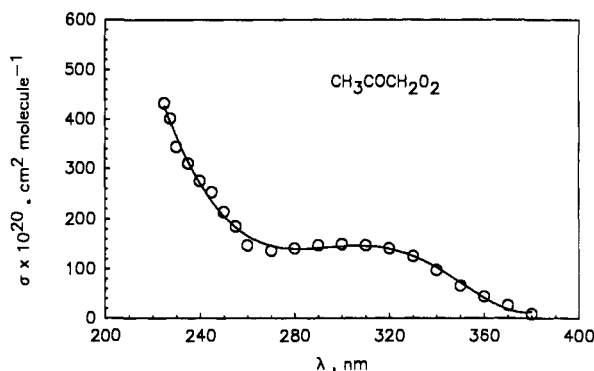
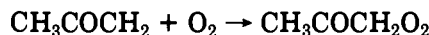
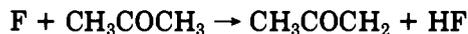
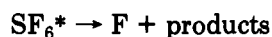


Figure 12. Absorption cross section data for $\text{CH}_3\text{COCH}_2\text{O}_2$ reported by Cox et al.³⁶ The solid line is a fifth-order fit.

O. $\text{CH}_3\text{COCH}_2\text{O}_2$

The absorption spectrum of acetyl peroxy radicals has been measured by Cox et al.³⁶ using the pulse radiolysis technique. Peroxy radicals were generated by the pulsed radiolysis of $\text{SF}_6/\text{CH}_3\text{COCH}_3/\text{O}_2$ mixtures:



The spectrum derived by Cox et al.³⁶ was calibrated by measuring the F atom yield by radiolysis of SF_6/CH_4 mixtures and quantifying the methyl radical production using a value of $\sigma(\text{CH}_3) = 4.12 \times 10^{-17} \text{ cm}^2 \text{ molecule}^{-1}$ at 216.4 nm, and is shown in Figure 12. As the only published data available it is the basis of our recommendation.

P. $\text{CF}_3\text{CCl}_2\text{O}_2$, CF_3CFHO_2 , $\text{CFCl}_2\text{CH}_2\text{O}_2$, and $\text{CF}_2\text{ClCH}_2\text{O}_2$

Absolute UV absorption spectra for this series of halogenated ethyl peroxy radicals have been reported by Jemi-Alade et al.⁴³ using the flash photolysis of mixtures of Cl_2 in synthetic air together with either $\text{CF}_3\text{CCl}_2\text{H}$, CF_3CFH_2 , CFCl_2CH_3 , or CF_2ClCH_3 . The resulting spectra are shown in Figures 13 and 14. The spectra of $\text{CFCl}_2\text{CH}_2\text{O}_2$, $\text{CF}_2\text{ClCH}_2\text{O}_2$ have the same shape as that of ethyl peroxy and are shifted to the blue by approximately 10 nm. The spectra of CF_3CFHO_2

TABLE II. Measured Branching Ratios of Peroxy Radical Reactions

k_a/k	k_b/k	k_c/k	technique ^a	substrates	temperature range	pressure	ref(s)
				$RO_2 + RO_2, R'O_2$			
				$CH_3O_2 + CH_3O_2 \rightarrow CH_3O + CH_3O + O_2$ (a)			
				$\rightarrow HCHO + CH_3OH + O_2$ (b)			
				$\rightarrow CH_3OOCH_3 + O_2$ (c)			
0.33	0.67		MMS	$(CH_3)_2N_2/O_2/i-C_4H_{10}$	298	550	59
0.49	0.51		CP/IR/GLC/MS	$(CH_3)_2N_2/O_2/DMB$	373	60–200	60
0.43	0.50	0.07	CP/MS	$(CH_3)_2N_2/O_2$	298	100	61
0.41	0.59		therm/GLC/MS	DTBP/ O_2	410	500	62
0.40	0.53	0.07	CP/FTIR	$(CH_3)_2N_2$	298	700	63
0.32	0.60	0.08	CP/FTIR	$(CH_3)_2N_2$ and $CH_4/Cl_2/O_2$	297	700	64
0.08	0.92	–	MMS/GC/chemical	$(CH_3)_2N_2/O_2$	255	760	65
0.19	0.81	–			292		
0.10	0.90	–			303		
0.24	0.76	–			313		
0.25	0.75	–			323		
0.48	0.52	–			343		
0.49	0.51	–			350		
0.42	0.58	–			365		
0.55	0.45	–			379		
0.51	0.49	–			417		
0.31	0.69		MP/UVA	$Cl_2/CH_4/O_2$	300	240	22
0.29	0.71		FP/UVA	$CH_4/Cl_2/O_2$	388	760, 210	66
0.49	0.51				423		
0.64	0.36				473		
0.79	0.21				523		
0.82	0.18				573		
0.11	0.79	0.10	CP/MIS	$CH_4/Cl_2/O_2$	223	754–765	67
0.17	0.73	0.10			253		
0.22	0.68	0.10			273		
0.28	0.62	0.10			293		
0.31	0.59	0.10			313		
0.38	0.52	0.10			333		
				$CD_3O_2 + CD_3O_2 \rightarrow$ products			
				$(CD_3)_2N_2/O_2$			
0.45	0.41	0.14	CP/MS		298	100	61, 68
				$C_2H_5O_2 + C_2H_5O_2 \rightarrow C_2H_5O + C_2H_5O + O_2$ (a)			
				$\rightarrow CH_3CHO + C_2H_5OH + O_2$ (b)			
				$\rightarrow C_2H_5OOC_2H_5 + O_2$ (c)			
0.51	0.40	0.09	CP/FTIR	Cl_2/C_2H_6 and $(C_2H_5)_2N_2$	298	700	69
0.64	0.36	–	MMS/GC	$(C_2H_5)_2N_2$	302	500	26
0.68	0.32	–			333		
0.71	0.29	–			373		
0.65	0.30	0.05	MMS/GC/chemical	$(C_2H_5)_2N_2$	250	760	25
0.70	0.28	0.02			256		
0.65	0.28	0.07			267		
0.71	0.24	0.05			298		
0.72	0.25	0.03			306		
0.67	0.25	0.08			320		
0.72	0.21	0.07			352		
0.79	0.17	0.04			380		
0.81	0.14	0.05			390		
0.86	0.11	0.03			414		
0.84	0.12	0.04			416		
0.64	0.30	0.06	CP/FTIR	$C_2H_6/Cl_2/O_2$	295	700	70
				$(CH_3)_2CHO_2 + (CH_3)_2CHO_2 \rightarrow (CH_3)_2CHO + (CH_3)_2CHO + O_2$ (a)			
				$(CH_3)_2CHO_2 + (CH_3)_2CHO_2 \rightarrow (CH_3)_2CO + (CH_3)_2CHOH + O_2$ (b)			
0.58	0.42	–	CP/GC	$(CH_3)_2CHN_2CH(CH_3)_2/O_2$	302	500	71
0.65	0.35	–	CP/GC	$(CH_3)_2CHN_2CH(CH_3)_2/O_2$	333	500	72
0.74	0.26	–			373		
				$(CH_3)_3CO_2 + (CH_3)_3CO_2 \rightarrow (CH_3)_3CO + (CH_3)_3CO + O_2$ (a)			
				$(CH_3)_3CO_2 + (CH_3)_3CO_2 \rightarrow (CH_3)_3COOC(CH_3)_3 + O_2$ (c)			
0.88	–	0.12	CP/GC	$(CH_3)_3CN_2C(CH_3)_3$	298	760	73
0.975	–	0.025			333		
				$CH_3C(O)O_2 + CH_3C(O)O_2 \rightarrow CH_3C(O)O + CH_3C(O)O + O_2$ (a)			
				$CH_3C(O)O_2 + CH_3C(O)O_2 \rightarrow$ other products (b)			
1.00	–	–	FP/UVA	CH_3CHO/Cl_2	253–368	600	10
				$2 CH_2ClO_2 \rightarrow 2 CH_2ClO + O_2$ (a)			
				$\rightarrow ClCH_2OH + HCOCl + O_2$ (b)			
>0.90	–	–	CP/FTIR	$CH_2Cl/Cl_2/O_2$	298	700	74
				$HOCH_2O_2 + HOCH_2O_2 \rightarrow HOCH_2O + HOCH_2O + O_2$ (a)			
				$HOCH_2O_2 + HOCH_2O_2 \rightarrow HCOOH + CH_2(OH)_2 + O_2$ (b)			
0.91	0.09	–	MMS/UVA/IRA	HCHO/ O_2	303	700	39

TABLE II (Continued)

k_a/k	k_b/k	k_c/k	technique ^a	substrates	temperature range	pressure	ref(s)
0.69	0.31	-	CP/FTIR	$\text{CH}_2\text{ClCH}_2\text{O}_2 + \text{CH}_2\text{ClCH}_2\text{O}_2 \rightarrow \text{CH}_2\text{ClCH}_2\text{O} + \text{CH}_2\text{ClCH}_2\text{O} + \text{O}_2$ (a)	295	700	75
				$\rightarrow \text{CH}_2\text{ClCHO} + \text{CH}_2\text{ClCH}_2\text{OH} + \text{O}_2$ (b)			
0.18	0.82	-	MMS/UVA	$\text{HOCH}_2\text{CH}_2\text{O}_2 + \text{HOCH}_2\text{CH}_2\text{O}_2 \rightarrow \text{HOCH}_2\text{CH}_2\text{O} + \text{HOCH}_2\text{CH}_2\text{O} + \text{O}_2$ (a)	298	760	41
				$\text{HOCH}_2\text{CH}_2\text{O}_2 + \text{HOCH}_2\text{CH}_2\text{O}_2 \rightarrow \text{HOCH}_2\text{CHO} + \text{HOCH}_2\text{CH}_2\text{OH} + \text{O}_2$ (b)			
0.50	0.50	-	MMS/UVA	$\text{CH}_3\text{O}_2 + (\text{CH}_3)_3\text{CO}_2 \rightarrow \text{CH}_3\text{O} + (\text{CH}_3)_3\text{CO} + \text{O}_2$ (a)	298	760	30
				$\text{CH}_3\text{O}_2 + (\text{CH}_3)_3\text{CO}_2 \rightarrow \text{HCHO} + (\text{CH}_3)_3\text{COH} + \text{O}_2$ (b)			
0.50	0.50	-	CP/GC	$(\text{CH}_3)_3\text{CN}_2\text{C}(\text{CH}_3)_3$ and $\text{CH}_3\text{N}_2\text{CH}_3/i\text{-C}_4\text{H}_{10}$	333	760	73
0.63	0.37	-	CP/GC	$(\text{CH}_3)_3\text{CN}_2\text{C}(\text{CH}_3)_3$	373	760	73
0.16	0.84	-	CP/GC	$(\text{CH}_3)_3\text{CN}_2\text{C}(\text{CH}_3)_3$	313	200	76
0.23	0.77	-			343		
0.67	0.33	-			393		
0.07	0.93		FP/UVA	$\text{CH}_3\text{O}_2 + \text{CH}_3\text{C}(\text{O})\text{O}_2 \rightarrow \text{CH}_3\text{O} + \text{CH}_3\text{COO} + \text{O}_2$ (a)	253	600	10
				$\text{CH}_3\text{O}_2 + \text{CH}_3\text{C}(\text{O})\text{O}_2 \rightarrow \text{HCHO} + \text{CH}_3\text{COOH} + \text{O}_2$ (b)			
0.50	0.50			$\text{CH}_3\text{CHO}/\text{Cl}_2$	298		
0.77	0.23				333		
0.91	0.09				368		

^a Key: MMS, molecular modulation spectroscopy; CP, continuous photolysis; IR, infrared analysis; GLC, gas and liquid chromatography; MS, mass spectroscopy; therm, thermogravimetric analysis; FTIR, Fourier transform infrared spectroscopy; chemical, wet chemical techniques; MP, modulated photolysis; UVA, ultraviolet absorption spectroscopy; FP, flash photolysis; DMB, 2,3-dimethylbutane; DTBP, di-*tert*-butyl peroxide.

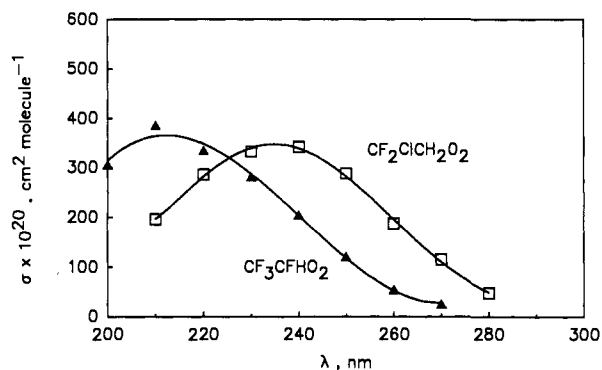


Figure 13. Absorption cross section data for CF_3CFHO_2 and $\text{CF}_2\text{ClCH}_2\text{O}_2$ reported by Jemi-Alade et al.⁴³ The solid lines are third-order fits.

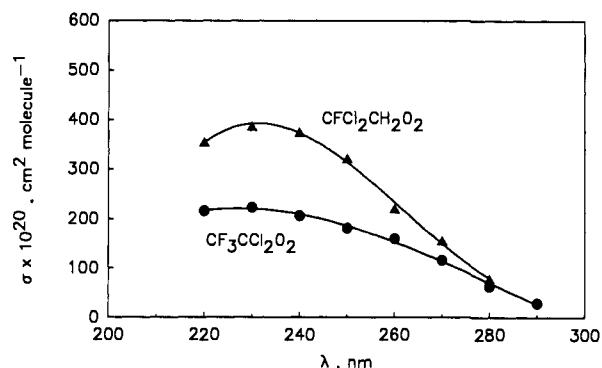


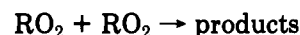
Figure 14. Absorption cross section data for $\text{CF}_3\text{CCl}_2\text{O}_2$ and $\text{CFCl}_2\text{CH}_2\text{O}_2$ reported by Jemi-Alade et al.⁴³ The solid lines are third-order fits.

and $\text{CF}_3\text{CCl}_2\text{O}_2$ differ substantially from that of ethyl peroxy. The absorption maximum of CF_3CFHO_2 is shifted by approximately 35 nm to the blue and $\text{CF}_3\text{CCl}_2\text{O}_2$ has an usually broad absorption spectrum in the region 200–300 nm with an absorption maximum of approximately $2 \times 10^{-18} \text{ cm}^2 \text{ molecule}^{-1}$ in the region

220–240 nm. This absorption maximum is a factor of 2 less than typically observed for alkyl peroxy radicals. As the only available data we recommend use of the spectra of Jemi-Alade et al.⁴³

III. Kinetics and Mechanisms of Peroxy Radical Self-Reactions and Cross Reactions

Kinetic and mechanistic data for the self-reaction and cross reaction of many different peroxy radicals have been reported. Mechanistic information has been generally deduced from the observed product distributions and is given in Table II. Kinetic information has, in all cases, been derived by monitoring the decay of peroxy radicals using their strong absorption in the UV from 200–300 nm. The actual measured parameter in the majority of the kinetic experiments is $k_{\text{obs}}/\sigma(\lambda)$ where k_{obs} is the observed second-order rate constant for the reaction



defined by

$$-d[\text{RO}_2]/dt = 2k_{\text{obs}}[\text{RO}_2]^2$$

and $\sigma(\lambda)$ is the RO_2 absorption cross section at the monitoring wavelength λ . The literature data for the kinetics of peroxy radical self-reactions and cross reactions is summarized in Table III. To maintain a consistency in the comparison between the various studies, we have used our recommended values for the absorption cross sections to place the reported values of $k_{\text{obs}}/\sigma(\lambda)$ on a common scale. Our recommendations for branching ratios and rate constants are summarized in Table IX.

A. $\text{CH}_3\text{O}_2 + \text{CH}_3\text{O}_2$

The branching ratios for the self-reaction of methyl peroxy radicals, as determined by product analysis, have

TABLE III. Kinetic Data for Peroxy Radical Self-Reactions

k_{obs}/σ^a	k_{obs}^b	λ (nm)	T (K)	pressure range (Torr)	technique ^c range	ref(s)
			$\text{CH}_3\text{O}_2 + \text{CH}_3\text{O}_2$			
0.75 ± 0.25	3.3 ± 1.1	240	298	200–800 ^d	MMS ($\text{CH}_3\text{N}_2\text{CH}_3$)	11
1.00 ± 0.18	4.4 ± 0.8	238	288–298	760	MMS ($\text{CH}_3\text{N}_2\text{CH}_3$)	12
1.31 ± 0.23	5.1 ± 0.9	248	295	760	FP ($\text{CH}_3\text{N}_2\text{CH}_3$)	16
0.8 ± 0.1	3.5 ± 0.4	240	298	300	MMS ($\text{CH}_3\text{N}_2\text{CH}_3$)	33
0.6 ± 0.2	2.7 ± 0.9		325			
2.05 ± 0.25	5.6 ± 0.7	265	296	50–695	FP ($\text{CH}_3\text{N}_2\text{CH}_3$)	13
1.33 ± 0.23	5.2 ± 0.9 ^d	210–280	298	not reported	MMS (CH_4/Cl_2)	17,18
1.08 ± 0.08	4.8 ± 0.4	240	298	570–610	FP ($\text{CH}_3\text{N}_2\text{CH}_3$)	14
1.27 ± 0.10	4.6 ± 0.4	253.7	298	80–800	FP (CH_4/Cl_2)	77
1.06 ± 0.07	4.5 ± 0.3	245	298	50–500	FP (CH_4/Cl_2)	78
2.84 ± 0.36	6.8 ± 0.9	270	298	350		
1.31 ± 0.23	5.1 ± 0.9	250	248	60–700	FP (CH_4/Cl_2)	19
1.40 ± 0.32	5.5 ± 1.3		270			
1.22 ± 0.18	4.8 ± 0.7		298			
1.18 ± 0.12	4.6 ± 0.5		329			
1.02 ± 0.16	4.0 ± 0.6		373			
0.95 ± 0.12	3.7 ± 0.5		417			
1.34 ± 0.23	5.3 ± 0.9	250	298	120–400	FP (CH_4/Cl_2)	8
1.35 ± 0.16	5.3 ± 0.6	250	228	100	FP (CH_4/Cl_2)	79
1.28 ± 0.20	5.0 ± 0.8		248	100		
1.16 ± 0.14	4.5 ± 0.5		273	100		
1.10 ± 0.14	4.3 ± 0.5		298	50–400		
1.21 ± 0.09	4.7 ± 0.4		340	100		
1.00 ± 0.12	3.9 ± 0.5		380	100		
1.11 ± 0.12	4.4 ± 0.5 ^e	210–270	298	760	MMS (CH_4/Cl_2)	20
1.27	5.6	240	255	550	MMS ($\text{CH}_3\text{N}_2\text{CH}_3$)	65
1.25	5.5		292			
1.02	4.5		303			
0.89	3.9		313			
1.39	6.1		323			
0.96	4.2		343			
0.89	3.9		350			
0.98	4.3		365			
1.00	4.4		379			
0.83	3.7		417			
1.27 ± 0.25	5.0 ± 1.0	250	248	210–760	FP (CH_4/Cl_2)	66
1.16 ± 0.15	4.5 ± 0.6		273			
1.17 ± 0.36	4.6 ± 1.4		298			
0.97 ± 0.13	3.8 ± 0.5		368			
1.04 ± 0.10	4.1 ± 0.4		373			
0.91 ± 0.08	3.6 ± 0.3		388			
0.91 ± 0.09	3.6 ± 0.4		423			
0.95 ± 0.04	3.7 ± 0.2		473			
0.90 ± 0.07	3.5 ± 0.3		523			
0.98 ± 0.06	3.8 ± 0.2		573			
1.16 ± 0.12	4.5 ± 0.5	250	300	240	MMS (CH_4/Cl_2)	22
1.07	4.6	230	268	11	MMS (CH_3I)	41
1.23	5.3		268	760		
1.13	4.9		273	760		
1.11	4.8		278	11		
1.05	4.5		283	760		
1.07	4.6		288	11		
1.22	5.2		293	760		
1.01 ± 0.09	4.3 ± 0.3		298	11–760		
1.01	4.3		303	760		
1.01	4.3		313	11		
1.00	4.3		318	760		
0.98	4.2		333	11		
0.95	4.1		343	760		
1.04	4.5		350	11		
1.02	4.4		350	760		
k_{obs}/σ^f	k_{obs}^g	λ (nm)	T (K)	pressure range (Torr)	technique	ref
			$\text{C}_2\text{H}_5\text{O}_2 + \text{C}_2\text{H}_5\text{O}_2$			
2.99 ± 0.23	12.4 ± 1.0 ^h	230–250	298	660–720	FP	23
1.53 ± 0.21	6.3 ± 0.9	240	303	420–710	MMS ($\text{C}_2\text{H}_5\text{N}_2\text{C}_2\text{H}_5$)	26
1.70 ± 0.18	7.1 ± 0.7		333			
1.91 ± 0.29	7.9 ± 1.3		373			
2.20 ± 0.31	9.1 ± 1.3		423			
2.34 ± 0.32	9.7 ± 1.3		457			
1.01 ± 0.05	4.2 ± 0.2	240	298	760	PR	24
4.06	12.0	260	268	28–740	MMS ($\text{C}_2\text{H}_6/\text{Cl}_2$)	27
3.79	11.2		279			
3.97	11.8		292			

TABLE III (Continued)

k_{obs}/σ^f	k_{obs}^g	λ (nm)	T (K)	pressure range (Torr)	technique	ref
4.23	12.5		308.5			
3.97	11.8		323.5			
4.13	12.2		347.5			
3.59	10.6	260	267	20	MMS ($\text{C}_2\text{H}_5\text{N}_2\text{C}_2\text{H}_5$)	27
3.83	11.3		275			
3.47	10.3		278			
4.23	12.5		287.5			
3.69	10.9		295			
3.61	10.7		298			
3.10	9.2		308			
2.90	8.6		313.5			
3.40	10.1		320.5			
1.48	6.1	240	254	not reported	MMS ($\text{C}_2\text{H}_5\text{N}_2\text{C}_2\text{H}_5$)	25
1.73	7.2		261			
1.75	7.3		265			
2.11	8.8		300			
2.31	9.6		325			
2.11	8.8		357			
2.54	10.5		361			
3.03	12.6		417			
2.34 ± 0.13	8.9 ± 0.5	250	228	25-400	FP ($\text{C}_2\text{H}_6/\text{Cl}_2$)	28
2.30 ± 0.15	8.7 ± 0.6		248			
2.39 ± 0.16	9.1 ± 0.6		273			
2.54 ± 0.19	9.6 ± 0.7		298			
2.74 ± 0.19	10.4 ± 0.7		340			
2.72 ± 0.19	10.3 ± 0.7		380			

k_{obs}/σ^i	k_{obs}^j	λ (nm)	T (K)	pressure range (Torr)	technique	ref
$1.21 \pm 0.10 \times 10^5$	0.38 ± 0.03	$n\text{-C}_3\text{H}_7\text{O}_2 + n\text{-C}_3\text{H}_7\text{O}_2$ 260	298	14-370	FP ($(\text{C}_3\text{H}_7\text{N})_2$)	29
not given	0.0013 ± 0.0001	$i\text{-C}_3\text{H}_7\text{O}_2 + i\text{-C}_3\text{H}_7\text{O}_2$ 265	300	760	MMS ($(i\text{-C}_3\text{H}_7\text{N})_2$)	55
	0.0018 ± 0.0002		313			
	0.0027 ± 0.0002		333			
	0.0042 ± 0.0005		353			
	0.0059 ± 0.0003		373			
420 ± 120	0.0020 ± 0.0006	240	298	733,740	FP ($(i\text{-C}_3\text{H}_7\text{N})_2$)	29
6.54 ± 1.45	$(2.9 \pm 0.6) \times 10^{-5}$	$t\text{-C}_4\text{H}_9\text{O}_2 + t\text{-C}_4\text{H}_9\text{O}_2$ 240	298	440,700	MMS ($(\text{C}(\text{CH}_3)_3\text{N})_2$)	30
4.0 ± 0.8	$(1.8 \pm 0.4) \times 10^{-5}$	240	298	260	FP ($(\text{C}(\text{CH}_3)_3\text{N})_2$)	32
6.4 ± 1.9	$(2.9 \pm 0.8) \times 10^{-5}$	240	298	310	FP ($(\text{C}(\text{CH}_3)_3\text{N})_2$)	33
22.0 ± 6.6	$(9.8 \pm 2.9) \times 10^{-5}$		325			
5.0	2.2×10^{-5}	240	293	50-760	FP ($\text{C}(\text{CH}_3)_4/\text{Cl}_2$)	34
123.0	5.5×10^{-4}		373	760		
362.0	1.6×10^{-3}		418	760		

k_a^k	k_b (s^{-1}) ^k	k_c (s^{-1}) ^k	λ (nm)	T (K)	pressure range (Torr)	technique	ref
1.57 ± 0.31	10.0 ± 2.0	2.0 ± 0.4	$\text{neo-C}_5\text{H}_{11}\text{O}_2 + \text{neo-C}_5\text{H}_{11}\text{O}_2$ 250	228	100	FP	35
0.84 ± 0.18	10.5 ± 2.1	2.2 ± 0.5		248		($\text{Cl}_2/\text{neo-C}_5\text{H}_{11}/\text{O}_2$)	
0.63 ± 0.13	13.0 ± 2.6	2.5 ± 0.5		273			
0.36 ± 0.07	15.0 ± 3.0	2.8 ± 0.6		298	25-100		
0.23 ± 0.04	18.0 ± 3.6	3.2 ± 0.6		340	100		
0.16 ± 0.03	20.0 ± 4.0	3.4 ± 0.7		380			

k_{obs}/σ^l	k_{obs}^m	λ (nm)	T (K)	pressure range (Torr)	technique	ref
na	4.58 ± 0.46	240	248	760	FP	34
	2.11 ± 0.32	220-280	273	760	($\text{Cl}_2/\text{neo-C}_5\text{H}_{11}/\text{O}_2$)	
	1.46 ± 0.21	210-270	288	50-760		
	1.04 ± 0.09	240	298	760		
	0.76 ± 0.06	240	333	760		
	0.56 ± 0.10	210-270	373	760		
2.25 ± 0.42	7.06 ± 1.31	250	$\text{CH}_2\text{ClO}_2 + \text{CH}_2\text{ClO}_2$ 228	100	FP ($\text{CH}_3\text{Cl}/\text{Cl}_2$)	37
1.97 ± 0.21	6.19 ± 0.65		248			
1.50 ± 0.19	4.72 ± 0.59		273			
1.20 ± 0.14	3.78 ± 0.45		298	25-400		
0.86 ± 0.06	2.71 ± 0.18		340	100		
0.63 ± 0.07	1.97 ± 0.23		380			

TABLE III (Continued)

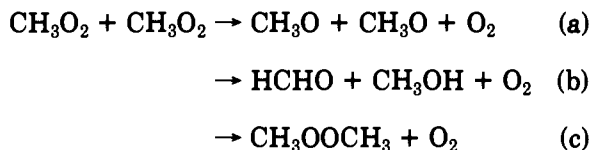
k_{obs}/σ^l	k_{obs}^m	λ (nm)	T (K)	pressure range (Torr)	technique	ref
1.88 ± 0.24	6.95 ± 0.88	240	$\text{CH}_2\text{FO}_2 + \text{CH}_2\text{FO}_2$		FP ($\text{CH}_3\text{F}/\text{Cl}_2$)	37
1.61 ± 0.29	5.97 ± 1.08		228	100		
1.19 ± 0.20	4.39 ± 0.74		248			
0.83 ± 0.18	3.07 ± 0.65		273			
0.74 ± 0.16	2.72 ± 0.58		298	25-400		
0.57 ± 0.21	2.10 ± 0.78		340	100		
			380			
		$\text{HOCH}_2\text{O}_2 + \text{HOCH}_2\text{O}_2 \rightarrow 2 \text{HOCH}_2\text{O} + \text{O}_2$ (a)				
		$\rightarrow \text{HCOOH} + \text{HOCH}_2\text{OH} + \text{O}_2$ (b)				
na	(k_a) 5.5 ± 1.1	250,1110.2 cm^{-1}	298-303	2-10	MMS (HCHO/Cl_2)	39
na	(k_b) 0.56 ± 0.28	250,1110.2 cm^{-1}	298-303	2-10	MMS (HCHO/Cl_2)	39
na	0.90 ± 0.20	250	275	85-170	FP (HCHO/Cl_2)	38
na	0.70 ± 0.21		295			
na	0.60 ± 0.20		323			
		$\text{CH}_2\text{ClCH}_2\text{O}_2 + \text{CH}_2\text{ClCH}_2\text{O}_2$				
2.23 ± 1.00	8.13 ± 2.23	250	228	100	FP ($\text{C}_2\text{H}_4/\text{Cl}_2$)	40
1.75 ± 0.26	6.40 ± 0.94		248			
1.38 ± 0.18	5.03 ± 0.65		273			
0.99 ± 0.16	3.60 ± 0.60		298	25-400		
0.59 ± 0.09	2.16 ± 0.32		340	100		
0.37 ± 0.08	1.35 ± 0.30		380			
0.68 ± 0.07	1.60 ± 0.17	230	$\text{HOCH}_2\text{CH}_2\text{O}_2 + \text{HOCH}_2\text{CH}_2\text{O}_2$		MMS ($\text{ICH}_2\text{CH}_2\text{OH}$)	41
			298	760		
		$\text{CH}_3\text{COO}_2 + \text{CH}_3\text{COO}_2$				
na	6.5 ± 3.0	210,240	302	28,715	MMS ($\text{CH}_3\text{CHO}/\text{Cl}_2$)	57
na	8.0 ± 1.3	198-208	298	153	FP ($\text{CH}_3\text{CHO}/\text{Cl}_2$)	58
na	23 ± 3	207	253	600	FP ($\text{CH}_3\text{CHO}/\text{Cl}_2$)	10
na	16 ± 3		298			
na	12 ± 2		368			
		$\text{CH}_3\text{OCH}_2\text{O}_2 + \text{CH}_3\text{OCH}_2\text{O}_2$				
	3.48 ± 0.58	240	228	25	FP ($\text{CH}_3\text{OCH}_3/\text{Cl}_2$)	42
	5.38 ± 0.36		50			
	5.60 ± 0.60		100			
	6.28 ± 0.69			200		
	2.17 ± 0.28			248		
	3.60 ± 0.58			25		
	4.16 ± 0.43			50		
	4.03 ± 0.62			100		
	4.52 ± 1.01			200		
	4.15 ± 0.36			400		
	1.36 ± 0.17			600		
	1.75 ± 0.28		273	25		
	2.57 ± 0.15			50		
	2.60 ± 0.21			100		
	2.85 ± 0.24			200		
	2.85 ± 0.24			400		
	3.01 ± 0.22			600		
	3.31 ± 0.26			800		
	0.69 ± 0.06		298	25		
	1.08 ± 0.08			50		
	1.54 ± 0.15			100		
	1.65 ± 0.14			200		
	2.03 ± 0.20			400		
	2.32 ± 0.18			600		
	2.36 ± 0.15			800		
	0.36 ± 0.07		340	25		
	0.41 ± 0.07			50		
	0.54 ± 0.07			100		
	0.64 ± 0.11			200		
	0.96 ± 0.26			400		
	1.06 ± 0.24			600		
	0.25 ± 0.06		380	25		
	0.23 ± 0.04			50		
	0.27 ± 0.05		100			
	0.33 ± 0.05		200			
	0.49 ± 0.17		400			
	0.60 ± 0.19		600			
	0.72 ± 0.14		800			

TABLE III (Continued)

k_{obs}/σ^f	k_{obs}^m	λ (nm)	T (K)	pressure range (Torr)	technique	ref
5.61 ± 1.08	8.3 ± 1.6	310	298	1000(SF ₆)	PR (SF ₆ /CH ₃ COCH ₃)	36
					CH ₃ COCH ₂ O ₂ + CH ₃ COCH ₂ O ₂	
na	15 ± 5	220,250 and IR	298	700	MMS (CH ₃ CHO/O ₂)	80, 96
na	1.3 ± 4.7	210,225	253	600	FP (CH ₃ CHO/Cl ₂)	10
na	5.5 ± 3		298			
na	6.8 ± 2		333			
na	13.3 ± 3		368			
					CH ₃ COO ₂ + CH ₃ O ₂ → CH ₃ COOH + HCHO + O ₂ —channel b	
na	16.3 ± 2	210,225	253	600	FP (CH ₃ CHO/Cl ₂)	10
na	5.5 ± 2		298			
na	2 ± 1.5		333			
na	1.3 ± 1.3		368			
					<i>t</i> -C ₄ H ₉ O ₂ + CH ₃ O ₂	
na	0.10 ± 0.05	240	298	760	MMS ((CH ₃ N) ₂ / <i>i</i> -C ₄ H ₁₀)	30

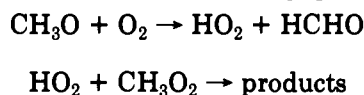
^a Units of 10⁶ cm s⁻¹. ^b Units of 10⁻¹³ cm³ molecule⁻¹ s⁻¹. ^c Key: MMS, molecular modulation spectroscopy; FP, flash photolysis; PR, pulse radiolysis. ^d Pressure range unclear, estimated from data given in tables and figure captions. ^e 250 nm. ^f Units of 10⁴ cm s⁻¹. ^g Units of 10⁻¹⁴ cm³ molecule⁻¹ s⁻¹. ^h Value of σ at 240 nm used to place this value on comparative basis. ⁱ Units of cm s⁻¹. ^j Units of 10⁻¹² cm³ molecule⁻¹ s⁻¹. ^k See text in section III.F for definition of k_a , k_b , and k_c . ^l Units of 10⁶ cm s⁻¹. ^m Units of 10⁻¹² cm³ molecule⁻¹ s⁻¹.

been reported by Parkes,⁵⁹ Alcock and Mile,⁶⁰ Weaver et al.,⁶¹ Selby et al.,⁶² Kan et al.,⁶³ Niki et al.,⁶⁴ Anastasi et al.,⁶⁵ Simon et al.,²² Lightfoot et al.,⁶⁶ and Horie et al.⁶⁷ Observed products are HO₂ radicals, HCHO, CH₃OH, and in certain instances CH₃OOCH₃. With the exception of the study of Lightfoot et al.,⁶⁶ the relative importance of channels a–c have been deduced from the ratio of the observed concentrations of the products HCHO, CH₃OH and CH₃OOCH₃.

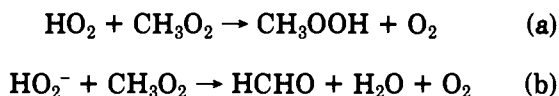


Lightfoot et al.⁶⁶ used measurements of the formation of HO₂ to establish the importance of channel a relative to the overall reaction.

There is a complication with both mechanistic and kinetic studies of the self-reaction of methyl peroxy radicals since reaction channel a yields CH₃O radicals which react rapidly with molecular oxygen to generate HO₂ which in turn reacts with CH₃O₂ radicals:



To relate observed product yields to the relative importance of channels a–c, information on the products of the reaction of CH₃O₂ with HO₂ is needed to make any necessary corrections. Jenkin et al.,²⁰ on the basis of experiments conducted at 11 Torr total pressure, have suggested that reaction of CH₃O₂ with HO₂ proceeds via two channels:



with $k_b/k = 0.4$. This result is supported by the measurements of Moortgat et al.⁸⁰ of the rate of CH₃OOH production during photolysis of acetaldehyde in 700 Torr of air. In their study, Moortgat et al.⁸⁰ found the

rate of CH₃OOH production to be approximately 30% less than the rate of loss of CH₃O₂ and HO₂ radicals implying the existence of a reaction channel other than that producing the hydroperoxide. However, recent work by Wallington and Japar⁸⁶ has shown that 92 ± 6% of the reaction of CH₃O₂ with HO₂ proceeds to yield the hydroperoxide. These authors monitored the production of CH₃OOH and the loss of CH₄ during photolysis of F₂ in the presence of CH₄ and H₂ in 700 Torr of air. There may be an effect of pressure on the branching ratio of the reaction of CH₃O₂ with HO₂ which would explain the apparent discrepancy between the results of Jenkin et al.²⁰ and Wallington and Japar.⁸⁶ However, such an effect cannot be invoked to explain the discrepancy between the results of Moortgat et al.⁸⁰ and Wallington and Japar.⁸⁶ The chemical system and subsequent data analysis of Wallington and Japar⁸⁶ appears to be less complex than those of Jenkin et al.²⁰ and Moortgat et al.⁸⁰ For this reason and the fact that the experiments of Wallington and Japar⁸⁶ were conducted in 700 Torr of air we assume for atmospheric applications that reaction of CH₃O₂ with HO₂ proceeds exclusively by one channel leading to CH₃OOH. Values of the branching ratios given in Table II have been calculated accordingly.

The branching ratios for the methyl peroxy self-reaction channels a–c determined at ambient temperature (298 ± 2 K) by Parkes,³⁰ Weaver et al.,⁶¹ Kan et al.,⁶³ Niki et al.,⁶⁴ and Simon et al.²² are all in agreement, within the experimental errors. Values of k_a/k range from 0.28 to 0.43, and upper limits of k_c/k from 0.07 to 0.10. This agreement is particularly impressive in view of the wide variety of experimental techniques and chemical systems used as given in Table II. The branching ratio k_a/k reported by Anastasi et al.⁶⁵ at 292 K is significantly lower than reported by all other workers for reasons that are unclear at the present time.

At temperatures greater than ambient there is considerable scatter in the literature data as shown in Figure 15. For example, the branching ratio k_a/k determined by Alcock and Mile⁶⁰ at 373 K is a factor of 2 larger than that reported by Lightfoot et al.⁶⁶ Also,

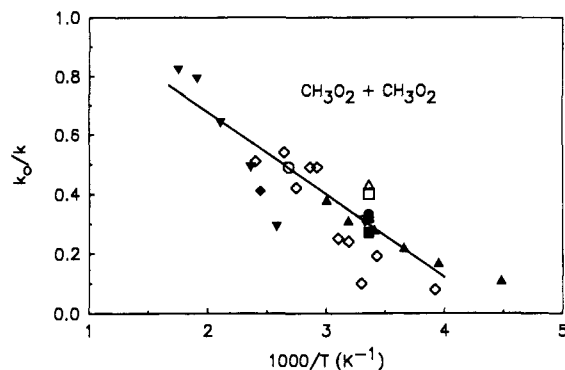


Figure 15. Plot of branching ratio k_a/k for self-reaction of methyl peroxy radicals as a function of temperature. Data is taken from Alcock and Mile⁶⁰ (open circle), Parkes⁵⁹ (filled circle), Weaver et al.⁶¹ (open triangle), Selby and Waddington⁶² (filled diamond), Kan et al.⁶³ (open square), Niki et al.⁶⁴ (filled squares), Anastasi et al.⁶⁵ (open diamonds), Simon et al.²² (open inverse triangle), Lightfoot et al.⁶⁶ (filled inverse triangles), and Horie et al.⁶⁷ (filled triangles). The solid line is our recommendation; see text.

while the data of Selby et al.,⁶² Anastasi et al.,⁶⁵ and Lightfoot et al.⁶⁶ are all in good agreement at 390–420 K, the 292 K branching ratio determined by Anastasi et al.⁶⁵ is (as mentioned above) approximately 50% lower than the average of five other studies (Parkes,² Weaver et al.,⁶¹ Kan et al.,⁶³ Niki et al.,⁶⁴ and Simon et al.²²). Further work is required to resolve these discrepancies. At 298 K we recommend using the average of the results of Parkes,²¹ Weaver et al.,⁶¹ Kan et al.,⁶³ Niki et al.,⁶⁴ Simon et al.,²² and Horie et al.⁶⁷ $k_a/k = 0.35$. As noted above, there have been some reports of the existence of a minor channel leading to the formation of CH_3OOCH_3 with a yield of approximately 7%. Thus, we recommend that for the purposes of modeling the oxidation of methane at 298 K, $k_a/k = 0.35$, $k_b/k = 0.58$, and $k_c/k = 0.07$.

From Figure 15 we see that, with the possible exception of the 388 K data point of Lightfoot et al.⁶⁶ and the 303 K data point of Anastasi et al.,⁶⁵ there are no data points which are anomalously high or low. We have chosen to conduct a linear least-squares analysis of all the data in the temperature range 250–600 K except these two points to yield our recommendation of

$$k_a/k = 1.24 - 280/T$$

with estimated uncertainties of $\pm 25\%$. We have restricted this analysis to temperatures above 250 K because of the sparsity of data below this temperature. Further work is necessary to refine the temperature dependence of this branching ratio, particularly at low temperatures relevant to the atmosphere, 220–280 K.

An alternate way to express the relative importance of the different reaction channels of the self reaction of CH_3O_2 radicals is to calculate the nonterminating to terminating branching ratio, $k_a/(k_b + k_c)$. We will define this parameter as β following the lead of Lightfoot et al.⁶⁶ Figure 16 shows a plot of $\ln(\beta)$ versus $1/T$ derived from the data listed in Table II. An unweighted linear least-squares fit to this data, (388 K, 303 K, and 223 K data points excluded) yields the expression

$$\ln(\beta) = (3.62 - 1350)/T$$

and is recommended over the temperature range 250–600 K. Again, no recommendation is made below

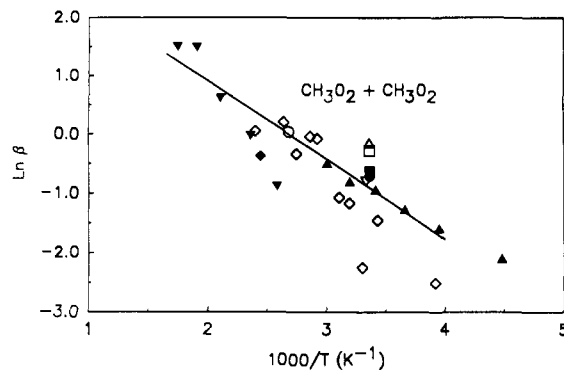


Figure 16. Plot of $\ln(k_a/k_b)$ for self-reaction of methyl peroxy radicals as a function of temperature. Data is taken from Alcock and Mile⁶⁰ (open circle), Parkes⁵⁹ (filled circle), Weaver et al.⁶¹ (open square and open triangle (CD_3O_2)), Selby and Waddington⁶² (filled diamond), Kan et al.⁶³ (open square), Niki et al.⁶⁴ (filled squares), Anastasi et al.⁶⁵ (open diamonds), Simon et al.²² (open inverse triangle), Lightfoot et al.⁶⁶ (filled inverse triangle), and Horie et al.⁶⁷ (filled triangles). The solid line is our recommendation; see text.

250 K because of the sparsity of data in this temperature region.

Finally, Alcock and Mile,⁶⁰ Weaver et al.,⁶¹ and Lightfoot et al.⁶⁶ have shown that (over the approximate temperature range 300–600 K) the branching ratios are invariant with total pressure between 100 and 760 Torr.

The kinetics of the self-reaction of methyl peroxy radicals



is the most widely studied aspect of peroxy reactions (Parkes et al.,¹¹ Parkes,¹² Hochenadel et al.,¹⁶ Anastasi et al.,^{33,65} Kan et al.,¹³ Cox and Tyndall,^{17,18} Adachi et al.,¹⁴ Sanhueza et al.,⁷⁷ Sander and Watson,^{78,19} McAdam et al.,⁸ Kurylo and Wallington,⁷⁹ Jenkin et al.,²⁰ Lightfoot et al.,⁶⁶ Simon et al.,²² and Jenkin and Cox⁴¹). All these studies used UV absorption over the range 200–300 nm to monitor the decay of CH_3O_2 radicals and determine $k_{\text{obs}}/\sigma(\lambda)$ as discussed above.

Values of k_{obs} were then obtained using appropriate values of $\sigma(\lambda)$. As stated earlier, to facilitate comparison between the various studies, we have placed the $k_{\text{obs}}/\sigma(\lambda)$ literature values on a common scale by using our recommended values of $\sigma(\text{CH}_3\text{O}_2)$ given in Table I. Values of k_{obs} so obtained are listed in Table III.

From Table III it can be seen that, with the possible exception of the results obtained at 270 nm by Sander and Watson,⁷⁸ there is good agreement in the values of k_{obs} derived from all studies near ambient temperature. The average value at 298 ± 6 K (excluding the 270 nm data of Sander and Watson⁷⁸) is $k_{\text{obs}} = 4.6 \times 10^{-13} \text{ cm}^3 \text{ molecule}^{-1} \text{ s}^{-1}$. No effect of pressure on k_{obs} over the range 80–800 Torr has been reported.

Studies of the temperature dependence of k_{obs} have been performed by Anastasi et al.,^{33,65} Sander and Watson,¹⁹ Kurylo and Wallington,⁷⁹ Lightfoot et al.,⁶⁶ and Jenkin and Cox.⁴¹ In all studies, except that of Jenkin and Cox,⁴¹ the effect of temperature on k_{obs} has been measured at one total pressure. Jenkin and Cox measured the temperature dependence of k_{obs} at two total pressures; 11 and 760 Torr. Analysis of the data at the two total pressures resulted in Arrhenius expressions which, at the 1σ level, were distinct. This observation led Jenkin and Cox to speculate that dif-

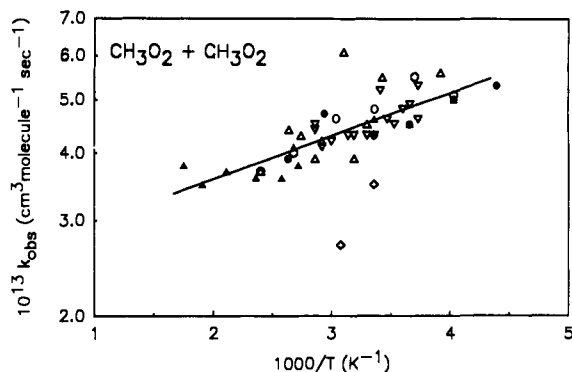


Figure 17. Arrhenius plot for k_{obs} for methyl peroxy self-reaction. Data is taken from Sander and Watson¹⁹ (open circles), Kurylo and Wallington⁷⁹ (filled circles), Anastasi et al.⁶⁵ (open triangles), Anastasi et al.³³ (open diamonds), Lightfoot et al.⁶⁶ (filled triangles), and Jenkin and Cox⁴¹ (open inverse triangles). Solid line is our recommendation.

ferent Arrhenius expressions are appropriate for the two pressures. In the present review, unless stated otherwise, all errors quoted represent 95% confidence limits, i.e. $\pm 2\sigma$. At the 2σ level the expressions derived by Jenkin and Cox are indistinguishable. At the present time we see no reason to distinguish between experiments performed at 10 Torr or 760 Torr. Accordingly, results from Anastasi et al.,^{33,65} Sander and Watson,¹⁹ Kurylo and Wallington,⁷⁹ Lightfoot et al.,⁶⁶ and Jenkin and Cox⁴¹ at all pressures are shown in the Arrhenius plot in Figure 17.

From Figure 17 it can be seen that, with the exception of the first study by Anastasi et al.,³³ and the 323 K data point from the most recent study of Anastasi et al.,⁶⁵ the results from all studies are in broad agreement. An unweighted linear least-squares analysis of the data of Sander and Watson,¹⁹ Kurylo and Wallington,⁷⁹ Anastasi et al.⁶⁵ (323 K data point excepted), Lightfoot et al.,⁶⁶ and Jenkin and Cox⁴¹ yields

$$k_{\text{obs}} = [(2.5 \pm 0.3) \times 10^{-13}] \exp(180 \pm 40/T) \text{ cm}^3 \text{ molecule}^{-1} \text{ s}^{-1}$$

which is recommended over the temperature range 230–600 K. Quoted errors represent 2σ from the least-squares analysis. This expression is plotted as a solid line in Figure 17. As discussed above, no effect of total pressure on k_{obs} has been discerned over the range 10–760 Torr. Additionally, several groups have demonstrated that k_{obs} is unaffected by the addition of up to 12.8 Torr of water vapor (Kan and Calvert,⁸¹ Sanhueza et al.,⁷⁷ Kurylo et al.,⁹³ and Lightfoot et al.⁶⁶).

It should be noted that the values of k_{obs} from all studies of the self-reaction of CH_3O_2 radicals are overestimates of the "true value" of the bimolecular rate constant. This is due to production of CH_3O radicals via channel a, which react with O_2 (necessarily present in all studies to convert CH_3 radicals to CH_3O_2), generating HO_2 radicals. The secondary reaction of the HO_2 radicals with CH_3O_2 results in k_{obs} being larger than the true bimolecular rate constant, k_1 . Assuming that each HO_2 radical generated in the system rapidly removes an additional CH_3O_2 radical, k_{obs} is related to k_1 by $k_{\text{obs}} = k_1[1 + k_a/(k_a + k_b + k_c)]$. At 298 K the recommended value for the branching ratio k_a/k (where $k = k_a + k_b + k_c$) = 0.35, thus $k_1 = 0.74k_{\text{obs}} = 3.4 \times 10^{-13} \text{ cm}^3 \text{ molecule}^{-1} \text{ s}^{-1}$. Using the recommended expression for the temperature dependence of k_a/k , together with

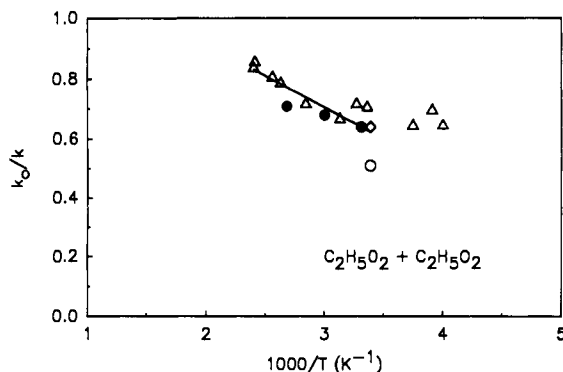


Figure 18. Plot of branching ratio k_a/k for self-reaction of ethyl peroxy radicals as a function of temperature. Data is taken from Niki et al.⁶⁹ (open circle), Anastasi et al.²⁶ (filled circles), Anastasi et al.²⁶ (open triangles), and Wallington et al.⁷⁰ (open diamond). The solid line is our recommendation; see text.

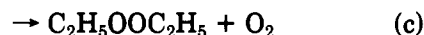
the fitted temperature dependence of k_{obs} , we derive the following Arrhenius expression

$$k = (9.2 \times 10^{-14}) \exp(390/T) \text{ cm}^3 \text{ molecule}^{-1} \text{ s}^{-1}$$

valid over the temperature range 250–600 K with estimated uncertainties of $\pm 25\%$.

B. $\text{C}_2\text{H}_5\text{O}_2 + \text{C}_2\text{H}_5\text{O}_2$

The branching ratio of the self-reaction of ethyl peroxy radicals has been studied by Niki et al.,⁶⁹ Anastasi et al.,^{25,26} and Wallington et al.⁷⁰ Anastasi et al.^{25,26} used the photolysis of azoethane in the presence of oxygen at 500 and 760 Torr total pressure in a molecular modulation spectrometer interfaced to a gas chromatograph with flame ionization detection, for the quantification of products. Wallington et al.⁷⁰ employed the photolysis of molecular chlorine in the presence of ethane at 700 Torr total pressure of air with FTIR quantification of both reactant loss and product formation. Niki et al.⁶⁹ used the photolysis of both azoethane and chlorine/ethane mixtures in 700 Torr of air with FTIR detection of product yields. In these studies, the observed product ratio $[\text{CH}_3\text{CHO}]/[\text{C}_2\text{H}_5\text{OH}]$ can be used to derive the importance of channels a and b.



As in the methyl peroxy self-reaction studies, the HO_2 radicals formed in these studies will react with $\text{C}_2\text{H}_5\text{O}_2$ radicals



Thus, an additional product observed in studies of the self-reaction of $\text{C}_2\text{H}_5\text{O}_2$ is $\text{C}_2\text{H}_5\text{OOH}$.

The fraction of the self-reaction proceeding through channel a is plotted as a function of temperature in Figure 18, from which it can be seen that all studies are in good agreement, although the room temperature result from Niki et al.⁶⁹ is somewhat lower than the others. At 298 K we recommend use of the average of the branching ratios reported by Niki et al.,⁶⁹ Anastasi et al.,^{25,26} and Wallington et al.,⁷⁰ $k_a/k = 0.63$. Finally,

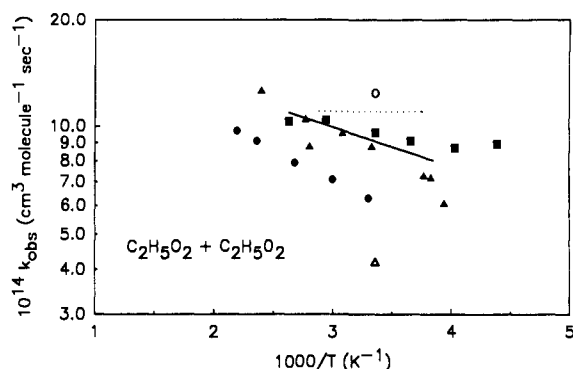


Figure 19. Arrhenius plot for k_{obs} for ethyl peroxy self-reaction. Data is taken from Adachi et al.²³ (open circle), Anastasi et al.²⁶ (filled circles), Munk et al.²⁴ (open triangle), Cattell et al.²⁷ (dotted line (see text)), Anastasi et al.²⁵ (filled triangles), and Wallington et al.²⁸ (filled squares). Solid line is our recommendation.

there is some experimental evidence for the formation of $\text{C}_2\text{H}_5\text{OOC}_2\text{H}_5$ as a minor product of the self-reaction of $\text{C}_2\text{H}_5\text{O}_2$ radicals. For purposes of modeling the oxidation of ethane in the atmosphere and in combustion systems, we recommend $k_c/k = 0.05$ independent of temperature²⁵ over the range 250–416 K. Linear least-squares analysis of the data in Figure 18 (250–267 K data of Anastasi et al.²⁵ excepted) yields $k_a/k = 1.33 - 209/T$. We chose to exclude the lower temperature data reported by Anastasi et al. as it appears to be inconsistent with the observed data trend at higher temperatures and requires additional confirmation.

The kinetics of the self-reaction of ethyl peroxy radicals has been studied by Adachi et al.,²³ Anastasi et al.,^{25,26} Munk et al.,²⁴ Cattell et al.,²⁷ and Wallington et al.²⁸ As before, the measured parameter in all these studies is $k_{\text{obs}}/\sigma(\lambda)$. The values of k_{obs} listed in Table III have been calculated using our recommended values of $\sigma(\text{C}_2\text{H}_5\text{O}_2)$ and are shown in an Arrhenius plot in Figure 19. Within the experimental errors, there was no observable effect of temperature over the range 267–347.5 K reported by Cattell et al.²⁷ For clarity, the average value of $k = 1.10 \times 10^{-13} \text{ cm}^3 \text{ molecule}^{-1} \text{ s}^{-1}$ reported by these workers is shown by the dotted line in Figure 19. As can be seen there is considerable scatter in the values of k_{obs} from the various studies. With the exception of the data points at the two extremes of temperature, there is agreement between the two most recent studies (Anastasi et al.²⁵ and Wallington et al.²⁸). Both these studies report values of k_{obs} which are significantly larger than that measured by Munk et al.²⁴ and reported in the first study of Anastasi et al.²⁶ The origin of this discrepancy is unclear. On the other hand, the room temperature data reported by Adachi et al.²³ and Cattell et al.²⁷ are both somewhat higher, than those of the latest work of Anastasi et al.²⁵ and Wallington et al.²⁸

An unweighted linear least-squares analysis of the data from Anastasi et al.²⁵ and Wallington et al.²⁸ between 260 and 380 K yields our recommendation of $k_{\text{obs}} = [(2.1 \pm 1.0) \times 10^{-13}] \exp[(-250 \pm 130)/T] \text{ cm}^3 \text{ molecule}^{-1} \text{ s}^{-1}$

Quoted errors represent 2σ . At 298 K this expression yields

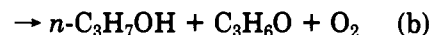
$$k_{298} = 9.1 \times 10^{-14} \text{ cm}^3 \text{ molecule}^{-1} \text{ s}^{-1}$$

with an estimated uncertainty of $\pm 25\%$.

As in the case of the CH_3O_2 self-reaction, the values of k_{obs} for the self-reaction of $\text{C}_2\text{H}_5\text{O}_2$ radicals are overestimates of the true bimolecular rate constant. This overestimation is caused by the production of $\text{C}_2\text{H}_5\text{O}$ radicals via channel a, which react with O_2 to produce HO_2 radicals. These HO_2 radicals react rapidly with $\text{C}_2\text{H}_5\text{O}_2$ causing k_{obs} to be larger than the true bimolecular rate constant that would be measured in the absence of such secondary reactions. Assuming that each HO_2 radical generated in the system rapidly removes an additional $\text{C}_2\text{H}_5\text{O}_2$ radical, the observed rate constant, k_{obs} , is related to the true rate constant, k , by $k_{\text{obs}} = k[1 + k_a/(k_a + k_b + k_c)]$. At 298 K our recommended value for the branching ratio k_a/k (where $k = k_a + k_b + k_c$) = 0.63. Thus $k = k_{\text{obs}}/1.63 = 5.6 \times 10^{-14} \text{ cm}^3 \text{ molecule}^{-1} \text{ s}^{-1}$. Using the recommended expression for the temperature dependence of k_a/k combined with the recommended temperature dependence of k_{obs} we derive the following Arrhenius expression; $k = (8.5 \times 10^{-14}) \exp(-125/T) \text{ cm}^3 \text{ molecule}^{-1} \text{ s}^{-1}$. This expression is valid over the range 260–380 K, we estimate the uncertainties of rate constants derived from this expression to be $\pm 35\%$.

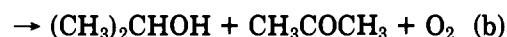
C. $n\text{-C}_3\text{H}_7\text{O}_2 + n\text{-C}_3\text{H}_7\text{O}_2$

No information is available about the branching ratio of this reaction. However, the kinetics of the self-reaction system were investigated by Adachi and Basco²⁹ using the flash photolysis and absorption spectroscopy technique at 298 K and pressures between 14 and 370 Torr. The results of this study are presented in Table III. No pressure dependence was reported. It should be noted that the rate constant reported in Table III has not been corrected for secondary removal of $n\text{-C}_3\text{H}_7\text{O}_2$ by reaction with HO_2 , as discussed above. In the absence of product data it is not possible to precisely correct for this effect. The correction factor is dependent on the branching ratio k_a/k and will lie in the range 1–2 as k_a/k varies from 0 to 1, hence, k will lie in the range $(1.75\text{--}4.1) \times 10^{-13} \text{ cm}^3 \text{ molecule}^{-1} \text{ s}^{-1}$. Our recommended value is then $k = (2.9 \pm 1.2) \times 10^{-13} \text{ cm}^3 \text{ molecule}^{-1} \text{ s}^{-1}$ for the rate constant at 298 K of the overall self-reaction:



D. $i\text{-C}_3\text{H}_7\text{O}_2 + i\text{-C}_3\text{H}_7\text{O}_2$

The branching ratio for the isopropyl peroxy radical self-reaction has been investigated by Kirsch et al.⁷¹ and Cowley et al.⁷² using continuous photolysis and gas chromatographic analysis (see Table II). These authors established that this reaction proceeds through two routes:



At 302 K Kirsch et al.⁷¹ report acetone, isopropyl alcohol, and isopropyl hydroperoxide as the main products following the self-reaction of isopropyl peroxy radicals. From their product data these workers derive values for the branching ratios $k_a/k = 0.58$ and $k_b/k =$

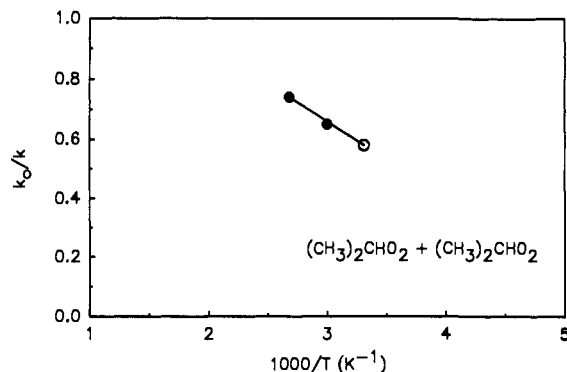


Figure 20. Plot of branching ratio k_a/k for self-reaction of isopropyl peroxy radicals as a function of temperature. Data is taken from Kirsch et al.⁷¹ (open circle) and Cowley et al.⁷² (filled circles). The solid line is our recommendation.

0.42. In a subsequent paper from the same research group, Cowley et al.⁷² report results of a product study at higher temperatures (333 and 373 K). In addition to the products observed at 302 K, Cowley et al.⁷² observed acetaldehyde, formaldehyde, and methanol. Branching ratios, k_a/k , reported by Cowley et al.⁷² and Kirsch et al.⁷¹ are compared in Figure 20. From this figure it can be seen that, over the limited temperature range for which data exist, there is a linear relationship between k_a/k and $1/T$ (K). Linear least squares analysis of the data in Figure 20 gives

$$k_a/k = 1.42 - 255/T$$

which is our recommendation over the temperatures range 302–373 K.

There have been two studies of the kinetics of this reaction. Kirsch et al.⁵⁵ used the molecular modulation technique over the temperature range 300–373 K, and Adachi and Basco²⁹ used the flash photolysis method to conduct an investigation at 298 K. The results of both studies are presented in Table III. At ambient temperature the value for k_{obs} reported by Adachi and Basco²⁹ is approximately 50% larger than that measured by Kirsch et al.⁵⁵ The origin of this discrepancy is unknown. It should be noted that in ref 29 it is stated that there is agreement between the two studies. However, this claim is based upon an inappropriate comparison of the k_{obs} value from the earlier study with a value of k corrected for reaction with HO_2 in the later study. The Arrhenius expression for k_{obs} derived by Kirsch et al.⁵⁵ is recommended over the temperature range 300–373 K:

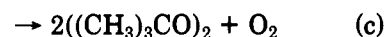
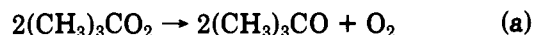
$$k_{\text{obs}} = [(2.3 \pm 0.2) \times 10^{-12}] \exp[-(2240 \pm 60)/T] \text{ cm}^3 \text{ molecule}^{-1} \text{ s}^{-1}$$

Kirsch and co-workers used their branching ratio data to correct k_{obs} for secondary loss of isopropyl peroxy radicals by reaction with HO_2 to yield the following values of k_a and k_b at 302 K: $k_a = (5.0 \pm 0.4) \times 10^{-16}$ and $k_b = (3.6 \pm 0.2) \times 10^{-16} \text{ cm}^3 \text{ molecule}^{-1} \text{ s}^{-1}$. Cowley et al.⁷² likewise derived the following Arrhenius expressions for k_a and k_b over the temperature range 300–373: $k_a = [(2.3 \pm 0.4) \times 10^{-12}] \exp[-(2560 \pm 180)/T]$ and $k_b = [(4.1 \pm 0.5) \times 10^{-14}] \exp[-(1440 \pm 120)/T] \text{ cm}^3 \text{ molecule}^{-1} \text{ s}^{-1}$ which we recommend.

E. *t*-C₄H₉O₂ + *t*-C₄H₉O₂

Product studies of the self-reaction of *tert*-butyl peroxy radicals have been carried out by Thomas and

Calvert,⁸² Kirsch and Parkes,⁷³ and Osbourne and Waddington.⁷⁶ All three studies used the photolysis of azobutane, $(\text{CH}_3)_3\text{CN}(\text{CH}_3)_3$, in the presence of oxygen as a source of *tert*-butyl peroxy radicals with product analysis performed using either GC^{73,76} or IR⁸² techniques. All studies observe acetone, *tert*-butyl alcohol, and *tert*-butyl hydroperoxide as major products and methanol as a minor product at 298 K. Additionally, formaldehyde is reported in significant yield by Thomas and Calvert⁸² and Osbourne and Waddington⁷⁶ but was not analyzed for by Kirsch and Parkes.⁷³ There is disagreement with regard to the formation of *tert*-butyl peroxide as a product. Thomas and Calvert⁸² in their experiments at 740 Torr at 298 K and Osbourne and Waddington⁷⁶ in experiments at 200 Torr and 313–393 K did not observe any peroxide formation and hence conclude that reaction proceeds via one channel, namely a:



In contrast, Kirsch and Parkes⁷³ report the observation of *tert*-butyl peroxide in experiments at 298 and 333 K at a pressure of 760 Torr. In this study,⁷³ the authors found k_c/k_a to be 0.14 and 0.025 at 298 and 333 K, respectively (to be compared to a value of 0.10 was previously reported by these workers at 298 K³¹). No evidence of reaction c was found at 373 K. The reasons for the discrepancies between the results of Thomas and Calvert⁸² and Osbourne and Waddington,⁷⁶ with those of Kirsch and Parkes,⁷³ concerning the importance of route c at 298 K, are not clear but may be related to experimental difficulties associated with detection of trace amounts of the peroxide in complex gas mixtures. Further work is needed to assess the exact mechanism of *tert*-butyl peroxy radicals self-reaction.

The kinetics of *tert*-butyl peroxy radicals self-reaction was measured by a number of workers: Parkes³⁰ using molecular modulation spectroscopy at room temperature, Anastasi et al.³² at room temperature, Anastasi et al.³³ at 298 and 325 K using the flash photolysis technique, and Lightfoot et al.³⁴ using flash photolysis over the range 293–423 K. Within the quoted experimental uncertainties there is good agreement between the values of $k_{\text{obs}}/\sigma(\lambda)$ reported in these studies. Values of k_{obs} given in Table III have been placed on a consistent basis using $\sigma(240) = 4.46 \times 10^{-18} \text{ cm}^2 \text{ molecule}^{-1}$. Results from the first study by Anastasi et al.³² are superseded by the second more extensive study by these workers³³ and hence are not considered further. The available literature data are shown in the Arrhenius plot in Figure 21. Linear-least-squares analysis of the data in Figure 21 yields our recommendation for the observed second-order rate constant for the self-reaction of *tert*-butyl peroxy radicals of

$$k_{\text{obs}} = (4.1 \times 10^{-11}) \exp(-4200/T) \text{ cm}^3 \text{ molecule}^{-1} \text{ s}^{-1}$$

As discussed above for other peroxy radical self-reactions, the measured second-order rate constant for the disappearance of *tert*-butyl peroxy radicals is frequently an overestimate of the true second-order rate constant due to secondary reactions. In the *tert*-butyl peroxy system these complications are particularly severe. The

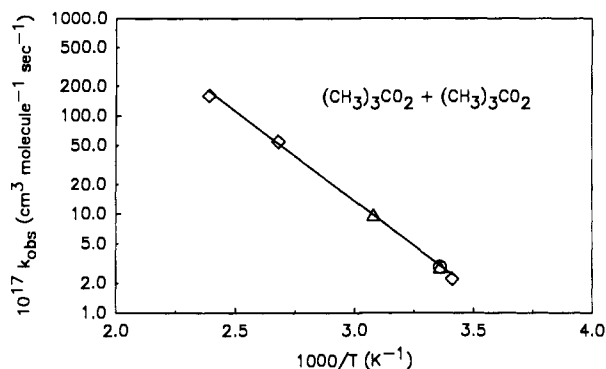
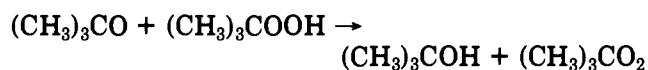
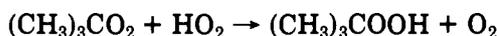
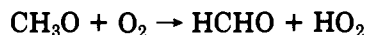
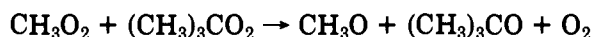
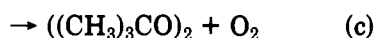
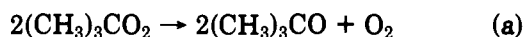


Figure 21. Plot of k_{obs} for the self-reaction of *tert*-butyl peroxy radicals: Parkes³⁰ (circle), Anastasi et al.³³ (triangles), and Lightfoot et al.³⁴ (diamonds). The solid line is a least-squares fit to the data.

majority of the self-reaction produces *tert*-butoxy radicals which decompose with at a rate of 650 s^{-1} at 298 K and 760 Torr³³ to give methyl radicals and acetone. The methyl radicals are rapidly converted to methyl peroxy radicals which in turn can react with *tert*-butyl peroxy radicals to produce more *tert*-butoxy radicals thereby starting a chain loss mechanism for *tert*-butyl peroxy. Important reactions following the self-reaction of *tert*-butyl peroxy radicals are given below:

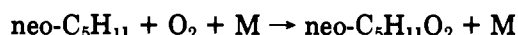
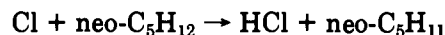
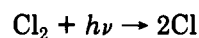


Unlike the other peroxy radicals previously discussed, it is not possible to apply a simple correction factor to account for these reactions. Instead the results from the kinetic studies need to be modeled using a mechanism which incorporates the above reactions. This approach has been used previously by Parkes³⁰ and by Lightfoot et al.³⁴ These workers calculate that k_{obs} is approximately a factor of 4 and approximately 40% larger, respectively, than the true second-order rate constant at ambient temperature in their systems. The large difference in assessment of the effect of secondary reaction arises as a result of differences in the chemical mechanisms used by these investigators. The chemical mechanism used by Lightfoot et al.³⁴ is more complete than that of Parkes, hence we prefer the expression derived by Lightfoot et al.³⁴ (placed on a consistent basis with $\sigma(240) = 4.46 \times 10^{-18} \text{ cm}^2 \text{ molecule}^{-1}$) to provide our recommended value for the true bimolecular rate constant of $k = (9.5 \times 10^{-12}) \exp(-3894/T) \text{ cm}^3 \text{ molecule}^{-1} \text{ s}^{-1}$.

F. neo-C₅H₁₂O₂ + neo-C₅H₁₂O₂

The kinetics of neopentyl peroxy radicals self-reaction has been investigated by Dagaut and Kurylo³⁵ and

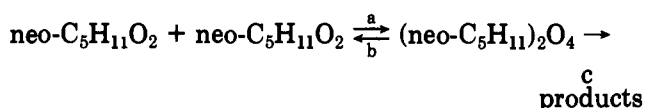
Lightfoot et al.³⁴ Both studies used flash photolysis/UV absorption spectroscopy. The photolysis of chlorine in presence of neopentane and oxygen in excess was used for radical generation:



The kinetics of the self-reaction was followed by monitoring the peroxy radicals by absorption in the UV.



Both studies observed distinctly non-second-order decay of absorption following the flash. Dagaut and Kurylo attributed this behavior to equilibration of neopentyl peroxy radicals with a dimer which could also decompose to products:



Kinetic modeling of the recorded transient absorption was used to assign Arrhenius parameters to each of these steps in the temperature range 228–380 K:

$$k_a = [(5.3 \pm 2.1) \times 10^{-15}] \exp[(1285 \pm 120)/T] \text{ cm}^3 \text{ molecule}^{-1} \text{ s}^{-1}$$

$$k_b = (61 \pm 11) \exp[-(423 \pm 52)/T] \text{ s}^{-1}$$

$$k_c = (7.9 \pm 0.6) \exp[-(315 \pm 22)/T] \text{ s}^{-1}$$

In contrast, Lightfoot et al. interpreted their kinetic data in terms of decomposition of neopentyl peroxy radicals, formed by the self-reaction of neopentyl peroxy radicals, into *tert*-butyl radicals and HCHO. Lightfoot et al. derived an overall rate constant for the self reaction of neopentyl peroxy radicals of

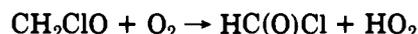
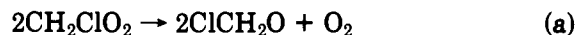
$$k = (3.02 \times 10^{-19}) (T/298)^{9.46} \exp(4260/T) \text{ cm}^3 \text{ molecule}^{-1} \text{ s}^{-1}$$

In view of the different mechanisms used by these two groups to interpret their results no recommendation is made here.

Clearly, a product study is needed to assess the mechanism of this self-reaction.

G. CH₂ClO₂ + CH₂ClO₂

End product analyses of the self-reaction of chloromethyl peroxy radicals has been carried out by Sanhueza and Hecklen³⁴ and by Niki et al.⁷⁴ The results of both studies are in agreement and indicate that the reaction proceeds essentially through channel a and is followed by formation of HO₂ and its reaction with a chloromethyl peroxy radical:



Niki et al.⁷⁴ report the HC(O)Cl product yield to be at least 90% with the remaining 10% removed presumably through reaction with HO₂ radicals to form an unidentified species with IR features and kinetics consistent with CH₂ClOOH.

The kinetics of the overall reaction was investigated by Dagaut et al.³⁷ using the flash photolysis/absorption spectroscopy technique over the temperature range 228–380 K at pressures of 25, 100, and 400 Torr. The results from this study are presented in Table III. The reaction is pressure independent and exhibits a negative activation energy. It should be noted that the rate constants for this reaction have not been corrected for secondary removal of CH₂ClO₂ by HO₂. The correction needed is probably smaller than that required for the self-reaction of CH₃O₂ and C₂H₅O₂ radicals as in the product investigation of Niki et al.⁷⁴ the observed hydroperoxide yield was low (<10%). This low hydroperoxide yield may reflect the fact that the rate constant of the chloromethyl peroxy radical self-reaction is faster than those measured for methyl and ethyl peroxy self-reactions and that the reaction of HO₂ with CH₂ClO₂ might be much smaller than the corresponding reaction with CH₃O₂. However, an alternative explanation for the low hydroperoxide yield is that there is an additional channel for the reaction of CH₂ClO₂ radicals with HO₂, namely:



If such a channel is of importance then the correction could be large. A study of the reaction of CH₂ClO₂ radicals with HO₂ is needed to resolve this uncertainty. At the present time we recommended the uncorrected Arrhenius expression of Dagaut et al.³⁷

$$k_{\text{obs}} = [(3.1 \pm 1.1) \times 10^{-13}] \exp[(735 \pm 95)/T] \text{ cm}^3 \text{ molecule}^{-1} \text{ s}^{-1}$$

H. CH₂FO₂ + CH₂FO₂

No information is available concerning the branching ratio for this reaction. However, as with CH₂ClO₂, the kinetics of the overall reaction was investigated by Dagaut et al.³⁷ using the flash photolysis/absorption spectroscopy technique over the temperature range 228–380 K at total pressures of 25, 100, and 400 Torr. The results from this study are presented in Table III. The reaction is pressure independent and exhibits a negative activation energy. As in the case of the CH₂ClO₂ self-reaction, no corrections to the rate constants were made to account for secondary removal of CH₂FO₂ by HO₂. A study of the reaction of CH₂FO₂ with HO₂ is needed before such corrections can be calculated. It is interesting to note that the kinetics of chloro- and fluoromethyl peroxy are indistinguishable in the temperature range covered by the study of Dagaut et al.³⁷ The Arrhenius expression of Dagaut et al.³⁷ is

$$k_{\text{obs}} = [(3.3 \pm 1.2) \times 10^{-13}] \exp[(700 \pm 100)/T] \text{ cm}^3 \text{ molecule}^{-1} \text{ s}^{-1}$$

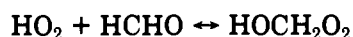
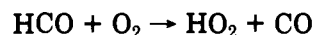
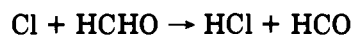
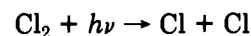
I. HOCH₂O₂ + HOCH₂O₂

The branching ratio of this reaction has been investigated at 298 K by Burrows et al.³⁹ who used a tunable infrared diode laser spectrometer to measure the

quantum yield of formic acid following photolysis of Cl₂/HCHO/O₂ mixtures at a total pressure of 2–10 Torr. Their results are reported in Table II for the reaction channels:



The kinetics of the self-reaction have been studied by Burrows et al.³⁹ using the molecular modulation technique at 298 K and by Veyret et al.³⁸ using flash photolysis at temperatures between 275 and 323 K. Both groups used the photolysis of Cl₂/HCHO/O₂ mixtures to generate HOCH₂O₂ radicals:



In the flash photolysis study of Veyret et al.³⁸ the decay of HOCH₂O₂ radicals was monitored via UV absorption at 250 nm. Self-reaction channel a yields HOCH₂O radicals which rapidly react with O₂ to generate HO₂ radicals, these in turn rapidly react with HCHO (present in large excess in the study of Veyret et al.³⁸) to regenerate HOCH₂O₂ radicals. Thus, Veyret et al.³⁸ measured the kinetics of self-reaction channel b only.

In the study of Burrows et al.³⁹ UV absorption was used to monitor the kinetic behavior of HOCH₂O₂ radicals, and IR spectroscopy was used to measure the yield of HCOOH. Such measurements allowed Burrows et al.³⁹ to determine the rate constants of both channels *k_a* and *k_b* at 298 K.

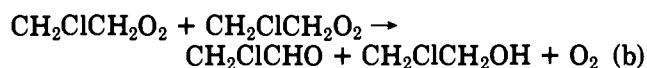
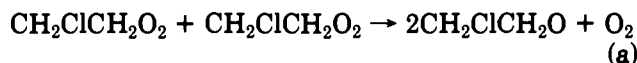
The results of both studies are reported in Table III from which it can be seen that both studies are in agreement with regard to the value of *k_b* at 298 K. The following Arrhenius expression of Veyret et al.³⁸ is recommended for *k_b* over the temperature range 275–320 K:

$$r_b = (5.65 \times 10^{-14}) \exp[(750 \pm 400)/T] \text{ cm}^3 \text{ molecule}^{-1} \text{ s}^{-1}$$

At 298 K we recommend use of the value of *k_a* = 5.5 × 10⁻¹² cm³ molecule⁻¹ s⁻¹ reported by Burrows et al.; no recommendation is made for *k_a* at other temperatures. Further work on the kinetics of this reaction would be useful.

J. CH₂CICH₂O₂ + CH₂CICH₂O₂

The branching ratio for this reaction has been investigated at 298 K and 700 Torr by Wallington et al.⁷⁵ using Fourier transform infrared spectroscopy to identify and quantify the products formed in the photolysis of C₂H₄/Cl₂ mixtures in 700 Torr of air at 295 K. From the observed rate of production of CH₂CICH₂OH and CH₂CICH₂CHO branching ratios for the reaction channels of *k_a*/(*k_a* + *k_b*) = 0.69 and *k_b*/(*k_a* + *k_b*) = 0.31 were established:



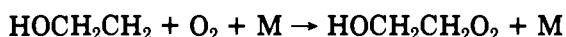
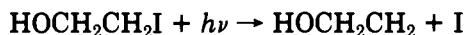
The kinetics of the self-reaction has been measured by Dagaut et al.⁴⁰ using flash photolysis/UV absorption over the temperature range 228–380 K at pressures ranging from 25 to 400 Torr. Their results, listed in Table III, exhibit no pressure dependence. The Arrhenius expression determined by Dagaut et al.⁴⁰ is

$$k_{\text{obs}} = [(1.1 \pm 0.7) \times 10^{-13}] \exp[(1020 \pm 170)/T] \text{ cm}^3 \text{ molecule}^{-1} \text{ s}^{-1}$$

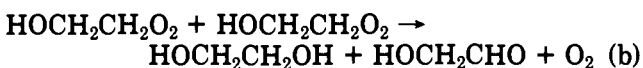
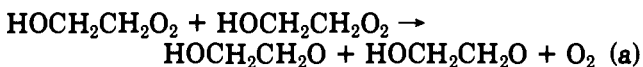
These authors did not correct the kinetic data for possible secondary removal of $\text{CH}_2\text{ClCH}_2\text{O}_2$ by HO_2 . Using the branching ratio measured by Wallington et al.⁷⁵ at 298 K this effect can be corrected for to yield $k = k_{\text{obs}}/1.69 = 2.1 \times 10^{-12} \text{ cm}^3 \text{ molecule}^{-1} \text{ s}^{-1}$ at 298 K.

K. $\text{HOCH}_2\text{CH}_2\text{O}_2 + \text{HOCH}_2\text{CH}_2\text{O}_2$

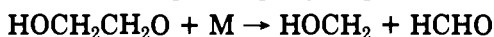
The kinetics and mechanism of the self-reaction of $\text{HOCH}_2\text{CH}_2\text{O}_2$ radicals has been investigated recently by Jenkin and Cox⁴¹ using the molecular modulation technique coupled with UV absorption spectroscopy. In this study $\text{HOCH}_2\text{CH}_2\text{O}_2$ radicals were generated using the photolysis of $\text{HOCH}_2\text{CH}_2\text{I}$ in the presence of O_2 :



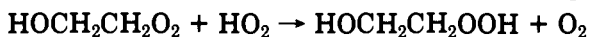
From the change in absorption at 230 nm following modulated photolysis an observed second-order rate constant $k_{\text{obs}} = (1.60 \pm 0.17) \times 10^{-12} \text{ cm}^3 \text{ molecule}^{-1} \text{ s}^{-1}$ was derived. The self-reaction of $\text{HOCH}_2\text{CH}_2\text{O}_2$ radicals is expected to proceed via propagating and terminating channels:



In a study of the products of the OH radical addition to ethene in the presence of NO, Niki and co-workers⁸⁵ have shown that under ambient conditions $\text{HOCH}_2\text{C-H}_2\text{O}$ radicals decompose rapidly to give HCHO.



In fact, Jenkin and Cox observed HCHO as a significant product (~30% yield) of the self-reaction of $\text{HOCH}_2\text{-CH}_2\text{O}_2$ radicals. Using HCHO as a tracer for channel a Jenkin and Cox established the branching ratio $k_a/(k_a + k_b) = 0.18 \pm 0.02$. This branching ratio can then be used to correct the observed second-order rate for the effect of reaction of the peroxy radicals with HO_2

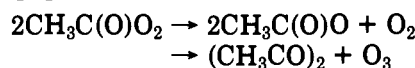


Assuming that every HO_2 radical produced via $\text{HOCH}_2\text{-CH}_2\text{O}$ decomposition reacts with $\text{HOCH}_2\text{CH}_2\text{O}_2$, then the "true" second-order rate constant for the self-reaction = $k_{\text{obs}}/1.18 = (1.36 \pm 0.21) \times 10^{-12} \text{ cm}^3 \text{ molecule}^{-1} \text{ s}^{-1}$.

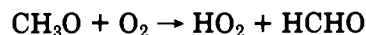
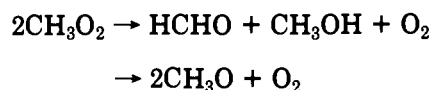
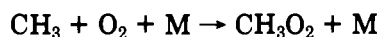
L. $\text{CH}_3\text{C(O)O}_2 + \text{CH}_3\text{C(O)O}_2$

The branching ratio for acetyl peroxy self-reaction has been investigated by Moortgat et al.¹⁰ in a flash

photolysis/UV absorption study at 600 Torr and temperatures in the range 253–368 K. The authors established that this reaction proceeds through a single channel and that a previous postulated path forming O_3 was negligible (estimated at 2%).



The kinetics of the overall reaction has been investigated by Addison et al.⁵⁷ by molecular modulation spectroscopy at 302 K, by Basco and Parmar⁵⁸ by flash photolysis at 298 K, and by Moortgat et al.¹⁰ by flash photolysis at 253–368 K. A complication for interpreting the data arises from the formation of CH_3O_2 radicals which react through self-reaction and with acetyl peroxy radicals:



The value of the rate constant determined by Moortgat et al.¹⁰ at 298 K is a factor of ~2 higher than previous determinations. The lower values obtained by Addison et al. and Basco and Parmar are probably in error due to erroneous values of $\sigma(\text{CH}_3\text{O}_2)$ and $k(\text{CH}_3\text{O}_2 + \text{CH}_3\text{C(O)O}_2)$ used in their calculations. Thus, the Arrhenius expression of Moortgat et al.¹⁰ is recommended for acetyl peroxy radicals self-reaction:

$$k = [(2.8 \pm 0.5) \times 10^{-12}] \exp[(530 \pm 100)/T] \text{ cm}^3 \text{ molecule}^{-1} \text{ s}^{-1}$$

M. $\text{CH}_3\text{OCH}_2\text{O}_2 + \text{CH}_3\text{OCH}_2\text{O}_2$

No information is available about the branching ratio of this reaction. However, the kinetics of the overall reaction were investigated by Dagaut et al.⁴² using the flash photolysis/absorption spectroscopy technique over the temperature range 228–380 K at pressures of 25–800 Torr. The results of this study are presented in Table III. The reaction is pressure dependent and exhibits an inverse temperature dependence. As with other substituted methyl peroxy radical self-reaction systems, no corrections for secondary removal of $\text{CH}_3\text{OCH}_2\text{O}_2$ by HO_2 were made. The authors used Troe's formalism for association reactions to represent their complete temperature-pressure data set:

$$k(T) = [k_0(T)[\text{M}]/[1 + [k_0(T)[\text{M}]/k_\infty(T)]]F_c^{1/\alpha}$$

where

$$\alpha = 1 + [(1/N) \log [k_0(T)[\text{M}]/k_\infty(T)]]^2$$

and

$$N = 0.75 - 1.27 \log(F_c)$$

$$k_0(T) = k_0(300 \text{ K}) [T/300]^{-n}$$

and

$$k_\infty(T) = k_\infty(300 \text{ K}) \{T/300\}^{-m}$$

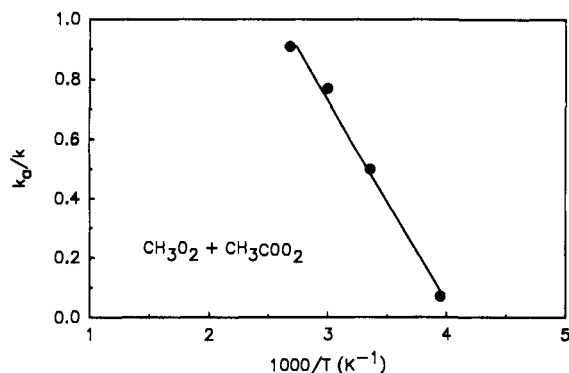


Figure 22. Plot of branching ratio k_a/k for reaction $\text{CH}_3\text{O}_2 + \text{CH}_3\text{COO}_2$ as a function of temperature determined by Moortgat et al.¹⁰ Solid line is a linear least-squares fit to the data and is our recommendation.

Fixing $F_c = 0.6$, the authors obtained the following parameters values in molecular units:

$$k_0(300 \text{ K}) = (2.5 \pm 0.8) \times 10^{-30}$$

$$k_{\infty}(300 \text{ K}) = (2.7 \pm 0.4) \times 10^{-12}$$

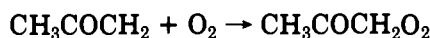
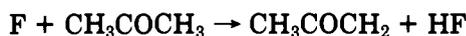
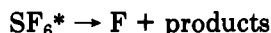
$$n = 5 \pm 1$$

$$m = 4.5 \pm 0.8$$

An end-product analysis study is needed to assess the mechanism of this reaction.

N. $\text{CH}_3\text{COCH}_2\text{O}_2 + \text{CH}_3\text{COCH}_2\text{O}_2$

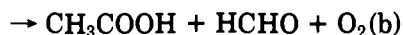
The kinetics of the self-reaction of $\text{CH}_3\text{COCH}_2\text{O}_2$ (acetyl peroxy) radicals have been studied at 298 K by Cox et al.³⁶ using the pulse radiolysis technique. Peroxy radicals were generated by the pulsed radiolysis of $\text{SF}_6/\text{CH}_3\text{COCH}_3/\text{O}_2$ mixtures:



From the observed second-order decay of the absorption signal at 310 nm a value of $k_{\text{obs}} = (8.3 \pm 1.6) \times 10^{-12} \text{ cm}^3 \text{ molecule}^{-1} \text{ s}^{-1}$ in 1 atm pressure of SF_6 at 298 K was derived and is recommended.

O. $\text{CH}_3\text{C(O)O}_2 + \text{CH}_3\text{O}_2$

The branching ratio of the reaction of the acetyl peroxy radical with the methyl peroxy radical was recently measured by Moortgat et al.¹⁰ using the flash photolysis/UV absorption spectroscopy at 298–368 K and 760 Torr (see Table II). Figure 22 shows the variation of k_a/k with temperature observed by these workers. As seen from this figure, over the temperature range studied, the branching ratio is well represented by the expression $k_a/k = 2.76 - (676/T)$ which we recommend.



These authors also derived rate constants for reaction channels a and b over the same range of conditions. Their kinetic data at 298 K are in good agreement with a previous determination by Moortgat et al.⁹⁶ obtained by kinetic modeling of acetaldehyde oxidation (see Table III). In the absence of other studies the Arrhenius expressions of Moortgat et al. for reactions a and b are recommended:

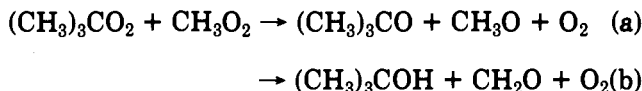
$$k_a = (1.8 \times 10^{-9}) \exp[-(1800 \pm 1100)/T] \text{ cm}^3 \text{ molecule}^{-1} \text{ s}^{-1}$$

$$k_b = (4.1 \times 10^{-15}) \exp[(2100 \pm 1200)/T] \text{ cm}^3 \text{ molecule}^{-1} \text{ s}^{-1}$$

The preexponential factor for channel a is clearly too large. The Arrhenius expression for k_a given above is, however, a good representation of the experimental data over the temperature range studied (298–368 K). Further work on the mechanisms and kinetics of this reaction are needed to confirm the data reported by Moortgat et al.¹⁰

P. $(\text{CH}_3)_3\text{CO}_2 + \text{CH}_3\text{O}_2$

The reaction of methyl peroxy radical with *tert*-butyl peroxy radical occurs during the photooxidation of *tert*-butyl radicals, as demonstrated by Parkes and co-workers in molecular modulation spectroscopy studies.^{30,73} The branching ratio for this reaction was reported by Parkes at 298 K, by Kirsch and Parkes⁷³ at 333 and 373 K, and by Osbourne and Waddington⁷⁶ at 313, 343, and 393 K (see Table II).



As seen from Table II there is a significant disagreement between these studies as to the relative importance of channels a and b and thus we offer no recommendation at this time. There have been no direct studies of the kinetics of this reaction. However, kinetic data has been derived indirectly by modeling the observed product yields. Using this approach Parkes reported a rate constant value of $(1.0 \pm 0.5) \times 10^{-13} \text{ cm}^3 \text{ molecule}^{-1} \text{ s}^{-1}$ for the overall reaction at 298 K whereas Osbourne and Waddington⁷⁶ prefer a value which is 2 orders of magnitude lower. Clearly no recommendation can be made in the absence of further work.

IV. Kinetics and Mechanisms of $\text{RO}_2 + \text{HO}_2$ Reactions

The literature data for the branching ratios and the kinetics of the reactions of peroxy radicals with HO_2 radicals are given in Tables IV and V and are discussed below.

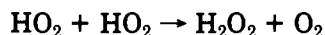
A. $\text{HO}_2 + \text{HO}_2$

A substantial body of data exists for hydroperoxy radicals self-reaction at temperatures below 500 K, as discussed in recent evaluations of kinetic data for atmospheric chemistry (DeMore et al.⁹⁰ and Atkinson et al.⁴⁷). At ambient temperature the reaction exhibits both a pressure and water vapor dependence. At higher

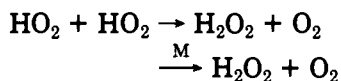
TABLE IV. Measured Branching Ratios for HO₂ + Peroxy Radical Reactions

k_a/k	k_b/k	technique	substrates	temperature range (K)	pressure (Torr)	ref
0.92	-	CP/FTIR	RO ₂ + HO ₂	295	700	86
			CH ₃ O ₂ + HO ₂ → CH ₃ OOH + O ₂ (a)			
			CH ₃ O ₂ + HO ₂ → HCHO + H ₂ O + O ₂ (b)			
0.60	0.40	MMS	CD ₃ O ₂ + HO ₂ → CD ₃ OOH + O ₂ (a)	300	10.8	20
			CD ₃ O ₂ + HO ₂ → DCDO + HD ₂ O + O ₂ (b)			
			CD ₄ /CH ₃ OH/Cl ₂			
0.60	0.40	MMS/UVA	HOCH ₂ O ₂ + HO ₂ → HOCH ₂ OOH + O ₂ (a)	298	2	39
			HOCH ₂ O ₂ + HO ₂ → HCOOH + H ₂ O + O ₂ (b)			
			HCHO/Cl ₂			
1.00	-	CP/FTIR	C ₂ H ₅ O ₂ + HO ₂ → C ₂ H ₅ OOH + O ₂ (a)	295	700	87
			C ₂ H ₆ /CH ₃ OH/Cl ₂			
0.75	0.25	CP/FTIR	CH ₃ C(O)O ₂ + HO ₂ → CH ₃ C(O)OOH + O ₂ (a)	298	700	88
			CH ₃ C(O)O ₂ + HO ₂ → CH ₃ C(O)OH + O ₃ (b)			
0.67	0.33	FP/UVA	CH ₃ CHO/CH ₃ OH/Cl ₂	253–368	600–650	89

temperatures recent data obtained by Lightfoot et al.⁴⁶ using the flash photolysis/UV absorption spectroscopy technique, reconcile the previous low-temperature data with the measurements of Troe⁹¹ at 1100 K by demonstrating that the rate constant increases with temperature above 600 K. These results are interpreted in terms of a direct bimolecular pathway accessible at high temperatures (>600 K)



competing with the low-temperature mechanism



Lightfoot et al.⁴⁶ fitted their data, together with the existing high-temperature data (298–1100 K, 760 Torr), and obtained the expression:

$$k = [(2.1 \pm 1.6) \times 10^{-10}] \exp[-(5051 \pm 722)/T] + [(1.8 \times 0.2) \times 10^{-13}] \exp(885/T)$$

in units of cm³ molecule⁻¹ s⁻¹.

Recently, Hippler et al.⁹² have used a shock tube/ultraviolet absorption system to measure the kinetics of the self-reaction of HO₂ radicals over the temperature range 720–1120 K. Two sources of HO₂ radicals were used: thermal dissociation of CH₃OOCH₃ in the presence of excess O₂ and thermal dissociation of H₂O₂. The kinetic data were derived using $\sigma(\text{HO}_2)_{230\text{nm},1000\text{K}} = 2.56 \times 10^{-18}$ cm² molecule⁻¹. Hippler et al.⁹² found no significant difference between their experimental data acquired at 5 bar total pressure, and data reported by Lightfoot et al.⁴⁶ at 1 bar showing that, in contrast to the situation at lower temperature, there is no evidence for any pressure effect at high temperatures. Hippler et al.⁹² combined their high-temperature results with the low-temperature kinetic expression appropriate for 760 Torr recommended by Atkinson et al.⁴⁷ to derive the following expression valid over the temperature range 300–1100 K:

$$k = [6.97 \times 10^{-10}] \exp(-6030/T) + [2.16 \times 10^{-13}] \exp(820/T) \text{ cm}^3 \text{ molecule}^{-1} \text{ s}^{-1}$$

Although the kinetic expressions listed in Table V appear markedly different, where comparison is possible, they in fact yield essentially identical results as

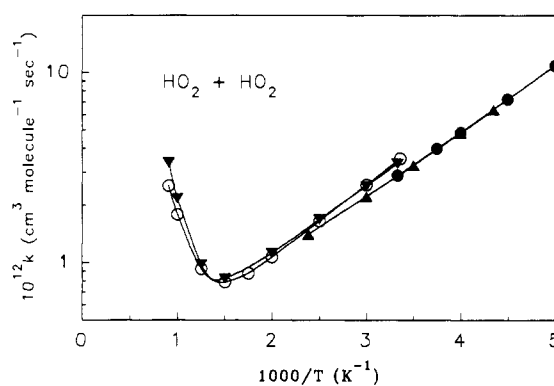
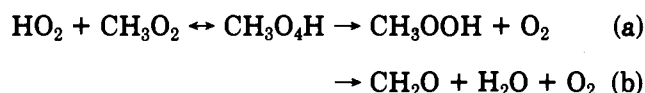


Figure 23. Kinetic data for the self-reaction of HO₂ radicals derived from the expressions recommended by DeMore et al.⁹⁰ (filled circles), Atkinson et al.⁴⁷ (filled triangles), Lightfoot et al.⁴⁶ (open circles), and Hippler et al.⁹² (filled inverse triangles). Solid lines are cubic-spline fits over the temperature range for which each recommendation is valid.

shown in Figure 23 where these expressions have been evaluated at a constant number density of 2.46×10^{19} molecules cm⁻³ of N₂. We recommend use of the expression given by Atkinson et al.⁴⁷ below 500 K and that of Hippler et al.⁹² above 500 K.

B. HO₂ + CH₃O₂

The branching ratio of the reaction of CH₃O₂ with HO₂ radicals has been studied by Wallington and Japar⁸⁶ using FTIR analysis (see Table IV). The authors found $k_a/k = 0.92$ at 295 K by continuous photolysis of CH₄/H₂/F₂/O₂/N₂ mixtures at 700 Torr total pressure.



Another value of this branching ratio can be obtained from the study of CH₃CHO photolysis by Moortgat et al.⁸⁰ In the study by Moortgat et al. the rate of the reaction channel producing CH₃OOH product (3.5×10^{-12} cm³ molecule⁻¹ s⁻¹) was reported to be significantly slower than the rate of the overall reaction (4.8×10^{-12} cm³ molecule⁻¹ s⁻¹) suggesting that $k_a/k = 0.73$ at 300 K and 760 Torr pressure. As discussed below, Jenkin et al.²⁰ have reported the observation of a significant

TABLE V. Kinetic Data for HO₂ + Peroxy Radical Reactions

k^a	λ (nm)	T (K)	technique ^b	ref
HO ₂ + HO ₂				
		200–300	review	90
$k = [(2.3 \times 10^{-13}) \exp(600 \pm 200)/T] + 1.7 \times 10^{-33}$ [air]		230–420	review	47
		exp[(1000 ± 400)/T] × [1 + (1.4 × 10 ⁻²¹) [H ₂ O] exp(2200/T)]		cm ³ molecule ⁻¹ s ⁻¹
$k = [(2.2 \times 10^{-13}) \exp(600/T) + 1.9 \times 10^{-33}$ [N ₂]		980–1250	shock tube/UVA	91
1.7–3.3	210	298–777	FP/UVA (CH ₃ OH/Cl ₂ /O ₂)	46
		exp(980/T) × [1 + (1.4 × 10 ⁻²¹) [H ₂ O] exp(2200/T)]		cm ³ molecule ⁻¹ s ⁻¹
		exp[-(5051 ± 722)/T] + [(1.8 ± 0.1) × 10 ⁻¹³] exp(885/T)	shock tube/UVA (H ₂ O ₂ ; (CH ₃ O) ₂ /O ₂)	92
	230	750–1120		
		exp(-6030/T) + [2.16 × 10 ⁻¹³] exp(820/T)		cm ³ molecule ⁻¹ s ⁻¹
		230		
HO ₂ + CH ₃ O ₂				
8.5 ± 1.2	210, 250	274	MMS/UVA (CH ₄ /H ₂ /Cl ₂ /O ₂)	17, 18
6.5 ± 1.0		298		
3.5 ± 0.5		338		
1.3		298	FTIR (CH ₃ NNCH ₃ /O ₂)	63
≤6.7 ± 2.2	220, 250	298	MMS/UVA (CH ₃ CHO/air)	80
4.8 ± 0.2	220, 250	298	MMS/UVA (CH ₃ CHO/air)	80
6.4 ± 1.0	210, 240	298	FP/UVA (CH ₄ /CH ₃ OH/Cl ₂ /O ₂)	8
2.9 ± 0.4	215–280	298	FP/UVA (CH ₄ /CH ₃ OH/Cl ₂ /O ₂)	93
6.8 ± 0.5	250	228	FP/UVA (CH ₄ /CH ₃ OH/Cl ₂ /O ₂)	94
5.5 ± 0.3		248		
4.1 ± 0.3		273		
2.4 ± 0.5		340		
2.1 ± 0.3		380		
5.4 ± 1.1	260, 1110 cm ⁻¹	300	MMS/UVA/IRA (CH ₄ /H ₂ O ₂ /Cl ₂ /O ₂)	20
6.8 ± 0.9	260	303	MMS/UVA (CH ₄ /H ₂ /Cl ₂ /O ₂)	
10.37 ± 4.72	210, 260	248	FP/UVA (CH ₄ /CH ₃ OH/Cl ₂ /O ₂)	48
7.63 ± 1.70		273		
5.63 ± 1.02		298		
5.22 ± 1.24		323		
2.98 ± 0.84		368		
3.11 ± 0.48		373		
2.39 ± 0.36		473		
1.83 ± 0.38		573		
HO ₂ + C ₂ H ₅ O ₂				
6.3 ± 0.9	210, 260, 1117 cm ⁻¹	295	MMS/UVA/IR (C ₂ H ₆ /CH ₃ OH/Cl ₂ /O ₂)	27
7.3 ± 1.0	230–280	248	FP/UVA (C ₂ H ₆ /CH ₃ OH/Cl ₂ /O ₂)	95
6.0 ± 0.5		273		
5.4 ± 1.2		298		
3.4 ± 1.0		340		
3.1 ± 0.5		380		
HO ₂ + HOCH ₂ O ₂				
12 ± 3	250, 1110 cm ⁻¹	298	MMS/UVA/IR (Cl ₂ /CH ₂ O/O ₂)	39
25 ± 5	210, 240	275	FP/UVA (Cl ₂ /CH ₂ O/O ₂)	38
12 ± 4		295		
12 ± 6		308		
6 ± 4		323		
6 ± 2		333		
HO ₂ + HOCH ₂ CH ₂ O ₂				
4.8 ± 1.5	220, 230, 240, 250	298	MMS/UVA (HOCH ₂ CH ₂ I)	41
HO ₂ + CH ₃ COO ₂				
27 ± 5	210	258	FP/UVA (Cl ₂ /CH ₃ CHO/CH ₃ OH/O ₂)	89
13 ± 3	210	298		
7.45 ± 3.0	207	368		

^aIn units of 10⁻¹² cm³ molecule⁻¹ s⁻¹. ^bKey: CPS, continuous near-UV photolysis in static conditions; MMS, molecular modulation spectroscopy; CP, continuous photolysis; IR, infrared analysis; FTIR, Fourier transform infrared spectroscopy; chemical, wet chemical techniques; MP, modulated photolysis; UVA, ultraviolet absorption spectroscopy; FP, flash photolysis.

yield of HDO following the continuous near-UV photolysis of CD₄/CH₃OH/O₂/Cl₂/N₂ mixtures at 10.8 Torr from which branching ratios of $k_a/k = 0.6$ and $k_b/k = 0.4$ were derived for the reaction of per-deuteromethyl peroxy with HO₂.

Of the three branching ratio determinations, the study of Wallington and Japar is the most direct and does not rely on simulation of the observed data using a complex chemical mechanism. Thus, we recommend use of the branching ratio of $k_a/k = 0.92 \pm 0.08$ at 295

K and 700 Torr from Wallington and Japar. Clearly, further work is needed to better define this branching ratio. The influence of temperature and pressure on the branching ratio has still to be examined.

The kinetics of the reaction of HO₂ with CH₃O₂ has been studied by Cox and Tyndall,^{17,18} Kan et al.,⁶³ Moortgat et al.,^{80,96} McAdam et al.,⁸ Kurylo et al.,⁹³ Dagaut et al.,⁹⁴ Jenkin et al.,²⁰ and Lightfoot et al.⁴⁸ These studies cover the temperature range 228–573 K and reveal a marked negative activation energy for the

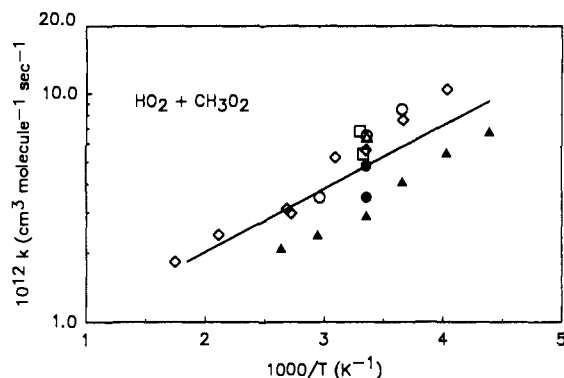


Figure 24. Arrhenius plot for the reaction $\text{HO}_2 + \text{CH}_3\text{O}_2$. The full line represents the Arrhenius fit to the data (our recommendation) from Cox and Tyndall¹⁷ (open circles), Moortgat et al.⁸⁰ (filled circles), McAdam et al.⁸ (open triangle), Kurylo et al.⁹³ and Dagaut et al.⁹⁴ (filled triangles), Jenkin et al.²⁰ (open squares), and Lightfoot et al.⁴⁸ (open diamonds).

rate constant of the overall reaction, consistent with a complex mechanism. However, no pressure dependence was found between 25 and 760 Torr, and no effect of added water vapor concentration up to 13 Torr^{94,48} was observed.

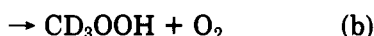
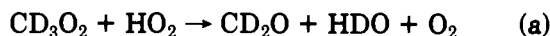
The kinetic data available for this reaction are plotted in Figure 24. As can be seen the data are rather scattered. Some of the discrepancies observed may be attributed to differences in the absorption coefficients used by the different authors but cannot be easily accounted for due to the complex nature of the kinetic analyses used. However, a general agreement is observed for the temperature dependence of the overall reaction. The best Arrhenius fit to the data (excluding the estimation of Kan et al.⁶³ and the upper limit value of Moortgat et al.⁸⁰) is represented by the following expression:

$$k = [(5.64 \pm 2.00) \times 10^{-13}] \exp[(640 \pm 105)/T] \text{ cm}^3 \text{ molecule}^{-1} \text{ s}^{-1}$$

where the errors represent 1σ .

C. $\text{HO}_2 + \text{CD}_3\text{O}_2$

The branching ratio of the reaction of HO_2 with CD_3O_2 has been determined by Jenkin et al.²⁰ at 300 K using continuous near-UV photolysis of a $\text{CD}_4/\text{CH}_3\text{OH}/\text{O}_2/\text{Cl}_2/\text{N}_2$ mixture at 10.8 Torr.



HDO production was monitored in the infrared and the branching ratio $k_a/(k_a + k_b) = 0.4$ was determined by comparing the measured HDO yield with the calculated flux of CD_3O_2 radicals reacting with HO_2 . A complex chemical mechanism was used in the calculations. The uncertainty on the resulting branching ratio could be large due to uncertainties in cross sections and kinetic data used in the simulation. No recommendation is made for the branching ratio of this reaction.

D. $\text{HO}_2 + \text{C}_2\text{H}_5\text{O}_2$

The branching ratio of this reaction has been investigated by Wallington and Japar⁸⁷ by photolyzing

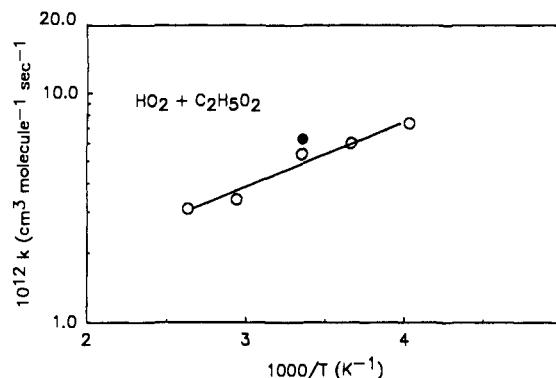


Figure 25. Arrhenius plot for the reaction $\text{HO}_2 + \text{C}_2\text{H}_5\text{O}_2$. The full line represents the Arrhenius fit to the data (our recommendation) from Cattell et al.²⁷ (filled circle) and Dagaut et al.⁹⁵ (open circles).

$\text{C}_2\text{H}_6/\text{CH}_3\text{OH}/\text{Cl}_2/\text{air}$ mixtures and analyzing the products using FTIR spectroscopy. It was shown that, at 295 K and over the pressure range 20–700 Torr, reaction of $\text{C}_2\text{H}_5\text{O}_2$ with HO_2 proceeds by a single reactive route forming $\text{C}_2\text{H}_5\text{OOH}$ and O_2 .



The kinetics of the reaction of HO_2 with $\text{C}_2\text{H}_5\text{O}_2$ has been investigated by Cattell et al.²⁷ at room temperature and 2.4 Torr and Dagaut et al.⁹⁵ from 228 to 380 K at pressures up to 400 Torr (see Table IV). Cattell et al.²⁷ produced ethyl peroxy and hydroperoxy radicals by modulated photolysis of $\text{C}_2\text{H}_6/\text{CH}_3\text{OH}/\text{Cl}_2/\text{O}_2/\text{N}_2$ and azoethane/ O_2 mixtures. They monitored $\text{C}_2\text{H}_5\text{O}_2$ and HO_2 by UV absorption at 260 and 210 nm. HO_2 was also monitored in the infrared at 1117 cm^{-1} using a tunable diode laser source. Dagaut et al.⁹⁵ used the flash photolysis/UV absorption spectroscopy technique in their kinetic study; radicals were produced by photolysis of $\text{C}_2\text{H}_6/\text{CH}_3\text{OH}/\text{Cl}_2/\text{O}_2/\text{N}_2$ mixtures. In both studies, the oxygen concentration was high enough to assure rapid conversion of ethyl radicals to ethyl peroxy radicals.

The kinetic data obtained by Cattell et al.²⁷ at 295 K is in good agreement with that of Dagaut et al.⁹⁵ (see Figure 25) and demonstrates the absence of pressure dependence above 2.4 Torr.

Dagaut et al. observed a residual absorption in their low-temperature experiments ($T = 228 - 238 \text{ K}$) with a maximum at about 250 nm. This result was interpreted by the authors in terms of an intermediate adduct stabilized at low temperature.



This stabilization will be more efficient than for the $\text{HO}_2 + \text{CH}_3\text{O}_2$ reaction due to the greater density of states associated with the ethyl compared to the methyl group.

The Arrhenius expression of Dagaut et al.⁹⁵ is recommended over the temperature range 250–380 K.

$$k = [(5.6 \pm 2.4) \times 10^{-13}] \exp[(650 \pm 125)/T] \text{ cm}^3 \text{ molecule}^{-1} \text{ s}^{-1}$$

E. $\text{HO}_2 + \text{HOCH}_2\text{O}_2$

The kinetics of this reaction have been investigated by Burrows et al.⁸⁹ using molecular modulation spec-

TABLE VI. Kinetic Data for Reaction of RO₂ + NO

10 ¹² k	T (K)	pressure range (Torr)	technique	ref
8.3 (at 298 K)	232–1271 $k = (3.7 \times 10^{-12}) \exp[(240 \pm 80)/T]$	HO ₂ + NO 1–12.5 cm ³ molecule ⁻¹ s ⁻¹	review	90
>1	298	CH ₃ O ₂ + NO 300 (N ₂)	MMS	33
8.0 ± 2.0	295	3 (He)	DF-MS	97
3.0 ± 0.2	298	760	FP-UVA	98
3.2 ± 1.8	296	760	RR ^a	99
6.5 ± 2.0	298	540	MMS	18
6.1 ± 0.7	298	75 (He)	FP-UVA	78
6.3 ± 0.9		350 (He)		
8.1 ± 1.1		700 (He)		
8.9 ± 0.7		700 (N ₂)		
8.4 ± 1.5	240	40 (Ar)	LP-LIF	100
8.6 ± 1.1	250	40 (Ar)		
9.0 ± 1.1	270	40 (Ar)		
7.8 ± 1.2	298	40–100 (Ar)		
7.8 ± 1.4	339	40 (Ar)		
13 ± 1.4	218	200 (CH ₄ /O ₂)	FP-UVA	101
17 ± 2.2	218	600 (CH ₄ /O ₂)		
7.7 ± 0.9	296	100–600 (CH ₄ /O ₂)		
6.3 ± 1.0	365	200 (CH ₄ /O ₂)		
8.6 ± 2.0	295	6 (He)	DF-MS	102
7 ± 2	298	8 (N ₂)	LP-UVA	103
		C ₂ H ₅ O ₂ + NO		
2.7 ± 0.2	298	350–760	FP-UVA	104
8.9 ± 3.0	295	5 (He)	DF-MS	105
		(CH ₃) ₂ CHO ₂ + NO		
3.5 ± 0.3	298	65 (Ar)	FP-UVA	106
		(CH ₃) ₃ CO ₂ + NO		
>1	298	300	MMS	33
		CFCl ₂ O ₂ + NO		
16 ± 2	298	1–6 (O ₂)	LP-MS	107
14.5 ± 2	298	1–10 (N ₂)	LP-MS	108
	230–430	1–10	LP-MS	108
		$k = [(1.45 \pm 0.2) \times 10^{-11}] (T/298)^{-(1.3 \pm 0.2)}$		
		cm ³ molecule ⁻¹ s ⁻¹		
		CF ₂ ClO ₂ + NO		
16 ± 3	298	1–10 (N ₂)	LP-MS	108
	230–430	1–10 (N ₂)	LP-MS	108
		$k = [(1.6 \pm 0.3) \times 10^{-11}] (T/298)^{-(1.5 \pm 0.4)}$		
		cm ³ molecule ⁻¹ s ⁻¹		
		CF ₃ O ₂ + NO		
17.8 ± 3.6	295	2–5 (He)	DF-MS	109
14.5 ± 2	298	1–10 (N ₂)	LP-MS	108
	230–430	1–10	LP-MS	108
		$k = [(1.45 \pm 0.2) \times 10^{-11}] (T/298)^{-(1.2 \pm 0.2)}$		
		cm ³ molecule ⁻¹ s ⁻¹		
		CCl ₃ O ₂ + NO		
18.6 ± 2.8	295	2–8 (He/O ₂)	DF-MS	110
17 ± 2	298	1–10 (N ₂)	LP-MS	108
	230–430	1–10	LP-MS	108
		$k = [(1.7 \pm 0.2) \times 10^{-11}] (T/298)^{-(1.0 \pm 0.2)}$		
		cm ³ molecule ⁻¹ s ⁻¹		

^aRelative to CH₃O₂ + SO₂ = 8.2 × 10⁻¹⁵.

V. Kinetics and Mechanisms of RO₂ + NO Reactions

The literature data for the branching ratios and the kinetics of the reactions of peroxy radicals with NO and NO₂ are given in Tables VI and VII, respectively, and are discussed below.

A. HO₂ + NO

The kinetics and mechanism of this reaction have been extensively reviewed in the latest JPL/NASA⁹⁰ and IUPAC⁴⁷ evaluations. In Table VI we report the

latest JPL/NASA recommendations based upon the results of several studies carried out near room temperature. The data of Howard and Evenson,¹¹⁹ Leu,¹²⁰ Howard,¹²¹ Glaschick-Schimpf et al.,¹²² Hack et al.,¹²³ and Thrush and Wilkinson¹²⁴ are in good agreement and are used. Other determinations by Burrows et al.¹²⁵ and Rozenshtein¹²⁶ were disregarded due to problems interpreting the data. The temperature dependence is that of Howard,¹²¹ which agrees with that of Leu.¹²⁰ The experiments described in ref 119–124, which are the basis of the NASA/JPL recommendation, were performed at low total pressure (<12.5 Torr). An absolute rate investigation of this reaction at high pressure is needed.

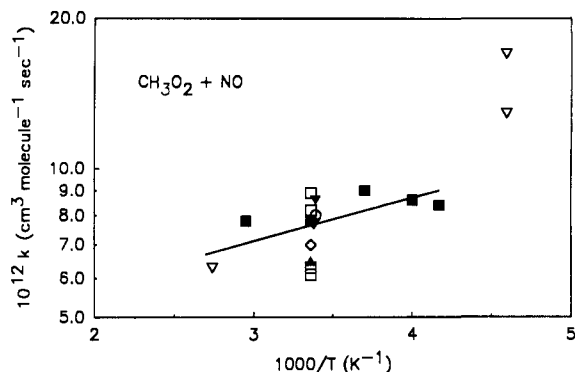
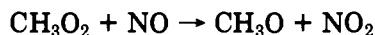


Figure 26. Arrhenius plot for the reaction $\text{CH}_3\text{O}_2 + \text{NO}$. Data taken from Plumb et al.^{97,102} (open circle and filled inverse triangle, respectively), Cox and Tyndall¹⁸ (filled triangle), Sander and Watson⁷⁸ (open squares), Ravishankara et al.¹⁰⁰ (filled squares), Simonaitis and Hecklen¹⁰¹ (open inverse triangles), and Zellner et al.¹⁰³ (open diamond). The solid line represents our recommendation.

B. $\text{CH}_3\text{O}_2 + \text{NO}$

Direct measurements of the formation of NO_2 and CH_3O as products of the reaction of methyl peroxy radicals with NO have been made by Ravishankara et al.¹⁰⁰ and Zellner et al.^{103,127} and demonstrate that this reaction proceeds predominantly (>80%) if not solely, via the channel



Kinetic studies have been performed by Anastasi and Smith,³³ Plumb et al.,^{97,102} Adachi and Basco,⁹⁸ Simonaitis and Hecklen,^{99,101} Cox and Tyndall,¹⁸ Sander and Watson,⁷⁸ Ravishankara et al.,¹⁰⁰ and Zellner et al.¹⁰³ As seen from Table VI, with the exception of the early studies of Adachi and Basco⁹⁸ and Simonaitis and Hecklen,⁹⁹ there is general agreement among the various studies at room temperature. As suggested by Sander and Watson⁷⁸ the low rate constant reported by Adachi and Basco⁹⁸ may be due to absorption by CH_3ONO at the monitoring wavelength. Methyl nitrite was present due to reaction of methoxy radicals (CH_3O) with NO which is present in large excess. Such a complication would lead to an underestimate of k . The rate constant reported in the first study of Simonaitis and Hecklen⁹⁹ was derived in an indirect manner relative to the rate of the reaction of methyl peroxy radicals with SO_2 and is hence superseded by the second and more direct study by these workers.

The rate constant for reaction of CH_3O_2 radicals with NO has been measured over a wide range of pressure and, with the possible exception of the study of Sander and Watson,⁷⁸ there is no evidence of any pressure dependence. Even in the study by Sander and Watson the rate constants reported at 75 and 700 Torr are indistinguishable within the combined experimental errors. Hence, our recommendation for the room temperature, pressure-independent rate constant is an arithmetic mean of the results of Plumb et al.,^{97,102} Simonaitis and Hecklen,¹⁰¹ Cox and Tyndall,¹⁸ Sander and Watson,⁷⁸ Ravishankara et al.,¹⁰⁰ and Zellner et al.,¹⁰³ $k = 7.5 \times 10^{-12} \text{ cm}^3 \text{ molecule}^{-1} \text{ s}^{-1}$ with an estimated uncertainty of $\pm 20\%$.

There have only been two studies of the temperature dependence of this reaction (Ravishankara et al.¹⁰⁰ and Simonaitis and Hecklen¹⁰¹). As seen from Figure 26,

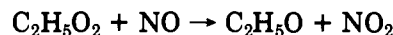
there is a significant difference between the near-zero temperature dependence reported by Ravishankara et al.¹⁰⁰ and the large negative temperature dependence reported by Simonaitis and Hecklen.¹⁰¹ The latter is in large part due to the lowest temperature data. For our recommendation we have performed a linear least-squares analysis of all the data shown in Figure 26 (with the exception of the lowest temperature data of Simonaitis and Hecklen) to yield

$$k = [(3.9 \pm 2.8) \times 10^{-12}] \exp[(200 \pm 190)/T] \text{ cm}^3 \text{ molecule}^{-1} \text{ s}^{-1}$$

valid over the temperature range 240–370 K. Quoted errors represent 2σ . Further studies of this reaction are needed to define the kinetics of this reaction at temperatures below 240 K and above 370 K.

C. $\text{C}_2\text{H}_5\text{O}_2 + \text{NO}$

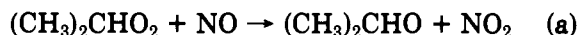
Plumb et al.¹⁰⁵ and Atkinson et al.^{128,129} have reported that $\text{C}_2\text{H}_5\text{O}$ and NO_2 are formed as a product of the reaction of $\text{C}_2\text{H}_5\text{O}_2$ with NO in a yield which is indistinguishable from unity within the experimental errors (20%). Thus we recommend use of a single channel for this reaction:



There have been two studies of the kinetics of this reaction. The results reported by Adachi and Basco¹⁰⁴ are a factor of 3 lower than those of Plumb et al.¹⁰⁵ The origin of this discrepancy probably lies in monitoring complications associated with the formation of $\text{C}_2\text{H}_5\text{O}-\text{NO}$ by the reaction of ethoxy radicals with the excess NO on a time scale comparable to that of the decay of ethyl peroxy radicals. The 250-nm monitoring wavelength used by Adachi and Basco was absorbed appreciably by ethyl nitrite. Hence we prefer the data reported by Plumb et al.¹⁰⁵ and recommend use of a pressure-independent rate constant at 298 K of $k = 9 \times 10^{-12} \text{ cm}^3 \text{ molecule}^{-1} \text{ s}^{-1}$ with an estimated uncertainty of $\pm 40\%$.

D. $(\text{CH}_3)_2\text{CHO}_2 + \text{NO}$

The mechanism of the reaction of isopropyl peroxy radicals with NO has been studied by Atkinson et al.^{128,129} using FTIR analysis of reaction mixtures following the continuous near UV irradiation of $\text{Cl}_2/\text{NO}/\text{C}_3\text{H}_8$ and $\text{CH}_3\text{ONO}/\text{NO}/\text{C}_3\text{H}_8$ mixtures in air at 735 Torr and 298 K. Atkinson et al.^{128,129} report branching ratios of $k_a/(k_a + k_b) = 0.96$ and $k_b/(k_a + k_b) = 0.04$:



The only study of the kinetics of this reaction was performed by Adachi and Basco¹⁰⁶ who report a rate constant at room temperature of $(3.5 \pm 0.3) \times 10^{-12} \text{ cm}^3 \text{ molecule}^{-1} \text{ s}^{-1}$. This value is considerably lower than our recommended values for the reactions of methyl and ethyl peroxy radicals with NO . In light of the underestimation of the rate constants for the reactions of methyl and ethyl peroxy radicals by Adachi and Basco,^{98,104} it seems likely that their study of isopropyl

TABLE VII (Continued)

$10^{12}k$	T (K)	pressure range (Torr)	technique	ref	$10^{12}k$	T (K)	pressure range (Torr)	technique	ref
$\text{CF}_2\text{ClO}_2 + \text{NO}_2$									
0.75 ± 0.13	298	1 (CF_2ClBr)	FP/MS	117	1.60 ± 0.23		6		
0.82 ± 0.33		1.5			1.72 ± 0.48		7		
1.27 ± 0.04		2			1.52 ± 0.40		8		
1.37 ± 0.07		3			2.18 ± 0.71		9		
1.51 ± 0.13		4			2.83 ± 0.20		10		
1.41 ± 0.18		5							
$\text{CF}_3\text{O}_2 + \text{NO}_2$									
1.34	233	0.8 (O_2)	LP/MS	118	1.47		6		
2.03		1.6			1.76		10		
3.95		4.7			0.37	373	2.5		
4.55		6.3			0.62		7.5		
5.15		7.9			0.69		12.5		
0.52	298	1				$\approx 233\text{--}373$		review	90
0.92		2			$k_o = [(2.2 \pm 0.5) \times 10^{-29}](T/300)^{-(6\pm 1)} \text{ cm}^6 \text{ molecule}^{-2} \text{ s}^{-1} \text{ (in air)}$				
1.1		3			$k_\infty = [(6.0 \pm 1.0) \times 10^{-12}](T/300)^{-(2.5\pm 1)} \text{ cm}^3 \text{ molecule}^{-1} \text{ s}^{-1} \text{ (in air)}$				
$\text{CCl}_3\text{O}_2 + \text{NO}_2$									
3.25	233	1.2 (O_2)	LP/MS	118	3.17		10		
3.85		1.6			0.91	373	5		
4.87		2.3			1.04		2.6		
5.87		3.3			1.32		4.3		
1.22	298	2				$\approx 233\text{--}373$		review	90
1.58		3			$k_o = [(5.0 \pm 1.0) \times 10^{-29}](T/300)^{-(5\pm 1)} \text{ cm}^6 \text{ molecule}^{-2} \text{ s}^{-1} \text{ (in air)}$				
2.45		6			$k_\infty = [(6.0 \pm 1.0) \times 10^{-12}](T/300)^{-(2.5\pm 1)} \text{ cm}^3 \text{ molecule}^{-1} \text{ s}^{-1} \text{ (in air)}$				

^aExperiments performed at "room temperature" which was taken to be 295 K.

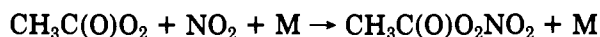
peroxy radicals may also be subject to similar interferences. No recommendation is made regarding the kinetics of this reaction, and further experimental work is needed.

E. $(\text{CH}_3)_3\text{CO}_2 + \text{NO}$

The reaction of *tert*-butyl peroxy radicals with NO has been studied by Anastasi et al.³³ who derived a lower limit to the rate constant of $1 \times 10^{-12} \text{ cm}^3 \text{ molecule}^{-1} \text{ s}^{-1}$ consistent with the body of kinetic data for other peroxy radical reaction with NO.

F. $\text{CH}_3\text{C}(\text{O})\text{O}_2 + \text{NO}$

To date there have been no direct studies of the kinetics of the reaction of acetyl peroxy radicals with NO. However, there have been a number of indirect studies in which the rate of reaction of $\text{CH}_3\text{C}(\text{O})\text{O}_2$ with NO is measured relative to that with NO_2 .



Cox et al.¹³⁰ reported a ratio $k_{\text{AcO}_2+\text{NO}}/k_{\text{AcO}_2+\text{NO}_2} = 1.7$ from observations of the effect of $[\text{NO}]/[\text{NO}_2]$ on the peroxy acetyl nitrate (PAN) product yield on photolysis of HONO/ CH_3CHO mixtures in 1 atm of air at 300 K. Further work by Cox and Roffey¹³¹ followed the rate of disappearance of PAN in mixtures with NO at one atmosphere pressure of air. Over the temperature range 303–328 K there was no significant variation of $k_{\text{AcO}_2+\text{NO}}/k_{\text{AcO}_2+\text{NO}_2}$ with a mean value of 1.9 ± 0.6 . In a similar experiment, Hendry and Kenley¹³² report $k_{\text{AcO}_2+\text{NO}}/k_{\text{AcO}_2+\text{NO}_2} = 3.1 \pm 0.5$ at atmospheric pressure independent of temperature over the range 298–318 K.

More recently, Kirchner et al.¹³³ and Tuazon et al.¹³⁴ have also monitored the decay rate of PAN in the presence of known concentrations of NO and NO_2 to

measure the rate constant ratio $k_{\text{AcO}_2+\text{NO}}/k_{\text{AcO}_2+\text{NO}_2}$. Tuazon et al.¹³⁴ report a rate constant ratio $k_{\text{AcO}_2+\text{NO}}/k_{\text{AcO}_2+\text{NO}_2} = 1.95 \pm 0.28$ at 740 Torr of air independent of temperature over the range 283–313 K. Kirchner et al.¹³³ report rate constant ratios, $k_{\text{AcO}_2+\text{NO}}/k_{\text{AcO}_2+\text{NO}_2}$, at atmospheric pressure of air of 2.2 ± 0.3 (304 K), 2.4 ± 0.1 (313 K), and 2.4 ± 0.1 (321 K). In addition, Kirchner et al.¹³³ measured the ratio $k_{\text{AcO}_2+\text{NO}}/k_{\text{AcO}_2+\text{NO}_2}$ as a function of pressure over the pressure range 30–1000 mbar of air at a fixed temperature of 313 K; results were as follows: 2.4 ± 0.1 , 1000 mbar; 2.6 ± 0.1 , 300 mbar; 3.6 ± 0.6 , 100 mbar; and 4.0 ± 0.8 , 30 mbar. Consistent with previous studies, the results of Kirchner et al. show that at atmospheric pressure there is no observable effect of temperature on the ratio $k_{\text{AcO}_2+\text{NO}}/k_{\text{AcO}_2+\text{NO}_2}$ over the range 304–321 K.

With the exception of the data reported by Hendry and Kenley,¹³² all studies of the rate constant ratio $k_{\text{AcO}_2+\text{NO}}/k_{\text{AcO}_2+\text{NO}_2}$ are in agreement. At atmospheric pressure there is no observable effect of temperature over the range 283–328 K; the average of the values reported by Cox and Roffey,¹³¹ Tuazon et al.,¹³⁴ and Kirchner et al.¹³³ is $k_{\text{AcO}_2+\text{NO}}/k_{\text{AcO}_2+\text{NO}_2} = 2.1$. This rate constant ratio can be combined with our recommended kinetic data for the reaction of $\text{CH}_3\text{C}(\text{O})\text{O}_2$ radicals with NO_2 (see next section) to provide a value for the rate constant of the reaction of $\text{CH}_3\text{C}(\text{O})\text{O}_2$ radicals with NO. At 760 Torr our recommended expression for $k_{\text{AcO}_2+\text{NO}_2}$ yields effective second-order rate constants of 8.4×10^{-12} and $1.0 \times 10^{-11} \text{ cm}^3 \text{ molecule}^{-1} \text{ s}^{-1}$ at 283 and 328 K. Taking an average of $k_{\text{AcO}_2+\text{NO}_2} = 9.2 \times 10^{-12} \text{ cm}^3 \text{ molecule}^{-1} \text{ s}^{-1}$ then yields our recommendation of $k_{\text{AcO}_2+\text{NO}} = 1.9 \times 10^{-11} \text{ cm}^3 \text{ molecule}^{-1} \text{ s}^{-1}$ at 760 Torr over the temperature range 283–328 K. We estimate the uncertainties associated with this rate constant to be $\pm 50\%$. The rate constant values $k_{\text{AcO}_2+\text{NO}}/k_{\text{AcO}_2+\text{NO}_2}$ reported by Kirchner et al.¹³³ at pressure less than 760 Torr can also be combined with values of $k_{\text{AcO}_2+\text{NO}_2}$ calculated from our recommended expression (5.6, 7.3,

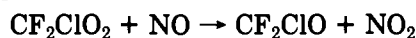
and $8.3 \times 10^{-12} \text{ cm}^3 \text{ molecule}^{-1} \text{ s}^{-1}$ at 30, 100, and 300 mbar) to give values of $k_{\text{AcO}_2+\text{NO}}$ of (2.2 ± 0.5) , (2.6 ± 0.5) , and $(2.2 \pm 0.1) \times 10^{-12} \text{ cm}^3 \text{ molecule}^{-1} \text{ s}^{-1}$ at 30, 100, and 300 mbar, respectively. Consistent with the body of data for reactions of peroxy radicals with NO there is no evidence for any effect of pressure over the range 30–1000 mbar on the kinetics of the reaction of $\text{CH}_3\text{C}(\text{O})\text{O}_2$ radicals with NO. Clearly, there is a need for direct kinetic studies on this reaction.

G. $\text{CFCl}_2\text{O}_2 + \text{NO}$

The kinetics of the reaction of CFCl_2O_2 radicals with NO has been studied by Lesclaux and co-workers^{107,108} using pulsed laser photolysis of CFCl_3 in the presence of O_2 and NO combined with time resolved mass spectroscopy. Rate constants of $(1.6 \pm 0.2)^{107}$ and $(1.45 \pm 0.2)^{108} \times 10^{-11} \text{ cm}^3 \text{ molecule}^{-1} \text{ s}^{-1}$ were determined independent of pressure over the range 1–10 Torr of O_2/N_2 at 295 K. No evidence for the existence of reaction channels other than that leading to the alkoxy radical and NO_2 were detected. Experiments performed over the temperature range 230–430 K by Dognon et al.¹⁰⁸ have shown this reaction to have an inverse temperature dependence the rate expression of Dognon et al.¹⁰⁸ given in Table VI is recommended.

H. $\text{CF}_2\text{ClO}_2 + \text{NO}$

The kinetics and mechanism of this reaction has been studied by Dognon et al.¹⁰⁸ by laser photolysis/mass spectroscopy over the pressure range 1–10 Torr at temperatures ranging from 230 to 430 K. An inverse temperature dependence was observed. No significant effect of pressure was observed. In the absence of other determinations the rate expression of Dognon et al.¹⁰⁸ given in Table VI is recommended. The major product observed in this reaction was NO_2 suggesting that the reaction proceeds via one channel:



I. $\text{CF}_3\text{O}_2 + \text{NO}$

The reaction of CF_3O_2 radicals with NO has been studied by Plumb and Ryan¹⁰⁹ using discharge flow mass spectroscopy and by Dognon et al.¹⁰⁸ using laser photolysis combined with mass spectroscopy. As seen from Table VI the results from both studies are in good agreement with a rate constant of $(1.6 \pm 0.2) \times 10^{-11} \text{ cm}^3 \text{ molecule}^{-1} \text{ s}^{-1}$ at 298 K, independent of pressure over the range 1–10 Torr. This value is consistent with the kinetics of other reactions of CX_3O_2 ($\text{X} = \text{F}$ or Cl) with NO. Dognon et al.¹⁰⁸ have studied the effect of temperature on the kinetics of this reaction over the range 230–430 K; an inverse temperature dependence was observed. The rate expression of Dognon et al.¹⁰⁸ given in Table VI is recommended. No evidence for the existence of reaction channels other than that leading to the alkoxy radical and NO_2 were detected by Dognon et al.¹⁰⁸ under their experimental conditions.

J. $\text{CCl}_3\text{O}_2 + \text{NO}$

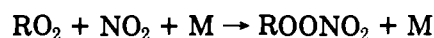
The kinetics of this reaction have been studied by Ryan and Plumb¹¹⁰ using the discharge flow mass

spectroscopy at 298 K and by Dognon et al.¹⁰⁸ using a laser photolysis mass spectroscopy over the temperature range 230–430 K. At 298 K results from both studies are in good agreement (see Table VI). Over the temperature range 230–430 K an inverse temperature dependence was observed. No significant effect of pressure was observed. The kinetic data reported by Dognon et al.¹⁰⁸ for this reaction are consistent with that of other reactions of CX_3O_2 ($\text{X} = \text{F}$ or Cl) with NO, and the expression calculated by these authors (given in Table VI) is recommended. The major product observed in this reaction was NO_2 suggesting that the reaction proceeds via one channel:



VI. Kinetics and Mechanisms of $\text{RO}_2 + \text{NO}_2$ Reactions

The reactions of alkyl peroxy radicals with NO_2 are known to proceed exclusively via combination to yield peroxy nitrates



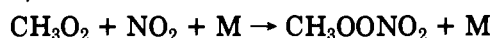
As combination reactions they are all expected to be pressure dependent with the rate increasing with increasing pressure and to have a negative temperature dependence. The available kinetic data for these reactions are listed in Table VII. As in all other classes of alkyl peroxy radical studies the best-characterized reaction is that of the simplest alkyl peroxy radical CH_3O_2 .

A. $\text{HO}_2 + \text{NO}_2$

The kinetics and mechanism of this reaction have been extensively reviewed by Atkinson et al.⁴⁷ and DeMore et al.⁹⁰ Both recommend the use of the kinetic expression derived by Kurylo and Ouellette^{135,136} from a fit of their experimental data combined with that of Sander and Peterson.¹³⁷ This recommended expression (given in Table VII) is consistent with the previous studies by Howard,¹²¹ Simonaitis and Heicklen,¹³⁸ and Cox and Patrick.¹³⁹ Further studies of the temperature dependence of the kinetics of this reaction at pressures above 1 atm are needed to better characterize the temperature dependence of the high-pressure limit.

B. $\text{CH}_3\text{O}_2 + \text{NO}_2$

The kinetics of this reaction have been studied by Adachi and Basco,¹¹¹ Cox and Tyndall,¹⁸ Sander and Watson,⁷⁸ and Ravishankara et al.¹¹²



Sander and Watson observed $k(298 \text{ K})$ to increase by factors of 3–4 on going from 50 to 700 Torr of either He, N_2 , or SF_6 . This dependence was confirmed by the study of Ravishankara et al.¹¹² using nitrogen as third body. Ravishankara et al.¹¹² also performed experiments at temperatures other than ambient and observed a negative temperature dependence. The study of Cox and Tyndall¹⁸ at 50 Torr of a mixture of methane and argon is consistent with the results of both Sander and Watson⁷⁸ and Ravishankara et al.¹¹² However, the rate constant measured in the presence of 540 Torr of

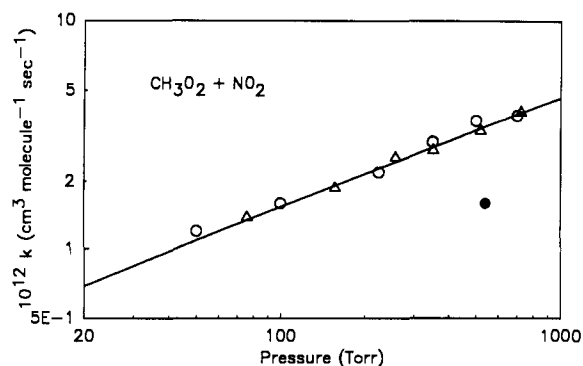


Figure 27. Falloff plot for the reaction $\text{CH}_3\text{O}_2 + \text{NO}_2$ at 298 K in nitrogen diluent. Data is taken from Cox and Tyndall¹⁷ (filled circle), Sander and Watson⁷⁸ (open circles), and Ravishankara et al.¹¹² (triangles). Solid line represents our recommendation.

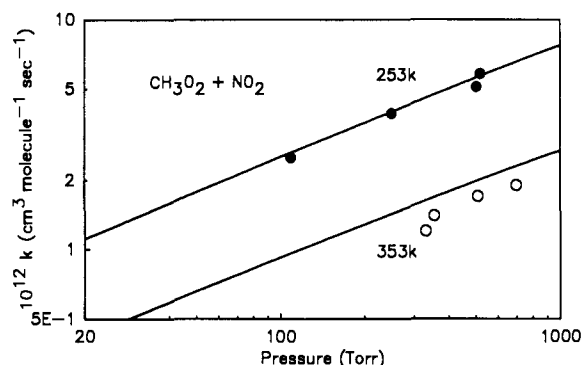


Figure 28. Falloff plot for the reaction $\text{CH}_3\text{O}_2 + \text{NO}_2$ at 253 and 353 K in nitrogen diluent. Data taken from Ravishankara et al.¹¹² Solid lines represent our recommendation; see discussion in text.

N_2 by Cox and Tyndall¹⁸ is considerably lower (by a factor of 2) than that measured by Sander and Watson and Ravishankara et al.¹¹² As suggested by Sander and Watson, the origin of this discrepancy may lie in the relatively long time scale employed in the molecular modulation technique which may allow significant dissociation of peroxy methyl nitrate to reactants and hence led to an underestimation of the rate constant for the association reaction. In the work of Adachi and Basco¹¹¹ the rate of reaction of CH_3O_2 with NO_2 was reported to be independent of pressure over the range 53–580 Torr of argon. This result is clearly inconsistent with the other studies of this reaction and strongly suggests that the results from ref 111 are in error.

In Figure 27 we show the 298 K N_2 data reported by Sander and Watson,⁷⁸ Ravishankara et al.,¹¹² and Cox and Tyndall.¹⁸ In Figure 28 we show the data obtained at 253 and 353 K (again in N_2) obtained by Ravishankara et al.¹¹² Watson and Sander fitted their 298 K kinetic data to the three-parameter expression proposed by Troe and co-workers.^{140,141}

$$k(M, T) = k_0(T)[M]/[1 + \{k_0[M]/k_\infty(T)\}] \times F_c^{[1 + \{\log_{10}[k_0(T)[M]/k_\infty(T)]\}^2]^{-1}}$$

using $k_0 = 2.3 \times 10^{-30} \text{ cm}^6 \text{ molecule}^{-2} \text{ s}^{-1}$, $k_\infty = 8 \times 10^{-12} \text{ cm}^3 \text{ molecule}^{-1} \text{ s}^{-1}$ and $F_c = 0.4$. Use of these parameters gives an excellent fit to the data reported by both Sander and Watson as well as that measured by Ravishankara et al. as shown by the solid line in Figure 27 and is our recommendation for 298 K. For temperatures other than ambient we recommend use of the

expressions derived in ref 112:

$$k_0(T) = (2.3 \times 10^{-30})(T/298)^{-2.5} \text{ cm}^6 \text{ molecule}^{-2} \text{ s}^{-1}$$

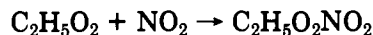
and

$$k_\infty(T) = (8.0 \times 10^{-12})(T/298)^{-3.5} \text{ cm}^3 \text{ molecule}^{-1} \text{ s}^{-1}$$

The fit of this expression to the existing data at 253 K is excellent. At 353 K the fit is only fair as shown in Figure 28. Our recommendation is thus biased toward the ambient and subambient data as they are most useful to the atmospheric chemistry community.

C. $\text{C}_2\text{H}_5\text{O}_2 + \text{NO}_2$

The kinetics of the reaction of $\text{C}_2\text{H}_5\text{O}_2 + \text{NO}_2$ has been studied by Adachi and Basco¹¹³ and Elfers et al.¹¹⁴ Adachi and Basco¹¹³ used flash photolysis/UV absorption technique to derive a rate constant of $1.2 \times 10^{-12} \text{ cm}^3 \text{ molecule}^{-1} \text{ s}^{-1}$ for this reaction which was independent of pressure over the range 44–676 Torr of argon. As noted above the measurements of Adachi and Basco¹¹³ may be subject to large systematic errors. Elfers et al.¹¹⁴ studied the kinetics of the reaction of $\text{C}_2\text{H}_5\text{O}_2$ radicals with NO_2 using a relative rate approach by measuring the rate of reaction of $\text{C}_2\text{H}_5\text{O}_2$ with NO_2 relative to that with NO at ambient temperature at pressures of ~ 8 –755 Torr of N_2/O_2 mixtures:



The reacting species were prepared by the photolysis of $\text{Cl}_2/\text{C}_2\text{H}_6/\text{NO}_x/\text{O}_2/\text{N}_2$ mixtures and FTIR spectroscopy was used to monitor changes in the concentrations of NO , NO_2 , and $\text{C}_2\text{H}_5\text{O}_2\text{NO}_2$. The results were placed upon an absolute basis using a value of 8.9×10^{-12} for the rate constant of the reaction with NO .¹⁰⁵ Using the Troe formalism the authors proposed use of the following falloff parameters: $k_0 = 4.8 \times 10^{-29} [\text{N}_2] \text{ cm}^3 \text{ molecule}^{-1} \text{ s}^{-1}$, $k_\infty = 1.0 \times 10^{-11} \text{ cm}^3 \text{ molecule}^{-1} \text{ s}^{-1}$, with $F_c = 0.3$. Further work is needed to better define the kinetics of the reaction of ethyl peroxy radicals with NO_2 . Nevertheless, we recommend use of the expression derived by Elfers et al.¹¹⁴

D. $(\text{CH}_3)_2\text{CHO}_2 + \text{NO}_2$

The kinetics of the reaction of $(\text{CH}_3)_2\text{CHO}_2 + \text{NO}_2$ has been studied by Adachi and Basco¹⁰⁶ using a flash photolysis UV absorption technique at 298 K to derive a rate constant of $5.6 \times 10^{-12} \text{ cm}^3 \text{ molecule}^{-1} \text{ s}^{-1}$ independent of pressure over the range 55–400 Torr of argon. As noted above the measurements of Adachi and Basco¹⁰⁶ may be subject to large systematic errors, in the absence of confirmatory measurements no recommendation is made.

E. $\text{CF}_2\text{ClO}_2 + \text{NO}_2$

The kinetics of the reaction $\text{CF}_2\text{ClO}_2 + \text{NO}_2$ has been studied by Moore and Carr¹¹⁷ using flash photolysis coupled with time-resolved mass spectrometry over the pressure range 1–10 Torr in CF_2ClBr at 298 K. At the pressures investigated the reaction is in the falloff region between second- and third-order kinetic behavior.

Moore and Carr¹¹⁷ fitted their kinetic data to the Troe expression

$$k(M,T) = k_0(T)[M]/[1 + [k_0[M]/k_\infty(T)]] \times F_c^{[1 + \log_{10}[k_0(T)[M]/k_\infty(T)]]^{-1}}$$

using $k_0 = 3.5 \pm 1.8 \times 10^{-29} \text{ cm}^6 \text{ molecule}^{-2} \text{ s}^{-1}$, $k_\infty = 5.2 \times 10^{-12} \text{ cm}^3 \text{ molecule}^{-1} \text{ s}^{-1}$, and $F_c = 0.6$.

The kinetic data obtained by Moore and Carr are consistent with the trend observed in the reactions of $\text{CF}_x\text{Cl}_{3-x}\text{O}_2$ reactions with NO_2 ; both k_0 and k_∞ increase with the number of Cl atoms in the peroxy radical. Measurements of the kinetics of the reaction of CF_2ClO_2 with NO_2 as a function of temperature at high pressures are necessary to better define the high-pressure limit and its temperature dependence. We recommend use of the expression of Moore and Carr for this reaction at 298 K.

F. $\text{CFCl}_2\text{O}_2 + \text{NO}_2$

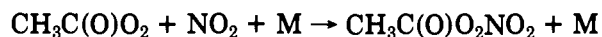
The kinetics of the reaction of CFCl_2O_2 with NO_2 has been studied by Lesclaux and Caralp¹⁰⁷ and Caralp et al.¹¹⁸ using laser flash photolysis of CFCl_3 in the presence of O_2 and NO_2 . Rate constant data were measured over the pressure range 1–12 Torr of oxygen at either 298 K¹⁰⁷ or 233, 298, and 373 K.¹¹⁸ At 298 K the results from both studies by Caralp and co-workers are in agreement. At the pressures investigated this reaction is in the falloff region between second- and third-order kinetic behavior. Caralp et al.¹⁰⁷ fitted their kinetic data to the Troe formalism with a temperature-dependent F_c value given by $F_c = \exp(-T/342)$. DeMore et al.⁹⁰ have shown that the data of Caralp et al.¹⁰⁷ can equally well be fitted by the Troe formalization with F_c held constant at $F_c = 0.6$. For the sake of simplicity and consistency with the bulk of the data reported in the present review we recommend use of the expression given by DeMore et al.⁹⁰

$$k(M,T) = k_0(T)[M]/[1 + [k_0[M]/k_\infty(T)]] \times F_c^{[1 + \log_{10}[k_0(T)[M]/k_\infty(T)]]^{-1}}$$

using $k_0 = [(3.5 \pm 0.5) \times 10^{-29}](T/300)^{[-5 \pm 1]} \text{ cm}^6 \text{ molecule}^{-2} \text{ s}^{-1}$, $k_\infty = [(6.0 \pm 1.0) \times 10^{-12}](T/300)^{[-2.5 \pm 1]} \text{ cm}^3 \text{ molecule}^{-1} \text{ s}^{-1}$, and $F_c = 0.6$.

G. $\text{CH}_3\text{C}(\text{O})\text{O}_2 + \text{NO}_2$

The kinetics of the reaction of acetyl peroxy radicals, $\text{CH}_3\text{C}(\text{O})\text{O}_2$, with NO_2 was first studied by Cox and Roffey¹³¹ and Hendry and Kenley.¹³² In both of these studies the measured experimental parameter was the rate of the reverse reaction, i.e. the thermal decomposition of PAN. By using estimates of the thermochemistry of the system the equilibrium constant was estimated and then the rate of the association reaction was calculated.



The results from both studies are in good agreement, yielding estimates of the rate constant $k = 1.4$ and $1.0 \times 10^{-12} \text{ cm}^3 \text{ molecule}^{-1} \text{ s}^{-1}$ at 1 atm pressure of either air or N_2 , respectively,^{131,132} with an estimated uncertainty of ± 1 order of magnitude.

The first absolute study of the kinetics of the reaction of acetyl peroxy radicals with NO_2 was performed by

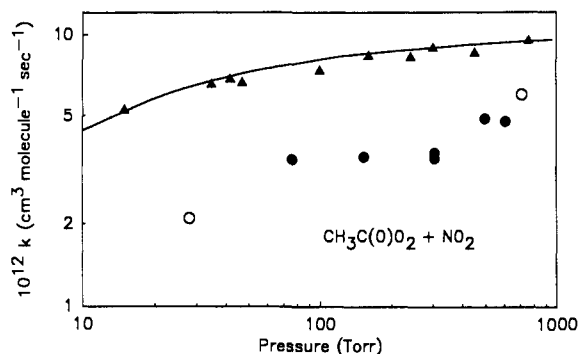


Figure 29. Falloff plot for the reaction $\text{CH}_3\text{C}(\text{O})\text{O}_2 + \text{NO}_2$ at 298 K in nitrogen diluent. Data is taken from Addison et al.⁵⁷ (open circles), Basco and Parmer⁵⁸ (filled circles), and Bridier et al.¹¹⁶ (triangles). The solid line is our recommendation.

Addison et al.⁵⁷ using the molecular modulation technique. As expected for an association reaction Addison et al.⁵⁷ observed a significant effect of pressure with the rate constant decreasing by a factor of 3 over the pressure range 715–28 Torr of added nitrogen. This behavior was confirmed by Basco and Parmer.¹¹⁵ In the latest and most comprehensive study of the kinetics of the reaction of acetyl peroxy radicals with NO_2 , Bridier et al.¹¹⁶ have employed the flash photolysis technique to measure the kinetics of this reaction at total pressures between 15 and 760 Torr and temperatures in the range 248–393 K. Figure 29 shows the kinetic data reported by Addison,⁵⁷ Basco and Parmer,¹¹⁵ and Bridier et al.¹¹⁶ as a function of pressure at 298 K. As seen from this figure the latest data from Bridier et al.¹¹⁶ is a factor of 2 higher than previously reported by Addison⁵⁷ and Basco and Parmer.¹¹⁵ As discussed by Bridier et al.¹¹⁶ the origin of this discrepancy probably lies in the different chemical mechanism used to simulate the observed behavior of the UV absorption. The chemical mechanism used by Bridier et al.¹¹⁶ is more complete than those used in the earlier studies and so the results of Bridier et al.¹¹⁶ are to be preferred. For consistency with the other three-body association reactions we have fit the 298 K data of Bridier et al.¹¹⁶ to the Troe expression:

$$k(M,T) = k_0(T)[M]/[1 + [k_0[M]/k_\infty(T)]] \times F_c^{[1 + \log_{10}[k_0(T)[M]/k_\infty(T)]]^{-1}}$$

with F_c fixed at 0.3 (as recommended by Bridier et al.¹¹⁶) to obtain our recommendation of $k_0 = [(2.0 \pm 0.5) \times 10^{-28}](T/298)^{[-7.1 \pm 1.7]} \text{ cm}^6 \text{ molecule}^{-2} \text{ s}^{-1}$, $k_\infty = [(1.1 \pm 0.1) \times 10^{-12}](T/298)^{[-0.9 \pm 0.15]} \text{ cm}^3 \text{ molecule}^{-1} \text{ s}^{-1}$. Temperature dependencies were taken directly from Bridier et al.¹¹⁶ At 760 Torr of air this expression yields $k = 9.4 \times 10^{-12} \text{ cm}^3 \text{ molecule}^{-1} \text{ s}^{-1}$. Uncertainties are estimated to be $\pm 40\%$.

There is a clear need for further studies of the kinetics of this atmospherically important reaction to check the data reported by Bridier et al.¹¹⁶ over as wide a range of temperature and pressure as possible. The large impact of uncertainties in the temperature dependence of this reaction on our understanding of tropospheric ozone formation has been discussed by Dodge.¹⁴² In addition to the direct experimental studies reported above there have been a number of indirect studies in which relative rate techniques have been used. In these studies the competition between reaction

TABLE VIII. Recommended Absorption Cross Sections for Peroxy Radicals

wavelength (nm)	σ (10^{-20} cm ² molecule ⁻¹)												
	CH ₃ O ₂	C ₂ H ₅ O ₂	<i>n</i> - C ₃ H ₇ O ₂ ^a	<i>i</i> - C ₃ H ₇ O ₂ ^a	<i>t</i> - C ₄ H ₉ O ₂	(CH ₃) ₂ - CCH ₂ O ₂	CH ₂ - ClO ₂ ^a	CH ₂ - FO ₂ ^a	HOCH ₂ - O ₂ ^a	CH ₂ - ClCH ₂ O ₂ ^a	HOCH ₂ - CH ₂ O ₂ ^a	CH ₃ - COO ₂ ^a	CH ₃ - OCH ₂ O ₂ ^a
195												428	
200	165							273				702	
205	190										79	797	
207												814	
210	212				136	225	245	340	305	215	112	771	340
215	268	230	205		210	265	285	400	325		147	612	360
220	327	282	249	264	285	320	305	460	342	270	179	488	395
225	386	330	321	405	361	385	345	475	355		210	355	400
230	430	376	385	474	412	455	370	460	365	355	235	291	400
235	443	408	478	492	440	505	375	415	365	390	255	300	390
240	442	415	423	487	446	525	370	370	355	400	264	313	365
245	426	406	408	469	430	540	340	320	335	390	259	317	335
250	392	379	382	441	398	520	314	265	305	365	245	287	295
255	362	338	352	400	350	500	275	210	265	325		253	260
260	318	296	315	354	298	450	240	155	216	280	198	214	220
265	279	245	272	295	245	415	200	125	165	220		184	175
270	238	192	223	231	193	350	160	85	123	180	122	146	140
275	161	149	166	156	150	285	120	70	90			120	
280	145	112	138	123	106	220	90	50	65	110	58	94	80
285	104	85				170				85			
290	66	60				120	30	30		45	21		35
295	42	45				75							
300	8	25				25							

^a Recommendation based upon one measurement.

of acetyl peroxy radicals with either NO or NO₂ has been measured, results from these studies are discussed in the section dealing with the reaction of acetyl peroxy radicals and NO.

H. CCl₃O₂ + NO₂

The kinetics of the reaction CCl₃O₂ + NO₂ has been studied by Caralp et al.¹⁰⁷ using pulsed laser photolysis and time-resolved mass spectroscopy in the pressure range 1–10 Torr over the temperature range 233–373 K. These workers fitted their kinetic data to the Troe formalism with a temperature dependent F_c value given by $F_c = \exp(-T/260)$. DeMore et al.⁹⁰ have shown that the data of Caralp et al.¹⁰⁷ can equally well be fitted by the Troe formalization with F_c held constant at $F_c = 0.6$. For the sake of simplicity and consistency with the bulk of the data reported in the present review we recommend use of the expression given by DeMore et al.⁹⁰

$$k(M, T) = k_0(T)[M]/[1 + [k_0[M]/k_\infty(T)]] \times F_c^{[1 + \log_{10}[k_0(T)[M]/k_\infty(T)]]^2}$$

using $k_0 = (5.0 \pm 1.0 \times 10^{-29})(T/300)^{[5 \pm 1]}$ cm⁶ molecule⁻² s⁻¹, $k_\infty = [(6.0 \pm 1.0) \times 10^{-12}](T/300)^{[-2.5 \pm 1]}$ cm³ molecule⁻¹ s⁻¹, and $F_c = 0.6$.

I. CF₃O₂ + NO₂

The kinetics of the reaction CF₃O₂ + NO₂ has been studied by Caralp et al.¹⁰⁷ using pulsed laser photolysis and time-resolved mass spectroscopy in the pressure range 1–10 Torr over the temperature range 233–373 K. These workers fitted their kinetic data to the Troe formalism with a temperature-dependent F_c value given by $F_c = \exp(-T/416)$. DeMore et al.⁹⁰ have shown that the data of Caralp et al.¹⁰⁷ can equally well be fitted by the Troe formalization with F_c held constant at $F_c = 0.6$. For the sake of simplicity and consistency with the bulk of the data reported in the present review we

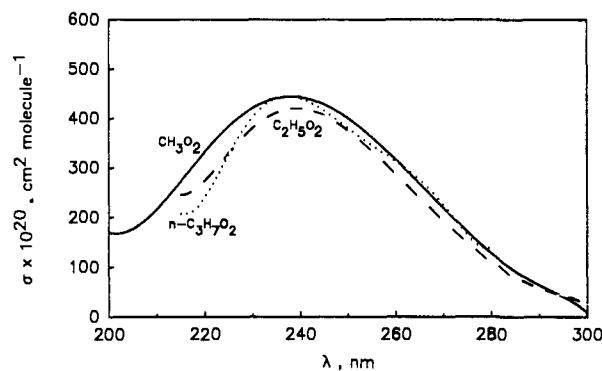


Figure 30. Recommended spectra for methyl, ethyl, and *n*-propyl peroxy radicals.

recommend use of the expression given by DeMore et al.⁹⁰

$$k(M, T) = k_0(T)[M]/[1 + [k_0[M]/k_\infty(T)]] \times F_c^{[1 + \log_{10}[k_0(T)[M]/k_\infty(T)]]^2}$$

using $k_0 = [(2.2 \pm 0.5) \times 10^{-29}](T/300)^{[-5 \pm 1]}$ cm⁶ molecule⁻² s⁻¹, $k_\infty = [(6.0 \pm 1.0) \times 10^{-12}](T/300)^{[-2.5 \pm 1]}$ cm³ molecule⁻¹ s⁻¹, and $F_c = 0.6$.

VII. Discussion

A. Absorption Spectra

Recommended values for the absorption cross sections of various peroxy radicals are given in Table VIII and are plotted in Figures 30–35. From these figures it can be seen that, with the exceptions of CH₃C(O)C-H₂O₂ and CH₃C(O)O₂, the general shapes of all the alkyl peroxy absorption spectra are similar with broad featureless absorptions maximizing at 225–245 nm. This fact is not surprising as the absorption arises through an electronic transition within orbitals associated with the peroxy group. Spectral assignment of the electronic transition is not straightforward. The lack of structure

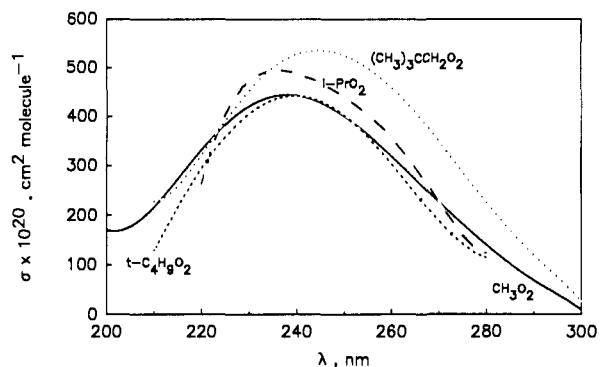


Figure 31. Recommended spectra of isopropyl, *tert*-butyl, and neopentyl peroxy radicals. The recommended spectrum of methyl peroxy radicals is included for comparison.

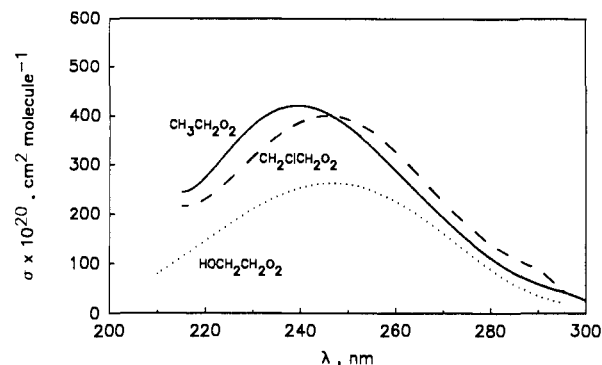


Figure 34. Recommended spectra of ethyl, 2-chloroethyl, and 2-hydroxyethyl peroxy radicals.

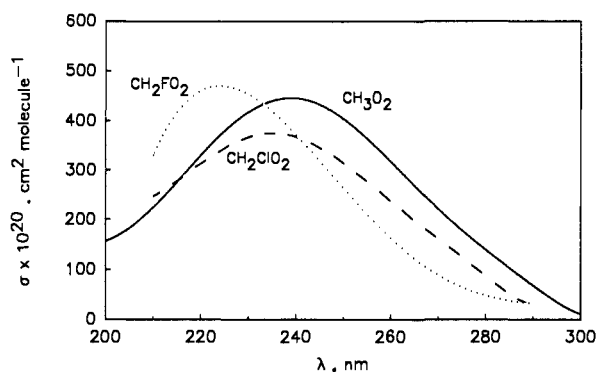


Figure 32. Recommended spectra of chloro- and fluoromethyl peroxy radicals compared to that of methyl peroxy radicals.

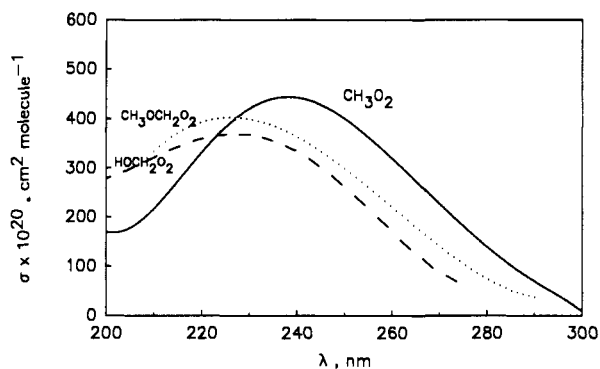


Figure 33. Recommended spectra of methoxy- and hydroxy-methyl peroxy radicals compared to that of methyl peroxy radicals.

on the absorption feature precludes an unambiguous assignment. In addition, the low (or lack of) symmetry in the peroxy radicals is a complicating factor. We make no recommendation for the assignment. A priori, the substitution of a variety of different chemical groups, X, in the radical CH_2XO_2 would not be expected to have a profound effect on the absorption spectrum. In the case of $\text{CH}_3\text{COCH}_2\text{O}_2$ and $\text{CH}_3\text{C}(\text{O})\text{O}_2$ the situation is complicated by the presence of two chromophores, the carbonyl group and the peroxy moiety. The UV spectra of both these radicals show two broad features (see Figure 35), indicating two different electronic transitions. The shorter wavelength feature is presumably associated with an allowed $\pi \rightarrow \pi^*$ transition (observed at about 180 nm in aldehydes¹⁴³) with the longer wavelength transition ascribed to a transition in the peroxy moiety.

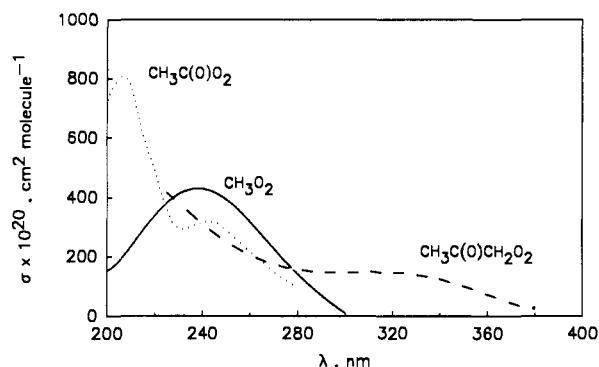


Figure 35. Recommended spectrum of acetyl and acetyl peroxy radical compared with that of methyl peroxy radical.

Our recommendations for CH_2ClO_2 , CH_2FO_2 , HOCH_2O_2 , $i\text{-PrO}_2$, $\text{ClCH}_2\text{CH}_2\text{O}_2$, $\text{HOCH}_2\text{CH}_2\text{O}_2$, $\text{CH}_3\text{OCH}_2\text{O}_2$, and $\text{CH}_3\text{COCH}_2\text{O}_2$ are based upon single experimental determinations and are thus subject to significant uncertainties. We estimate these uncertainties to be $\pm 25\%$. Further experimental investigations of these spectra are needed. In the case of CH_3O_2 our recommendation is based on the average value of six laboratory studies and we estimate the uncertainty of this to be $\pm 15\%$. The recommended absorption spectra of $\text{C}_2\text{H}_5\text{O}_2$, $t\text{-C}_4\text{H}_9\text{O}_2$, and neopentyl peroxy are based on at least two experimental determinations; we estimate the uncertainty associated with these recommendation to be $\pm 20\%$. Since our spectrum for CH_3O_2 is the most certain we feel that it is useful to compare and contrast the other peroxy radical spectra to that of CH_3O_2 .

As seen from Figures 30 and 31, with the exception of the 210-nm value for $t\text{-C}_4\text{H}_9\text{O}_2$, our recommended absorption spectra for CH_3O_2 , $\text{C}_2\text{H}_5\text{O}_2$, $n\text{-C}_3\text{H}_7\text{O}_2$, $i\text{-C}_3\text{H}_7\text{O}_2$, and $t\text{-C}_4\text{H}_9\text{O}_2$ are, for practical purposes, indistinguishable. Interestingly however, as seen from Figure 31, the peak absorption cross section for $(\text{C}-\text{H}_3)_3\text{CCH}_2\text{O}_2$ is larger than that of CH_3O_2 by approximately 20% and is shifted by 10 nm to the red. This is somewhat surprising in light of the fact that spectra of all the other unsubstituted alkyl peroxy radicals are so similar. Further studies of the absorption spectra of $t\text{-C}_4\text{H}_9\text{O}_2$, $i\text{-C}_3\text{H}_7\text{O}_2$, and $(\text{CH}_3)_3\text{CCH}_2\text{O}_2$ would be useful.

Figures 32 and 33 compare the spectra of CH_2ClO_2 , CH_2FO_2 , HOCH_2O_2 , and $\text{CH}_3\text{OCH}_2\text{O}_2$ to that of CH_3O_2 . From these figures it can be seen that the absorption maxima for fluoromethyl peroxy is shifted approximately 15 nm to shorter wavelength than methyl peroxy

TABLE IX. Recommended Data for Self-Reactions of Peroxy Radicals

T (K)	k ($\text{cm}^3 \text{ molecule}^{-1} \text{ s}^{-1}$)	
	$\text{CH}_3\text{O}_2 + \text{CH}_3\text{O}_2 \rightarrow \text{CH}_3\text{O} + \text{CH}_3\text{O} + \text{O}_2$	(a)
	$\rightarrow \text{HCHO} + \text{CH}_3\text{OH} + \text{O}_2$	(b)
	$\rightarrow \text{CH}_3\text{OOCH}_3 + \text{O}_2$	(c)
250-600	$k_a/k = 1.24 - 280/T$	
230-600	$k_{\text{obs}} = [(2.5 \pm 0.3) \times 10^{-13}] \exp[(180 \pm 40)/T]$	
250-600	$k_{\text{true}} = [9.2 \times 10^{-14}] \exp(390/T)$	
	$\text{C}_2\text{H}_5\text{O}_2 + \text{C}_2\text{H}_5\text{O}_2 \rightarrow \text{C}_2\text{H}_5\text{O} + \text{C}_2\text{H}_5\text{O} + \text{O}_2$	(a)
	$\rightarrow \text{CH}_3\text{CHO} + \text{C}_2\text{H}_5\text{OH} + \text{O}_2$	(b)
	$\rightarrow \text{C}_2\text{H}_5\text{OOC}_2\text{H}_5 + \text{O}_2$	(c)
250-416	$k_a/k = 1.33 - 209/T$	
260-380	$k_{\text{obs}} = [(2.1 \pm 1.0) \times 10^{-13}] \exp[-(250 \pm 130)/T]$	
260-380	$k_{\text{true}} = [8.5 \times 10^{-14}] \exp[-(125/T)]$	
	$\text{CH}_2\text{ClO}_2 + \text{CH}_2\text{ClO}_2 \rightarrow \text{CH}_2\text{ClO} + \text{CH}_2\text{ClO} + \text{O}_2$	(a)
	$\rightarrow \text{other products}$	(b)
300	$k_a/k > 0.9$	
250-500	$k_{\text{obs}} = [(3.1 \pm 1.1) \times 10^{-13}] \exp[(735 \pm 95)/T]$	
	$\text{CH}_2\text{FO}_2 + \text{CH}_2\text{FO}_2 \rightarrow \text{products}$	
250-500	$k_{\text{obs}} = [(3.3 \pm 1.2) \times 10^{-13}] \exp[(700 \pm 100)/T]$	
	$\text{HOCH}_2\text{O}_2 + \text{HOCH}_2\text{O}_2 \rightarrow \text{HOCH}_2\text{O} + \text{HOCH}_2\text{O} + \text{O}_2$	(a)
	$\text{HOCH}_2\text{O}_2 + \text{HOCH}_2\text{O}_2 \rightarrow \text{HC(O)OH} + \text{CH}_2(\text{OH})_2 + \text{O}_2$	(b)
300	$k_a/k = 0.9$	
270-320	$k_b = (5.65 \times 10^{-14}) \exp[(750 \pm 400)/T]$	
	$\text{CH}_2\text{ClCH}_2\text{O}_2 + \text{CH}_2\text{ClCH}_2\text{O}_2 \rightarrow \text{CH}_2\text{ClCH}_2\text{O} + \text{CH}_2\text{ClCH}_2\text{O} + \text{O}_2$	(a)
	$\rightarrow \text{CH}_2\text{ClCHO} + \text{CH}_2\text{ClCH}_2\text{OH} + \text{O}_2$	(b)
295	$k_a/k = 0.7$	
230-380	$k_{\text{obs}} = [(1.1 \pm 0.7) \times 10^{-13}] \exp[(1020 \pm 170)/T]$	
	$\text{HOCH}_2\text{CH}_2\text{O}_2 + \text{HOCH}_2\text{CH}_2\text{O}_2 \rightarrow \text{HOCH}_2\text{CH}_2\text{O} + \text{HOCH}_2\text{CH}_2\text{O} + \text{O}_2$	(a)
	$\text{HOCH}_2\text{CH}_2\text{O}_2 + \text{HOCH}_2\text{CH}_2\text{O}_2 \rightarrow \text{HOCH}_2\text{CH}_2\text{OH} + \text{HOCH}_2\text{CHO} + \text{O}_2$	(b)
298	$k_a/k = 0.18$	
298	$k_{\text{obs}} = (1.60 \pm 0.17) \times 10^{-12}$	
298	$k = (1.36 \pm 0.21) \times 10^{-12}$	
	$\text{CH}_3\text{C(O)O}_2 + \text{CH}_3\text{(O)O}_2 \rightarrow \text{CH}_3\text{C(O)O} + \text{CH}_3\text{(O)O} + \text{O}_2$	(a)
	$\text{CH}_3\text{C(O)O}_2 + \text{CH}_3\text{(O)O}_2 \rightarrow \text{other products}$	(b)
250-370	$k = [(2.8 \pm 0.5) \times 10^{-12}] \exp[(530 \pm 100)/T]$	
	$2 n\text{-C}_3\text{H}_7\text{O}_2 \rightarrow 2 n\text{-C}_3\text{H}_7\text{O} + \text{O}_2$	(a)
	$\rightarrow n\text{-C}_3\text{H}_7\text{OH} + \text{C}_3\text{H}_6\text{O} + \text{O}_2$	(b)
298	$k = (2.9 \pm 0.9) \times 10^{-13}$	
	$2 (\text{CH}_3)_2\text{CHO}_2 \rightarrow 2 (\text{CH}_3)_2\text{CHO} + \text{O}_2$	(a)
	$\rightarrow (\text{CH}_3)_2\text{CHOH} + \text{CH}_3\text{COCH}_3 + \text{O}_2$	(b)
300-373	$k_a = [(2.3 \pm 0.4) \times 10^{-12}] \exp[-(2560 \pm 180)/T]$	
300-373	$k_b = [(4.1 \pm 0.5) \times 10^{-14}] \exp[-(1440 \pm 120)/T]$	
	$2 (\text{CH}_3)_3\text{CO}_2 \rightarrow 2 (\text{CH}_3)_3\text{CO} + \text{O}_2$	(a)
	$\rightarrow ((\text{CH}_3)_3\text{CO})_2 + \text{O}_2$	(c)
290-420	$k_{\text{obs}} = (4.1 \pm 10^{-11}) \exp(-4200/T)$	
290-420	$k_{\text{true}} = (9.5 \times 10^{-12}) \exp(-3894/T)$	

and is $\sim 10\%$ more intense. In contrast the absorption spectrum for chloromethyl peroxy has an absorption maximum at the same wavelength as methyl peroxy and is $\sim 10\%$ less intense. The spectra of hydroxymethyl peroxy and methoxymethyl peroxy appear to be shifted to shorter wavelength by about 15 nm and reduced slightly in intensity.

Finally, Figure 34 shows a comparison of our recommended spectra for $\text{CH}_2\text{ClCH}_2\text{O}_2$ and $\text{HOCH}_2\text{CH}_2\text{O}_2$ with that of $\text{C}_2\text{H}_5\text{O}_2$. From this figure it can be seen that the spectrum of chloroethyl peroxy is nearly indistinguishable from that of $\text{C}_2\text{H}_5\text{O}_2$ while that of $\text{HOCH}_2\text{CH}_2\text{O}_2$ has the same shape but is reduced in intensity by approximately 35%. The contrast between $\text{HOCH}_2\text{CH}_2\text{O}_2$ and $\text{C}_2\text{H}_5\text{O}_2$ versus HOCH_2O_2 and CH_3O_2 may reflect possible interaction of the hydroxy H with the peroxy group in $\text{HOCH}_2\text{CH}_2\text{O}_2$ via a six-membered ring. Further investigations of the $\text{HOCH}_2\text{CH}_2\text{O}_2$ UV spectrum would be useful.

At this point it is appropriate to note that while UV absorption spectroscopy offers a convenient, sensitive method for monitoring peroxy radicals in kinetic studies there is a fundamental limitation to this technique. This limitation is that the UV absorptions of all the alkyl peroxy absorption spectra are similar and in some

cases indistinguishable (see for example Figures 30 and 31). Thus, in general, UV absorption spectroscopy is not well suited to the simultaneous detection of different peroxy radicals. Future advances in our understanding of peroxy radical chemistry may require the use of more selective monitoring techniques. One promising candidate is infrared spectroscopy. However, at present infrared spectral data exists for comparatively few peroxy radicals (see the recent compilation by Jacox and Dal-Favero¹⁴⁴); further work is needed in this area.

B. Kinetics and Mechanisms of Self-Reactions

Table IX lists our recommendations for the kinetics and mechanistic for the self-reaction of peroxy radicals. Whereas in Table III values for k_{obs} are reported without corrections for secondary chemistry, in Table IX such corrections are reflected in the recommendations wherever possible.

The effect of temperature on our recommended kinetic and mechanistic data for the self-reactions of peroxy radicals is shown in Figures 36-38. From these figures a number of interesting points arise.

(i) The kinetics of the self-reactions of peroxy radicals

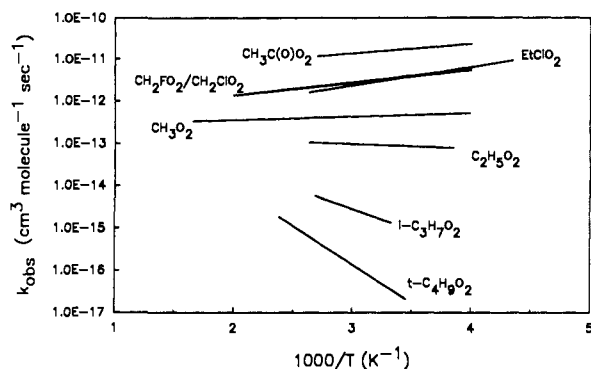


Figure 36. Recommended kinetic data for the observed second-order rate constant, k_{obs} , for the self-reaction of alkyl peroxy radicals.

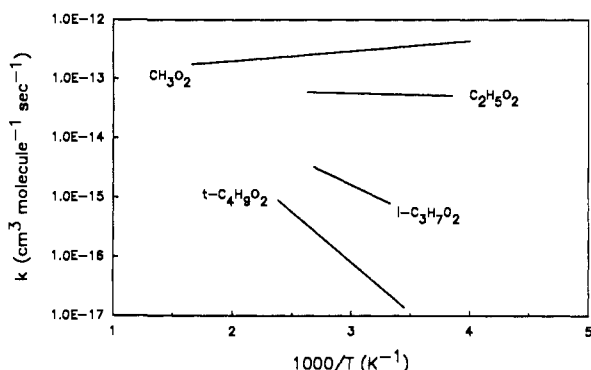


Figure 37. Recommended kinetic data for the true second-order rate constant for the self-reaction of alkyl peroxy radicals.

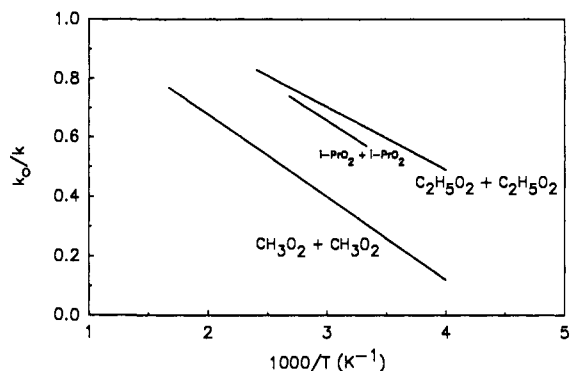


Figure 38. Recommended data for the branching ratio k_a/k for the self-reaction of methyl, ethyl, and isopropyl peroxy radicals.

vary greatly with the identity of the peroxy radical, spanning 6 orders of magnitude.

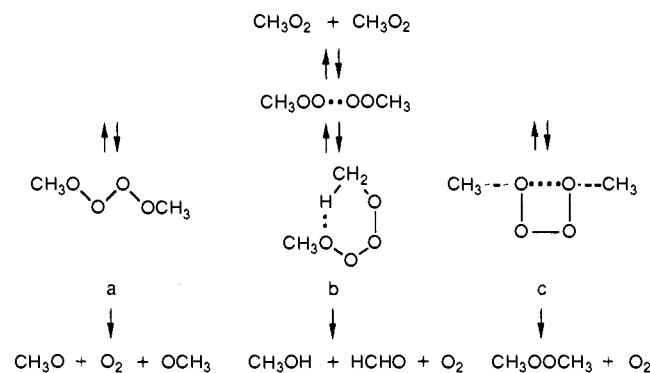
(ii) As seen from Figure 36 there is a trend in temperature dependence of k_{obs} with reactivity of the RO_2 radical. The least reactive radical shows the most positive temperature dependence. As the reactivity of the radical increases through the series $t\text{-C}_4\text{H}_9\text{O}_2$ to $i\text{-C}_3\text{H}_7\text{O}_2$ to $\text{C}_2\text{H}_5\text{O}_2$ the temperature dependence becomes less pronounced. At CH_3O_2 there is a slight negative temperature dependence. For the most reactive RO_2 radicals a significant negative temperature dependence is observed.

(iii) The same trend of large positive temperature dependence at low reactivity moving to a negative temperature dependence with more reactive radicals is observed in the data shown in Figure 37 for values of the rate constants of self-reaction corrected for loss of peroxy radicals via secondary reactions.

(iv) The majority of the reactions proceed via two main channels, with evidence for the existence of a third, minor channel, forming ROOR in a few systems. As seen from Figure 38, in all cases where studies of the branching ratios have been performed as a function of temperature, the observed trend is a rapid increase in the importance of channel a with increasing temperature and conversely a rapid decrease in the importance of the molecular channel b. The data from Figures 37 and 38 together show that the absolute magnitude of the rate constant for channel a shows a positive temperature dependence whereas channel b displays a negative temperature dependence.

(v) For methyl and ethyl peroxy self-reactions, despite the fact that there is a major change in the branching ratio over the temperature range studied, there is a relatively small change in the rate constant of the overall reaction over the temperature range.

The above observations can be rationalized in terms of the mechanism of self-reaction which is thought to involve the initial formation of a weakly bound tetraoxide adduct, RO_4R , which either decomposes back to reactants or rearranges to form products. Infrared absorptions consistent with this adduct have been observed in the self-reaction of CH_3O_2 by Ase et al.¹⁴⁵ studied using matrix isolation techniques. The mechanism of the self-reaction of peroxy radicals is thought to proceed via the following mechanism (CH_3O_2 used as example):



Pathway a involves the decomposition of the tetraoxide intermediate by the breaking of two O-O bonds (either concerted or stepwise) from a transition state that may be linear or cyclic. Pathway b was first suggested by Russell¹⁴⁶ and involves the formation of a six-membered ring by the partial formation of a H-O bond. The hydrogen is then transferred to form an alcohol, aldehyde, and O_2 . Pathway c, which is of minor importance, is thought to proceed via a four-membered ring to form the peroxide.

The above mechanism can be used to rationalize the observed trends in the kinetic and branching ratio data noted. Firstly, the large variation in reactivity observed experimentally is consistent with the formation of a somewhat constrained intermediate where the steric hindrance of, for example, a *tert*-butyl or isopropyl group will lead to a considerable decrease in reactivity. Secondly, the formation of a short-lived tetraoxide adduct can be used to explain the observed trend in decreasing temperature dependence with increasing reactivity. With the slower reacting species such as *tert*-butyl and isopropyl peroxy radicals the rate-determining step is the rearrangement and decomposition

TABLE XII. Recommended Kinetic Parameters for NO₂ + Peroxy Radical Reactions

peroxy radical	k_o (cm ⁶ molecule ⁻² s ⁻¹)	k_∞ (cm ³ molecule ⁻¹ s ⁻¹)	F_c
HO ₂	$(1.8 \times 10^{-31})(T/300)^{-3.2}$	$(4.7 \times 10^{-12})(T/300)^{-1.4}$	0.6
CH ₃ O ₂	$(2.3 \times 10^{-30})(T/300)^{-2.5 \pm 1}$	$(8.0 \times 10^{-12})(T/300)^{-3.5}$	0.4
C ₂ H ₅ O ₂	4.8×10^{-29}	1.0×10^{-11}	0.3
CH ₃ C(O)O ₂	$[(2.0 \pm 0.5) \times 10^{-28}](T/298)^{-7.1 \pm 1.7}$	$[(1.1 \pm 0.1) \times 10^{-11}](T/298)^{-0.9 \pm 0.15}$	0.3
CF ₂ ClO ₂	3.5×10^{-29}	5.2×10^{-12}	0.6
CFCl ₂ O ₂	$[(3.5 \pm 0.5) \times 10^{-29}](T/300)^{-15 \pm 1}$	$[(6.0 \pm 1.0) \times 10^{-12}](T/300)^{-2.5 \pm 1}$	0.6
CCl ₃ O ₂	$[(5.0 \pm 1.0) \times 10^{-29}](T/300)^{-15 \pm 1}$	$[(6.0 \pm 1.0) \times 10^{-12}](T/300)^{-2.5 \pm 1}$	0.6
CF ₃ O ₂	$[(2.2 \pm 0.5) \times 10^{-29}](T/300)^{-15 \pm 1}$	$[(6.0 \pm 1.0) \times 10^{-12}](T/300)^{-2.5 \pm 1}$	0.6

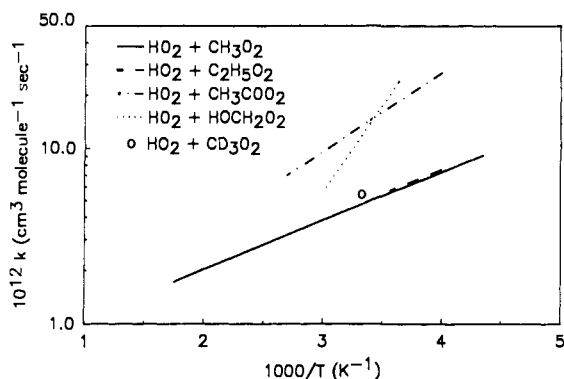
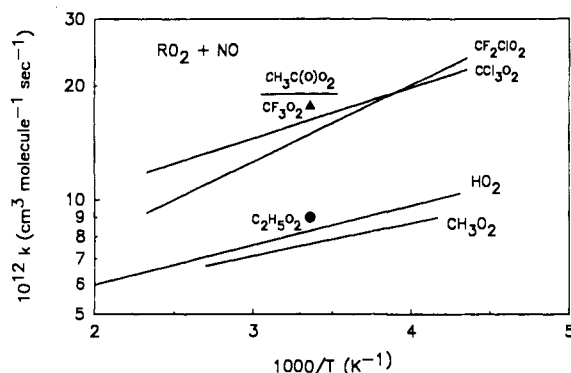
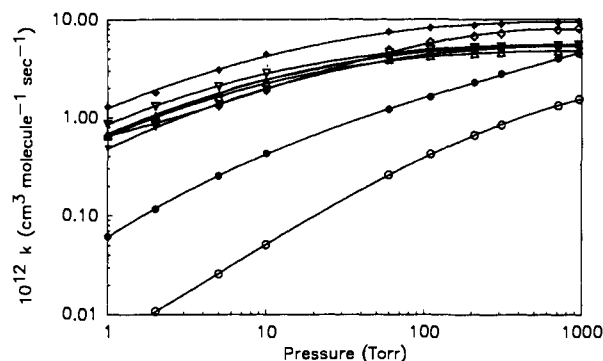
Figure 39. Recommended rate constants for HO₂ + RO₂ → products.

Figure 40. Recommended kinetic data for the reactions of peroxy radicals with NO.

general consistency between all reactions of this type. These reactions are rapid with rate constants at ambient temperature in the range $(0.7\text{--}2) \times 10^{-11}$ cm³ molecule⁻¹ s⁻¹, where recommendations are possible concerning the temperature dependence of the reactions a slight negative dependence is observed in all cases with the possible exception of the reaction with CH₃C(O)O₂ where data exist over a very limited temperature range, precluding the observation of any temperature dependence. In all cases reaction of RO₂ with NO are independent of pressure over the ranges studied (1–700 Torr) and the majority of the reaction proceeds via one channel to form an alkoxy radical plus NO₂.

The slight negative temperature dependence observed in the reactions of RO₂ radicals with NO may suggest that the reaction proceeds, at least in part, by a mechanism which involves the formation of a short-lived complex, ROONO, which dissociates into RO and NO₂ products.

Recommended kinetic data for the reactions of peroxy radicals with NO₂ are given in Table XII. Figure 41 shows a plot of our recommended kinetic data for the reaction of peroxy radicals with NO₂ at 298 K as a function of pressure over the range 1–1000 Torr (O₂,

Figure 41. Recommended kinetic data for the reactions of peroxy radicals with NO₂ at 298 K as a function of pressure. Data points were calculated using the rate expressions given in the text: HO₂ (open circles), CH₃O₂ (filled circles), CF₂ClO₂ (open triangles), CFCl₂O₂ (filled triangles), C₂H₅O₂ (open diamonds), CH₃C(O)O₂ (filled diamonds), CCl₃O₂ (open inverse triangles), and CF₃O₂ (filled inverse triangles). Solid lines are third-order fits.

N₂, or N₂/O₂ mixtures as third bodies). At pressures below 100 Torr all these reactions are in the falloff region between second- and third-order kinetics while at atmospheric pressure, 760 Torr, all reactions, with the exception of that of HO₂, are essentially at (within 20% of) the high-pressure limit.

The majority of our recommendations for the kinetics of the reactions of peroxy radicals with NO and NO₂ are based upon results from a single experimental study, and in many cases the experimental conditions were such that significant extrapolations are required to reach conditions typical of the atmosphere. In view of the importance of these reactions in models of atmospheric chemistry there is an urgent need for additional studies of these and other reactions of peroxy radicals with NO_x particularly as a function of temperature.

VIII. Conclusions

This article provides the first critical review of the ultraviolet spectra of alkyl peroxy radicals and the kinetics and mechanisms of the reactions of these radicals in the gas phase with other peroxy radicals, HO₂ radicals, and NO_x. Despite the substantial body of information available there remain large uncertainties associated with kinetics and mechanisms of many important aspects of the chemistry of these species. Of particular relevance to computer modeling of hydrocarbon oxidation in the atmosphere are the large uncertainties associated with both the kinetics and mechanisms of reactions of peroxy radicals with HO₂ radicals and the kinetics of the reaction of peroxy radicals with NO_x. Further experimental work, coupled with theoretical ab initio computational studies, is needed in these areas.

IX. Acknowledgment

We would like to thank Bob Hampson (National Institute of Standards and Technology) for helpful comments and suggestions.

Note Added in Proof. In a parallel, independent effort Drs. P. D. Lightfoot, R. A. Cox, J. N. Crowley, M. Destriau, G. D. Hayman, M. E. Jenkin, G. K. Moortgat, and F. Zabel have also reviewed the gas-phase peroxy radical literature data. Their review is complementary to ours and will be published essentially simultaneously in *Atmospheric Environment*. We thank these authors for sending us a preprint of their work.

X. References

- Finlayson-Pitts, B. J.; Pitts, J. N., Jr. *Atmospheric Chemistry*; Wiley: New York, 1986.
- Wayne, R. P. *Chemistry of Atmospheres*; Oxford University Press: Oxford, 1985.
- Madronich, S.; Calvert, J. G. *J. Geophys. Res.* **1990**, *95*, 5697.
- Paukert, T. T.; Johnston, H. S. *J. Chem. Phys.* **1972**, *56*, 2824.
- Cox, R. A.; Burrows, J. P. *J. Phys. Chem.* **1979**, *83*, 2560.
- Hochanadel, C. J.; Sworski, T. J.; Ogren, P. J. *J. Phys. Chem.* **1980**, *84*, 3274.
- Sander, S. P.; Peterson, M.; Watson, R. T.; Patrick, R. *J. Phys. Chem.* **1982**, *86*, 1236.
- McAdam, K.; Veyret, B.; Lesclaux, R. *Chem. Phys. Lett.* **1987**, *133*, 39.
- Kurylo, M. J.; Wallington, T. J.; Ouellette, P. A. *J. Photochem.* **1987**, *39*, 201.
- Moortgat, G. K.; Veyret, B.; Lesclaux, R. *J. Phys. Chem.* **1989**, *93*, 2362.
- Parkes, D. A.; Paul, D. M.; Quinn, C. P.; Robinson, R. C. *Chem. Phys. Lett.* **1973**, *23*, 425.
- Parkes, D. A. *Int. J. Chem. Kinet.* **1977**, *9*, 451.
- Kan, C. S.; McQuigg, R. D.; Whitbeck, M. R.; Calvert, J. C. *Int. J. Chem. Kinet.* **1979**, *11*, 921.
- Adachi, H.; Basco, N.; James, D. G. L. *Int. J. Chem. Kinet.* **1980**, *12*, 949.
- Pilling, M. J.; Smith, M. J. C. *J. Phys. Chem.* **1985**, *89*, 4713.
- Hochanadel, C. J.; Ghormley, J. A.; Boyle, J. W.; Ogren, P. J. *J. Phys. Chem.* **1977**, *81*, 3.
- Cox, R. A.; Tyndall, G. S. *Chem. Phys. Lett.* **1979**, *65*, 357.
- Cox, R. A.; Tyndall, G. S. *J. Chem. Soc. Faraday Trans. 2* **1980**, *76*, 153.
- Sander, S. P.; Watson, R. T. *J. Phys. Chem.* **1981**, *85*, 2960.
- Jenkin, M. E.; Cox, R. A.; Hayman, G. D.; Whyte, L. J. *J. Chem. Soc. Faraday Trans. 2* **1988**, *84*, 913.
- Dagaut, P.; Kurylo, M. J. *J. Photochem. Photobiol. A: Chem.* **1990**, *51*, 133.
- Simon, F.; Schneider, W.; Moortgat, G. K. *Int. J. Chem. Kinet.* **1990**, *22*, 791.
- Adachi, H.; Basco, N.; James, D. G. L. *Int. J. Chem. Kinet.* **1979**, *11*, 1211.
- Munk, J.; Pagsberg, P.; Ratajczak, E.; Sillesen, A. *J. Phys. Chem.* **1986**, *90*, 2752.
- Anastasi, C.; Brown, M. J.; Smith, D. B.; Waddington, D. J. Joint Meeting of the French and Italian Sections of the Combustion Institute, Amalfi, June 1987.
- Anastasi, C.; Waddington, D. J.; Woolley, A. *J. Chem. Soc., Faraday Trans. 1* **1983**, *79*, 505.
- Cattell, F. C.; Cavanagh, J.; Cox, R. A.; Jenkin, M. E. *J. Chem. Soc., Faraday 2* **1986**, *82*, 1999.
- Wallington, T. J.; Dagaut, P.; Kurylo, M. J. *J. Photochem. and Photobiol., A: Chem.* **1988**, *42*, 173.
- Adachi, H.; Basco, N. *Int. J. Chem. Kinet.* **1982**, *14*, 1125.
- Parkes, D. A. 15th Symposium (International) on Combustion, Tokyo 1974; The Combustion Institute: Pittsburgh, 1975; p 795.
- Kirsch, L. J.; Parkes, D. A. Proceedings of the 5th Int. Symposium on Gas Kinetics, Manchester, 1977; Royal Society of Chemistry: London, 1977; p 37.
- Anastasi, C.; Parkes, D. A.; Smith, I. W. M. Proceedings of the 5th Int. Symposium on Gas Kinetics, Manchester, 1977; Royal Society of Chemistry: London, 1977; p 60.
- Anastasi, C.; Smith, I. W. M.; Parkes, D. A. *J. Chem. Soc. Faraday Trans. 1* **1978**, *74*, 1693.
- Lightfoot, P. D.; Roussel, P.; Veyret, B.; Lesclaux, R. *J. Chem. Soc., Faraday Trans. 1990*, *86*, 2927.
- Dagaut, P.; Kurylo, M. J. *Int. J. Chem. Kinet.* **1990**, *22*, 1177.
- Cox, R. A.; Munk, J.; Nielsen, O. J.; Pagsberg, P.; Ratajczak, E. *Chem. Phys. Lett.* **1990**, *173*, 206.
- Dagaut, P.; Wallington, T. J.; Kurylo, M. J. *Int. J. Chem. Kinet.* **1988**, *20*, 815.
- Veyret, B.; Lesclaux, R.; Rayez, M.-T.; Rayez, J.-C.; Cox, R. A.; Moortgat, G. K. *J. Phys. Chem.* **1989**, *93*, 2368.
- Burrows, J. P.; Moortgat, G. K.; Tyndall, G. S.; Cox, R. A.; Jenkin, M. E.; Hayman, G. D.; Veyret, B. *J. Phys. Chem.* **1989**, *93*, 2375.
- Dagaut, P.; Wallington, T. J.; Kurylo, M. J. *Chem. Phys. Lett.* **1988**, *146*, 589.
- Jenkin, M. E.; Cox, R. A. *J. Phys. Chem.* **1990**, *95*, 3229.
- Dagaut, P.; Wallington, T. J.; Kurylo, M. J. *J. Photochem. Photobiol., A: Chem.* **1989**, *48*, 187.
- Jemi-Alade, A. A.; Lightfoot, P. D.; Lesclaux, R. *Chem. Phys. Lett.* **1991**, *179*, 119.
- Hochanadel, C. J.; Ghormley, J. A.; Ogren, P. J. *J. Chem. Phys.* **1972**, *56*, 4426.
- Kijewski, H.; Troe, J. *Helv. Chim. Acta* **1972**, *55*, 205.
- Lightfoot, P. D.; Veyret, B.; Lesclaux, R. *Chem. Phys. Lett.* **1988**, *150*, 120.
- Atkinson, R.; Baulch, D. L.; Cox, R. A.; Hampson, R. F.; Kerr, J. A.; Troe, J. *J. Phys. Chem., Ref. Data* **1989**, *18*, 881.
- Lightfoot, P. D.; Veyret, B.; Lesclaux, R. *J. Phys. Chem.* **1990**, *94*, 708.
- Troe, J. *Ber. Bunsen-Ges. Phys. Chem.* **1973**, *73*, 946.
- Plumb, I. C.; Ryan, K. R. *Int. J. Chem. Kinet.* **1981**, *13*, 1011.
- Slagle, I. R.; Feng, Q.; Gutman, D. *J. Phys. Chem.* **1984**, *88*, 3648.
- Wallington, T. J.; Andino, J. M.; Kaiser, E. W.; Japar, S. M. *Int. J. Chem. Kinet.* **1989**, *21*, 1113.
- Wagner, A. F.; Slagle, I. R.; Sarzynski, D.; Gutman, D. *J. Phys. Chem.* **1990**, *94*, 1853; **1991**, *95*, 1014.
- Kaiser, E. W.; Lorkovic, I. M.; Wallington, T. J. *J. Phys. Chem.* **1990**, *94*, 3352.
- Kirsch, L. J.; Parkes, D. A.; Waddington, D. J.; Woolley, A. *J. Chem. Soc., Faraday Trans. 1* **1978**, *74*, 2293.
- Lightfoot, P. D. Private communication.
- Addison, M. C.; Burrows, J. P.; Cox, R. A.; Patrick, R. *Chem. Phys. Lett.* **1980**, *73*, 283.
- Basco, N.; Parmar, S. S. *Int. J. Chem. Kinet.* **1985**, *17*, 891.
- Parkes, D. A. Proceedings of the 15th International Symposium on Combustion, Tokyo, 1974; The Combustion Institute: Pittsburgh, PA, 1974; p 795.
- Alcock, W. G.; Mile, B. *Combust. Flame* **1975**, *24*, 125.
- Weaver, J.; Meagher, J.; Shortridge, R.; Hecklen, J. *J. Photochem.* **1975**, *4*, 341.
- Selby, K.; Waddington, D. J. *J. Chem. Soc. Perkin Trans. 2* **1979**, *1259*.
- Kan, C. S.; Calvert, J. G.; Shaw, J. H. *J. Phys. Chem.* **1980**, *84*, 3411.
- Niki, H.; Maker, P. D.; Savage, C. M.; Breitenbach, L. P. *J. Phys. Chem.* **1981**, *85*, 877.
- Anastasi, C.; Couzens, P. J.; Waddington, D. J.; Brown, M. J.; Smith, D. B. 10th International Symposium on Gas Kinetics, Swansea, 1988; Royal Society of Chemistry: London, 1988.
- Lightfoot, P. D.; Lesclaux, R.; Veyret, B. *J. Phys. Chem.* **1990**, *94*, 700.
- Horie, O.; Crowley, J. N.; Moortgat, G. K. *J. Phys. Chem.* **1990**, *94*, 8198.
- Weaver, J.; Shortridge, R.; Meagher, J.; Hecklen, J. *J. Photochem.* **1975**, *4*, 109.
- Niki, H.; Maker, P. D.; Savage, C. M.; Breitenbach, L. P. *J. Phys. Chem.* **1982**, *86*, 3825.
- Wallington, T. J.; Gierczak, C. A.; Ball, J. C.; Japar, S. M. *Int. J. Chem. Kinet.* **1989**, *21*, 1077.
- Kirsch, L. J.; Parkes, D. A.; Waddington, D. J.; Woolley, A. *J. Chem. Soc., Faraday Trans. 1* **1979**, *75*, 2678.
- Cowley, L. T.; Waddington, D. J.; Woolley, A. *J. Chem. Soc., Faraday Trans. 1* **1982**, *78*, 2535.
- Kirsch, L. J.; Parkes, D. A. *J. Chem. Soc., Faraday Trans. 1* **1981**, *77*, 293.
- Niki, H.; Maker, P. D.; Savage, C. M.; Breitenbach, L. P. *Int. J. Chem. Kinet.* **1980**, *12*, 1001.
- Wallington, T. J.; Andino, J. M.; Japar, S. M. *Chem. Phys. Lett.* **1990**, *165*, 189.
- Osbourne, D. A.; Waddington, D. J. *J. Chem. Soc., Perkin Trans. 2* **1984**, 1861.
- Sanhueza, E.; Simonaitis, R.; Hecklen, J. *Int. J. Chem. Kinet.* **1979**, *11*, 907.
- Sander, S. P.; Watson, R. T. *J. Phys. Chem.* **1980**, *84*, 1664.
- Kurylo, M. J.; Wallington, T. J. *Chem. Phys. Lett.* **1987**, *138*, 543.
- Moortgat, G. K.; Cox, R. A.; Schuster, G.; Burrows, J. P.; Tyndall, G. S. *J. Chem. Soc., Faraday Trans. 2* **1989**, *85*, 809.
- Kan, C. S.; Calvert, J. G. *Chem. Phys. Lett.* **1979**, *63*, 111.
- Thomas, S. S.; Calvert, J. G. *J. Am. Chem. Soc.* **1962**, *84*, 4207.
- Batt, L.; Robinson, G. N. *Int. J. Chem. Kinet.* **1987**, *18*, 391.

- (84) Sanhueza, E.; Heicklen, J. *J. Phys. Chem.* **1975**, *79*, 7.
- (85) Niki, H.; Maker, P. D.; Savage, C. M.; Breitenbach, L. P. *Chem. Phys. Lett.* **1981**, *80*, 499.
- (86) Wallington, T. J.; Japar, S. M. *Chem. Phys. Lett.* **1990**, *167*, 513.
- (87) Wallington, T. J.; Japar, S. M. *Chem. Phys. Lett.* **1990**, *166*, 495.
- (88) Niki, H.; Maker, P. D.; Savage, C. M.; Breitenbach, L. P. *J. Phys. Chem.* **1985**, *89*, 588.
- (89) Moortgat, G. K.; Veyret, B.; Lesclaux, R. *Chem. Phys. Lett.* **1989**, *160*, 443.
- (90) DeMore, W. B.; Sander, S. P.; Golden, D. M.; Molina, M. J.; Hampson, R. F.; Kurylo, M. J.; Howard, C. J.; Ravishankara, A. R. *Chemical Kinetics and Photochemical Data for Use in Stratospheric Modeling. Evaluation Number 9*. NASA-JPL Publication 90-1, 1990; JPL: Pasadena, CA, 1990.
- (91) Troe, J. *Ber. Bunsen-Ges. Phys. Chem.* **1969**, *73*, 946.
- (92) Hippler, H.; Troe, J.; Willner, J. *J. Chem. Phys.* **1990**, *93*, 1755.
- (93) Kurylo, M. J.; Dagaut, P.; Wallington, T. J.; Neuman, D. M. *Chem. Phys. Lett.* **1987**, *139*, 513.
- (94) Dagaut, P.; Wallington, T. J.; Kurylo, M. J. *J. Phys. Chem.* **1988**, *92*, 3833.
- (95) Dagaut, P.; Wallington, T. J.; Kurylo, M. J. *J. Phys. Chem.* **1988**, *92*, 3836.
- (96) Moortgat, G. K.; Burrows, J. P.; Schneider, W.; Tyndall, G. S.; Cox, R. A. Proceedings of the 4th European Symposium on the Physical and Chemical Behavior of Atmospheric Pollutants, Stresa, September 1986; G. Angeletti and G. Restelli, Eds.; D. Reidel Publishing Co.: Dordrecht, 1987; pp 271-281.
- (97) Plumb, I. C.; Ryan, K. R.; Steven, J. R.; Mulcahy, M. F. R. *Chem. Phys. Lett.* **1979**, *63*, 255.
- (98) Adachi, H.; Basco, N. *Chem. Phys. Lett.* **1979**, *63*, 490.
- (99) Simonaitis, R.; Heicklen, J. *Chem. Phys. Lett.* **1979**, *65*, 361.
- (100) Ravishankara, A. R.; Eisele, F. L.; Kreutter, N. M.; Wine, P. H. *J. Chem. Phys.* **1981**, *74*, 2267.
- (101) Simonaitis, R.; Heicklen, J. *J. Phys. Chem.* **1981**, *85*, 2946.
- (102) Plumb, I. C.; Ryan, K. R.; Steven, J. R.; Mulcahy, M. F. R. *J. Phys. Chem.* **1981**, *85*, 3136.
- (103) Zellner, R.; Fritz, B.; Lorenz, K. *J. Atmos. Chem.* **1986**, *4*, 241.
- (104) Adachi, H.; Basco, N. *Chem. Phys. Lett.* **1979**, *64*, 431.
- (105) Plumb, I. C.; Ryan, K. R.; Steven, J. R.; Mulcahy, M. F. R. *Int. J. Chem. Kinet.* **1982**, *14*, 183.
- (106) Adachi, H.; Basco, N. *Int. J. Chem. Kinet.* **1982**, *14*, 1243.
- (107) Lesclaux, R.; Caralp, F. *Int. J. Chem. Kinet.* **1984**, *16*, 1117.
- (108) Dognon, A. M.; Caralp, F.; Lesclaux, R. *J. Chim. Phys.* **1985**, *82*, 349.
- (109) Plumb, I. C.; Ryan, K. R. *Chem. Phys. Lett.* **1982**, *92*, 236.
- (110) Ryan, K. R.; Plumb, I. C. *Int. J. Chem. Kinet.* **1984**, *16*, 591.
- (111) Adachi, H.; Basco, N. *Int. J. Chem. Kinet.* **1980**, *12*, 1.
- (112) Ravishankara, A. R.; Eisele, F. L.; Wine, P. H. *J. Chem. Phys.* **1980**, *73*, 3743.
- (113) Adachi, H.; Basco, N. *Chem. Phys. Lett.* **1979**, *67*, 324.
- (114) Elfers, G.; Zabel, F.; Becker, K. H. *Chem. Phys. Lett.* **1990**, *168*, 14.
- (115) Basco, N.; Parmer, S. S. *Int. J. Chem. Kinet.* **1987**, *19*, 115.
- (116) Bridier, I.; Caralp, F.; Loirat, H.; Lesclaux, R.; Veyret, B.; Becker, K. H.; Reimer, A.; Zabel, F. *J. Phys. Chem.* **1991**, *95*, 3594.
- (117) Moore, S. B.; Carr, R. W. *J. Phys. Chem.* **1990**, *94*, 1393.
- (118) Caralp, F.; Lesclaux, R.; Rayez, M. T.; Rayez, J. C.; Forst, W. *J. Chem. Soc., Faraday Trans. 2* **1988**, *84*, 569.
- (119) Howard, C. J.; Evenson, K. M. *Geophys. Res. Lett.* **1977**, *4*, 437.
- (120) Leu, M. T. *J. Chem. Phys.* **1979**, *70*, 1662.
- (121) Howard, C. J. *J. Chem. Phys.* **1977**, *67*, 5258.
- (122) Glaschick-Schimpf, I.; Leiss, A.; Monkhouse, P. B.; Schurath, U.; Becker, K. H.; Fink, E. H. *Chem. Phys. Lett.* **1979**, *67*, 318.
- (123) Hack, W.; Preuss, A. W.; Temps, F.; Wagner, H. Gg.; Hoyermann, K. *Int. J. Chem. Kinet.* **1980**, *12*, 851.
- (124) Thrush, B. A.; Wilkinson, J. P. T. *Chem. Phys. Lett.* **1981**, *81*, 1.
- (125) Burrows, J. P.; Cliff, D. I.; Thrush, B. A.; Wilkinson, J. P. T. *Proc. R. Soc. (London)* **1979**, *A368*, 463.
- (126) Rozenshtein, V. B.; Gershenzon, Yu. M.; Il'in, S. O.; Kishkovich, O. P. *Chem. Phys. Lett.* **1984**, *112*, 473.
- (127) Zellner, R. *J. Chim. Phys.-Chim. Biol.* **1987**, *84*, 403.
- (128) Atkinson, R.; Aschmann, S. M.; Carter, W. P. L.; Winer, A. M.; Pitts, J. N., Jr. *Int. J. Chem. Kinet.* **1984**, *16*, 1085.
- (129) Atkinson, R.; Aschmann, S. M.; Carter, W. P. L.; Winer, A. M.; Pitts, J. N., Jr. *J. Phys. Chem.* **1982**, *86*, 4563.
- (130) Cox, R. A.; Derwent, R. G.; Holt, P. M.; Kerr, J. A. *J. Chem. Soc. Faraday Trans. 1* **1976**, *72*, 2061.
- (131) Cox, R. A.; Roffey, M. J. *Environ. Sci. Technol.* **1977**, *11*, 900.
- (132) Hendry, D. G.; Kenley, R. A. *J. Am. Chem. Soc.* **1977**, *99*, 3198.
- (133) Kirchner, F.; Zabel, F.; Becker, K. H. *Ber. Bunsen-Ges. Phys. Chem.* **1990**, *94*, 1379.
- (134) Tuazon, E. C.; Carter, W. P. L.; Atkinson, R. *J. Phys. Chem.* **1991**, *95*, 2434.
- (135) Kurylo, M. J.; Ouellette, P. A. *J. Phys. Chem.* **1986**, *90*, 441.
- (136) Kurylo, M. J.; Ouellette, P. A. *J. Phys. Chem.* **1987**, *91*, 3365.
- (137) Sander, S. P.; Peterson, M. *J. Phys. Chem.* **1984**, *88*, 1566.
- (138) Simonaitis, R.; Heicklen, J. *Int. J. Chem. Kinet.* **1978**, *10*, 67.
- (139) Cox, R. A.; Patrick, R. *Int. J. Chem. Kinet.* **1979**, *11*, 635.
- (140) Troe, J. *Ber. Bunsen-Ges. Phys. Chem.* **1983**, *87*, 161.
- (141) Gilbert, R. G.; Luther, K.; Troe, J. *Ber. Bunsen-Ges. Phys. Chem.* **1983**, *87*, 169.
- (142) Dodge, M. C. *J. Geophys. Res.* **1989**, *94*, 5121.
- (143) Calvert, J. G.; Pitts, J. N., Jr. *Photochemistry*; John Wiley and Sons: New York, 1966.
- (144) Jacox, M. E.; Dal-Favero, M. E. *NIST Vibrational and Electronic Energy Levels of Small Polyatomic Transient Molecules*; NIST Standard Reference Database 26, 1992.
- (145) Ase, P.; Bock, W.; Snelson, A. *J. Phys. Chem.* **1986**, *90*, 2099.
- (146) Russell, J. A. *J. Am. Chem. Soc.* **1957**, *79*, 3871.
- (147) Patrick, R.; Barker, J. R.; Golden, D. M. *J. Phys. Chem.* **1984**, *88*, 128.